Developing a Tool to Estimate The Traffic Loading Frequency Equivalent to be Inserted into The Flexible Pavement Design Method

by

Mohammadmehdi SARHADI

THESIS PRESENTED TO ÉCOLE DE TECHNOLOGIE SUPÉRIEURE
IN PARTIAL FULFILLMENT OF A MASTER'S DEGREE
WITH THESIS IN CONSTRUCTION ENGINEERING
M.A.Sc.

MONTREAL, AUGUST 14, 2023

ÉCOLE DE TECHNOLOGIE SUPÉRIEURE
UNIVERSITÉ DU QUÉBEC

BOARD OF EXAMINERS

THIS THESIS HAS BEEN EVALUATED

BY THE FOLLOWING BOARD OF EXAMINERS

Mr. Prof. Alan Carter, Thesis supervisor
Department of Construction Engineering, École de technologie supérieure

Mr. Prof. Michel Vaillancourt, Co-supervisor
Department of Construction Engineering, École de technologie supérieure

Mr. Prof. Conrad Boton, President of the board of examiners
Department of Construction Engineering, École de technologie supérieure

Mr. Prof. Diego Ramirez Cardona, external independent examiner
Department of Construction Engineering, École de technologie supérieure

THIS THESIS WAS PRESENTED AND DEFENDED

IN THE PRESENCE OF A BOARD OF EXAMINERS AND THE PUBLIC

ON AUGUST 9, 2023

AT ÉCOLE DE TECHNOLOGIE SUPÉRIEURE

ACKNOWLEDGEMENTS

I would like to express my deepest gratitude to Prof. Alan Carter, my supervisor, whose unwavering support and guidance have been invaluable throughout my Master's thesis and related research. His persistence, inspiration, and profound expertise have played a pivotal role in shaping both the research project and the composition of this thesis.

In addition to my supervisor, I extend my heartfelt appreciation to Prof. Michel Vaillancourt, my co-supervisor, for his dedicated efforts in assisting me. His insightful comments, unwavering motivation, and thought-provoking questions have pushed me to explore new areas and expand the scope of my study. His brilliant approach has opened my eyes to new ways of learning and understanding.

I am also indebted to my family and friends who have consistently supported and encouraged me in all my endeavors. Your unwavering belief in me and your relentless pursuit of the best have always been evident. I am grateful to my parents and brother for teaching me the essence of happiness, self-awareness, and the importance of prioritizing others.

Their unwavering support has been a constant source of strength throughout this journey

Développement d'un outil pour estimer la fréquence équivalente de chargement de trafic à insérer dans la méthode de conception des chaussées flexibles

Mohammadmehdi SARHADI

RÉSUMÉ

Dans la conception des chaussées flexibles soumises à une charge dynamique de véhicules, il est essentiel de modéliser avec précision le comportement des couches d'asphalte. Pour y parvenir, il est nécessaire de transférer la charge de trafic du domaine temporel, où la charge s'applique sur la surface au fil du temps, au domaine fréquentiel, qui est utilisé pour simuler le comportement du matériau bitumineux en laboratoire. Dans ce contexte, un outil itératif/de conversion est développé pour estimer la fréquence angulaire équivalente de la charge de trafic. Cet outil est construit en analysant la déformation instantanée enregistrée par des jauges de contrainte installées au bas de la couche d'asphalte du système routier ULAVAL. L'analyse commence par le calcul de la rigidité de la couche d'asphalte pour chaque température d'essai en se basant sur le modèle 2S2P1D. Ensuite, les signaux de charge efficace sont extraits en estimant le temps de chargement efficace à l'aide de la méthode d'Odemark. Les signaux isolés sont ensuite transformés dans le domaine fréquentiel par une analyse de Fourier dans Microsoft Excel afin d'obtenir la fréquence équivalente pour chaque température en tant que fréquence maximale des signaux convertis.

Pour valider les résultats, les fréquences équivalentes calculées sont utilisées comme fréquence de chargement initiale dans le calcul 2S2P1D, et le processus est répété jusqu'à ce qu'il n'y ait aucune différence entre la fréquence de chargement initiale et la fréquence équivalente dans le résultat. En obtenant la fréquence équivalente pour le paramètre de chargement de trafic, le comportement des couches d'asphalte peut être modélisé avec plus de précision, ce qui conduit à une conception plus précise des chaussées flexibles soumises à une charge dynamique de véhicules. La méthodologie proposée dans cette étude permet d'estimer la fréquence équivalente pour différentes conditions de chaussée et vitesses de chargement. Elle offre un outil fiable et efficace aux ingénieurs pour estimer le temps de chargement efficace et la fréquence équivalente de la charge de trafic, qui sont des paramètres cruciaux pour concevoir des chaussées flexibles avec une précision améliorée.

Mots-clés: Comportement des chaussées souples, fréquence équivalente, méthode d'Odemarks, analyse de Fourier, modèle 2DP1D.

Developing a Tool to Estimate The Traffic Loading Frequency Equivalent to be Inserted into The Flexible Pavement Design Method

Mohammadmehdi SARHADI

ABSTRACT

In the design of flexible pavements subjected to dynamic vehicular loading, it is crucial to accurately model the behaviour of asphalt layers. To achieve this, it is necessary to transfer the traffic loading from the time domain, in which the loading applies on top of the surface through time, to the frequency domain, which is used to simulate the bituminous material behaviour in the laboratory. In this context, an iterative/conversion tool is developed to estimate the equivalent angular frequency for traffic loading. The tool is built by analyzing the instantaneous deformation recorded by strain gauges installed at the bottom of the asphalt layer of the ULAVAL paved system. The analysis begins by calculating the stiffness of the asphalt layer in each testing temperature based on the 2S2P1D model. Then, the effective loading signals are extracted through the estimation of effective loading time using the Odemark method. The isolated signals are then transformed into the frequency domain by Fourier analysis in Microsoft Excel to obtain the equivalent frequency for each temperature as the peak frequency in the converted signals.

To validate the results, the calculated equivalent frequencies are inputted into the 2S2P1D calculation as the initial loading frequency and the process is repeated until there are no differences between the initial loading frequency and the equivalent frequency in the result. By obtaining the equivalent frequency for the traffic loading parameter, the behaviour of the asphalt layers can be modelled more accurately, leading to a more precise design of flexible pavements under dynamic vehicular loading. The proposed methodology in this study allows for the estimation of equivalent frequency for various pavement conditions and loading speeds. It provides a reliable and efficient tool for engineers to estimate the effective loading time and equivalent frequency of traffic loading, which are crucial parameters for designing flexible pavements with improved accuracy.

Keywords: Flexible pavement behaviour, Equivalent frequency, Odemarks' method, Fourier analysis, FFT, 2S2P1D model.

TABLE OF CONTENTS

LIST OF TABLES

LIST OF FIGURES

Page

LIST OF ABREVIATIONS

2S2P1D	Two Springs, Two Parabolic Elements, One Dashpot
AASHTO	American Association of State Highway and Transportation Officials
DFT	Discrete-Fourier Transform
ESAL	Equivalent Single Axle Load
ETS	École de technologie supérieure
FFT	Fast-Fourier Transform
HMA	Hot Mixed Asphalt
LCMB	Laboratoire sur les Chaussées et Matériaux Bitumineux
LDS	Linear Displacement Sensor
LVE	Linear Viscoelastic
MEPDG	Mechanistic-Empirical Pavement Design Guide
MC	Medium Curing
NCHRP	The National Cooperative Highway Research Program
OPECC	Outil de Prédiction de l'Évolution du Comportement de la Chaussée
TML	Tokyo Measuring Instruments Laboratory
WLF	William-Landel-Ferry law

LIST OF SYMBOLS AND UNITS OF MEASUREMENTS

$\|E^*\|$	Dynamic complex modulus (Norm of complex modulus)
C_1 and C_2	Material dependent constants for WLF law
A_c	The square dimension of the contact area
a_c	The radius dimension of the contact area
a_τ	The temperature shift factor
E^*	Complex modulus (MPa)
E	Elastic or young modulus (MPa)
E_1	Real part of the complex modulus (MPa)
E_2	Imaginary part of the complex modulus (MPa)
E_0	Glassy modulus, when $\omega\tau$ tends to ∞ (MPa)
E_{00}	Static modulus, when $\omega\tau$ tends to 0 (MPa)
E_i	The elastic modulus of the $i^t h$ layer (MPa)
E_n	The elastic modulus of the $n^t h$ layer (MPa)
E_{SG}	The elastic modulus of the subgrade layer (MPa)
E_t	The relaxation modulus at the time t (MPa)
f	Frequency (Hz)
f_v	The equivalent frequency for the vehicle speed of "v" (Hz)
f_{100}	The equivalent frequency for the vehicle speed of 100 km/h (Hz)
G^*	Complex shear modulus (MPa)

G	Complex modulus (MPa)
h_i	The thickness of the $i^t h$ layer (mm)
h_n	The thickness of the $n^t h$ layer (mm)
i	Complex number $i^2 = -1$
L	Length of the contact area (mm)
L_{eff}	The effective loading length at the bottom of the asphalt layers (mm)
m	Number of Maxwell model pairs (one spring and one dashpot in series
N	Total number of samples in the Fourier analysis
n	The number of an n-th sample in the Fourier analysis
N_{eff}	Total number of the time intervals over the effective loading time
T	Temperature $^\circ C$
T_g	The Glass Transition temperature $^\circ C$
T_{ref}	Reference testing temperature $^\circ C$
t_{eff}	The effective loading time at the bottom of asphalt layers (s)
V_s	The vehicle speed on top of the asphalt surface (km/h)
$X(f)$	Function of data sets in frequency domain
X_k	K^{th} frequency representative
$x(t)$	Function of data sets in time domain
Z_{eff}	The effective loading depth over the asphalt layers (mm)
τ_m	Relaxation time

$\tau(T)$	Time constant that varies with temperature
σ	Stress (MPa)
ν	Viscosity
ϕ	Phase angle ($\circ$ or Rad)
ε	The tension deformation or strain
ω	Angular frequency or pulsation (Rad) = $2\pi f 2$
δ	Dimensionless constant for 2S2P1D model
β	Dimensionless constant for 2S2P1D model

INTRODUCTION

The highway network in Canada spans over one million kilometers, of which approximately 40% are paved roads. In densely populated areas, such as Quebec and Prince Edward Island, the percentage of paved roads in the overall road network is significantly higher, at approximately 57% and 70%, respectively. Over 95% of all paved roadways in Canada, or 380,000 kilometers, are constructed with bituminous material, which underscores the importance of pavement maintenance and design as an essential industry category (Badeli, 2018).

Historically, asphalt pavements were designed using an empirical approach prior to the early 1920s. However, this approach did not consider material mechanics. Later, the elastic mechanistic-empirical pavement design was developed as the first widely accepted analysis theory, based on the assumption that asphalt mixtures are homogeneous, isotropic linearly elastic solids. However, this assumption does not hold true due to the viscoelastic behaviour of bituminous materials. In the last phase of pavement design history to date, the viscoelastic mechanistic-empirical pavement design was introduced. According to this theory, the behaviour of bituminous material under dynamic traffic loads lies in the viscoelastic range. Therefore, viscoelastic theory must be applied, utilizing viscoelastic mechanical models, such as the generalized Maxwell model and the 2S2P1D model (Liao, 2007).

As flexible pavement design has progressed to the point where mechanical models can simulate the stiffness of bituminous material as a norm of complex modulus, the time domain loading parameter needs to be converted to the frequency domain. The equivalent frequency for the vehicular loading parameter is dependent on the effective loading time in the effective depth of pavement, estimated using the Odemarks' method (Carter *et al.*, 2018). For instance, a vehicular speed of 10 km/h in a parking lot is considered as 0.01 Hz, while a speed of 100 km/h on a highway is considered as 10 Hz. Thus, the effective loading time obtained using the Odemarks' method must be converted to an equivalent frequency using a conversion tool, based

on the Fourier analysis of the effective loading time, to be utilized in the mechanical models for pavement design.

Main objective is to develop a conversion tool that utilizes the Fourier analysis and Odemarks' method to determine the equivalent angular frequency of the vehicular loading parameter on the surface layer. This tool is intended to compare the results with the frequency variables assumed by simulation methods. To achieve this objective, the study analyzed the instantaneous deformation data that was measured by strain gauges installed under the wheel path of the lab pavement system with a total size of 6, 2, 2 m^3 (length, depth, and width) in three different areas at four varied temperatures; -8, 6, 16, and 20 $^{\circ}C$.

This study aims to develop a reliable calculation tool based on Fourier analysis and Odemarks' method for determining the equivalent angular frequency of vehicular loading parameters on the surface layer. The study comprises four phases to achieve this objective. In the first phase, the stiffness of the asphalt layer is calculated by the 2S2P1D mechanical model based on the test parameters and the assumed initial loading frequency (ranging from 0.1 to 10 Hz). Subsequently, the Odemarks' method is applied to calculate the effective loading time for each test temperature (-8, 6, 16, and 20°C) in the second phase. In the third step, the effective loading signals are extracted from the strain gauge recordings and are adjusted to power of two time factors to prepare them for conversion into the frequency domain using Fourier analysis. Finally, the equivalent frequency for the recorded loading signals is determined by finding the frequency factors of all curves' peak amplitudes as the equivalent frequency, and the calculation method is reevaluated by adjusting the input of the initial loading frequency.

An appendix is provided to explain the developed conversion tool in Microsoft Excel version 16.61.1, which is intended to be an accurate method for obtaining the equivalent frequency for every loading signal depending on the pavement and the loading parameters, assuming that the findings support the hypotheses. The hypotheses of this research are as follows.

- The duration of effective loading estimated using the Odemarks' method, considering the loading parameters and the pavement characteristics described in the data collection section, is nearly equivalent to the recorded loading duration captured by the strain gauges, which includes both loading and unloading phases.

- The highest level of longitudinal tension in the asphalt layer, which is indicated by the peak of the loading signals' curve and denoted as "ε_t", is observed precisely when the wheel is positioned directly on top of it. Furthermore, this peak occurs at the midpoint of the effective loading period.

- The hypothesis in data collection analysis indicates that the deformation data collected by the TML-REF is not affected by the idealized crack.

- The primary conjecture of this research is that the equivalent frequency for the effective loading time obtained from the loading and pavement parameters can be represented by the frequency component associated with the maximum strain amplitude in the frequency domain for each loading signal.

- It is postulated that utilizing a polynomial regression to determine the estimated equivalent frequencies for each effective loading time would serve as a precise calibration curve to derive the equivalent frequency for every required effective loading time.

This master's thesis is structured as follows. Following a brief introduction, Chapter 1 provides a comprehensive review of the literature on flexible pavement and its design. Chapter 2 outlines the research methodology, and Chapter 3 examines and discusses the results. Additionally, details on the developed tool are presented in Appendix 1.

CHAPTER 1

BACKGROUND AND LITERATURE REVIEW

Since the 1920s, pavement engineers have been striving to improve design methods for flexible pavements. The goal is to increase project durability, safety, and budget efficiency by simulating and calculating structural behavior under unstable environmental conditions more accurately. The dominant stress created by traffic loads on the surface of flexible pavements is carried and dispersed to the subgrade layers by the asphalt layers, which consist of bituminous material. This type of material exhibits fundamentally complex behavior under various types and intensities of stresses, referred to as "viscoelastic behavior," which is now incorporated in simulation methods using mechanical models for bituminous material. This chapter presents an overview of the flexible pavement structure, bituminous material behavior under moving loads, and an explanation of mechanical models. It is essential to determine the precise stress distribution throughout the layers and prepare them for use in simulation methods as equivalent loading frequency data inputs to predict how the asphalt layer under the wheel path will behave in hypothetical conditions. This chapter reviews and explains the mathematical methods used for loading distribution, along with the Fourier analysis used to convert time domain data to the frequency domain (Huang, 2004).

1.1 Introduction to Flexible Pavements

In the realm of pavement engineering, bituminous materials have been acknowledged as viscoelastic substances with intricate behavior since the commencement of the 1960s, presenting both viscous and elastic regions across a range of loading frequency and temperature. The main structural layers of flexible pavements are composed of asphalt mixes made of granular aggregates and bitumen. In this section, a detailed examination of these layers is presented (Badeli, 2018).

1.1.1 Structural Layered System

The primary objective of the pavement structure is to distribute the applied traffic loads by transmitting the vertical and shear stresses from the surface to the underlying layers. As a result, the individual pavement layers exhibit distinct structural behavior and response characteristics to the traffic loads. Deformation and stress are induced in each layer due to the interfacial bonding between the asphalt layers, which can vary based on the material and the design methods employed (Carter *et al.*, 2018). Flexible asphalt pavements are commonly constructed over subgrade layers, which may be either natural soil or fill material, and require proper grading and compaction (refer to Figure 1.1). The topmost layer, the surface or wearing layer, experiences the greatest environmental stresses and deflections due to direct contact with traffic loads. A smooth surface layer is crucial to minimize asphalt slippage and traffic noise, but it has a relatively small influence on bearing capacity. The asphalt base layer, as the main structural asphalt layer, transfers moving loads to the subgrade or granular foundation layer while also preventing fatigue cracking. The material used in this layer has a higher modulus to manage stresses for the subgrade or granular layer. If a thicker bituminous layer is needed, an alternative approach involves incorporating a binder or intermediate asphalt layer between the surface and base layers, rather than increasing the thickness of the asphalt base layer (Carter *et al.*, 2018).

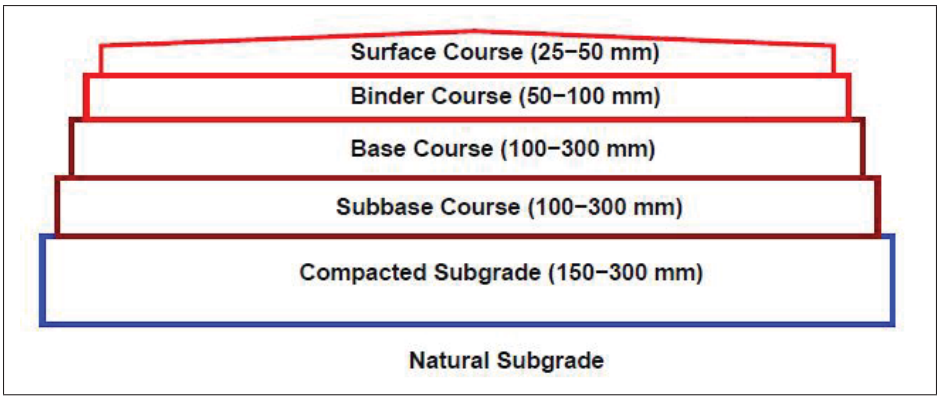

Figure 1.1 Typical flexible pavement
Taken from Alfaqawi et al.(2012)

In addition, to ensure proper adhesion between pavement layers, interface layers, such as prime coat, tack coat, and seal coat, must be applied. A prime coat is necessary to achieve the necessary bonding between the asphalt base and granular layers below. This is accomplished through a layer of asphalt emulsion, which serves to protect the underlying layers from moisture and provide water resistance. The prime coat can be made from either a cutback asphalt texture or a medium curing (MC) grade of liquid asphalt with low viscosity. Tack coats are also essential for achieving good adhesion and preventing slippage between bituminous material layers. A strong tack coat is required to dissipate shear stress within the pavement structure, and it is formed by applying a thin layer of asphalt emulsion (Cross & Shrestha, 2005). Ultimately, a protective seal coat should be added over the surface layer. This serves to shield the surface from oxidation and stiffening while also improving traction. The material used for this layer is asphalt emulsion, mainly composed of asphalt cement, water, and an emulsifying agent (David W. Janisch, 1998). Aggregate granular layers are composed of granular material without bituminous, which must be blended with appropriate sieves and compacted between the asphalt layers and subgrade base. The design requirements determine whether aggregate layers are divided into granular layers. The granular base layer's primary purpose is to withstand higher stresses than the sub-base and provide more bearing capacity and drainage capacity. The granular sub-base distributes loads across the base layer and provides thermal isolation, and this layer should be thick enough to prevent frost heave (Carter *et al.*, 2018).

1.1.2 Behaviour of Bituminous Materials to Various Situations

Since the 1920s, it has been assumed that bituminous materials behave elastically, which simplifies the design process. However, in reality, asphalt behaves viscoelastically above a certain temperature known as the glass transition temperature (T_g), as depicted in figure 1.2. In the viscoelastic range, the stiffness of bituminous material is determined by its complex modulus, which varies with different loading frequencies and temperature (Huang, 2004).

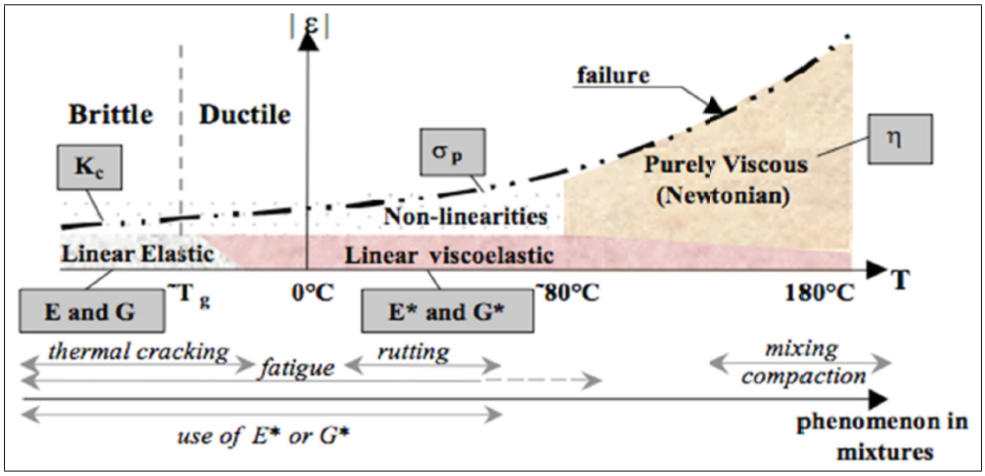

Figure 1.2 Range of the behaviour of the bituminous material
Taken from Oral et al. (2003)

As depicted in figure 1.3, the response of bituminous materials to typical traffic loading and low levels of strain amplitude falls within the Linear Viscoelastic (LVE) region, where the complex modulus is utilized for stiffness analysis of asphalt mixtures. However, under low cycles of vehicular loading and high strain levels, the behavior of bituminous materials falls within the non-linear viscoelastic region, and when subjected to thousands of loading cycles under low strain levels, it leads to fatigue failure, which represents the limits of bituminous material failure (Badeli, 2018).

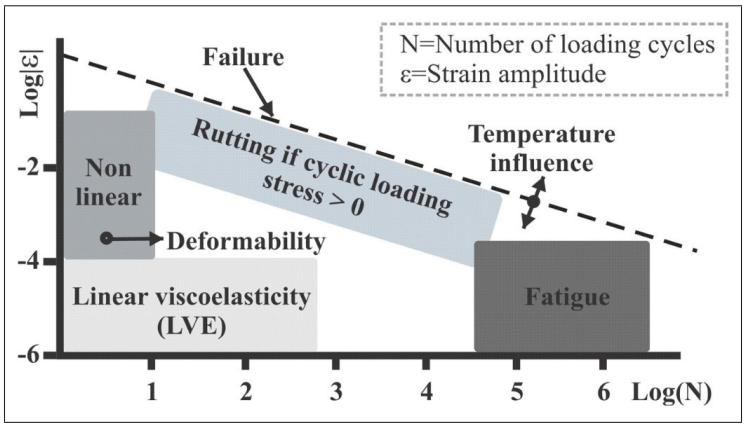

Figure 1.3 Typical behaviour of bituminous material
Taken from Ramirez et al. (2015)

1.1.2.1 Complex Modulus

As previously mentioned, bituminous material exhibits viscoelastic behavior when subjected to moving loads, and its stiffness in this region is described by the complex modulus, which represents the behavior of the asphalt material under various loading cycles and temperatures. The complex modulus, denoted as E^*, is commonly determined using equation 1.3, as shown in figure 1.4, which depicts the complex relationship between two stresses and deformation curves. Here, i is a complex number ($i^2 = -1$), σ_0 is peak stress and ε_0 is peak strain. Due to the viscoelastic nature of the bituminous material, sinusoidal strain appears with a time lag of φ/ω, which is referred to as the phase angle (φ) (Carter *et al.*, 2018).

$$\sigma(t) = \sigma_0 \sin(\omega t) \tag{1.1}$$

$$\varepsilon(t) = \varepsilon_0 \sin(\omega t - \varphi) \tag{1.2}$$

$$E^* = \frac{\sigma_0 . e^{i\omega t}}{\varepsilon_0 e^{\omega t - \varphi}} \tag{1.3}$$

According to Liao's work (Liao, 2007), the dynamic modulus can be calculated as the magnitude of the complex modulus, which is obtained by dividing the stress and strain peaks. Equation 1.4

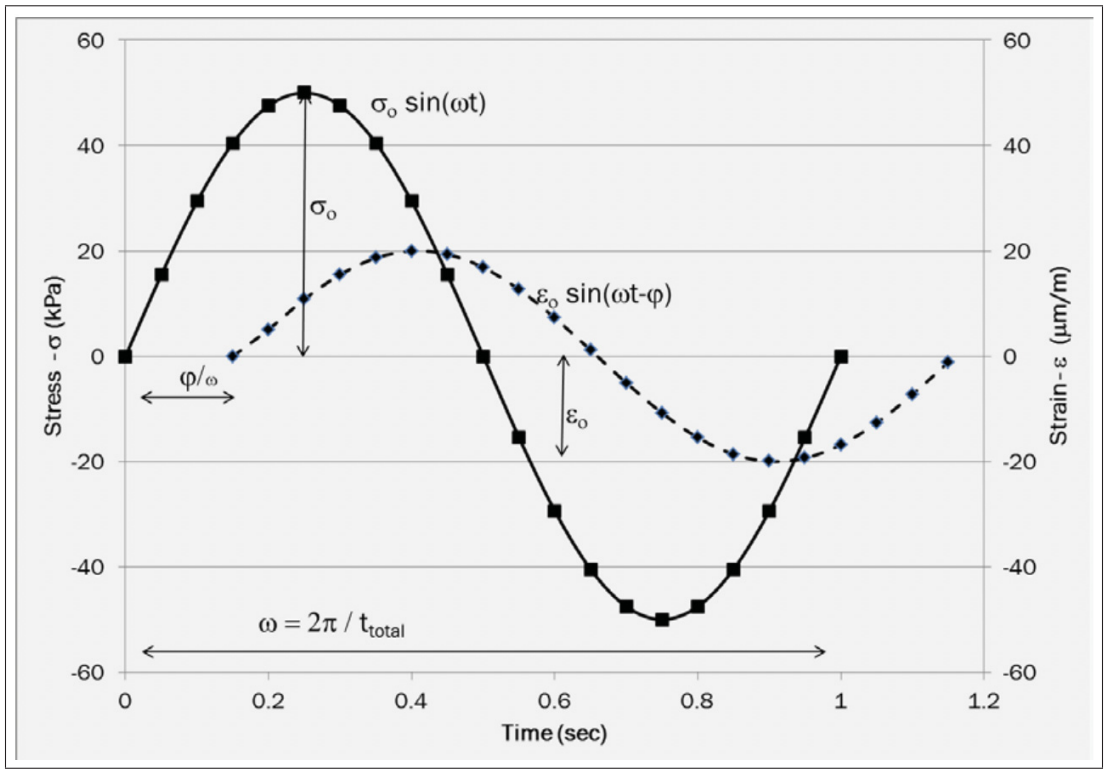

Figure 1.4 Sinusoidal stress and strain signals
Taken from Carter et al. (2018)

defines the dynamic modulus as the sum of the squares of the real part (E_1) and imaginary part (E_2) of the complex modulus.

$$|E^*| = \frac{\sigma_0}{\varepsilon_0} = \sqrt{{E_1}^2 + {E_2}^2} \tag{1.4}$$

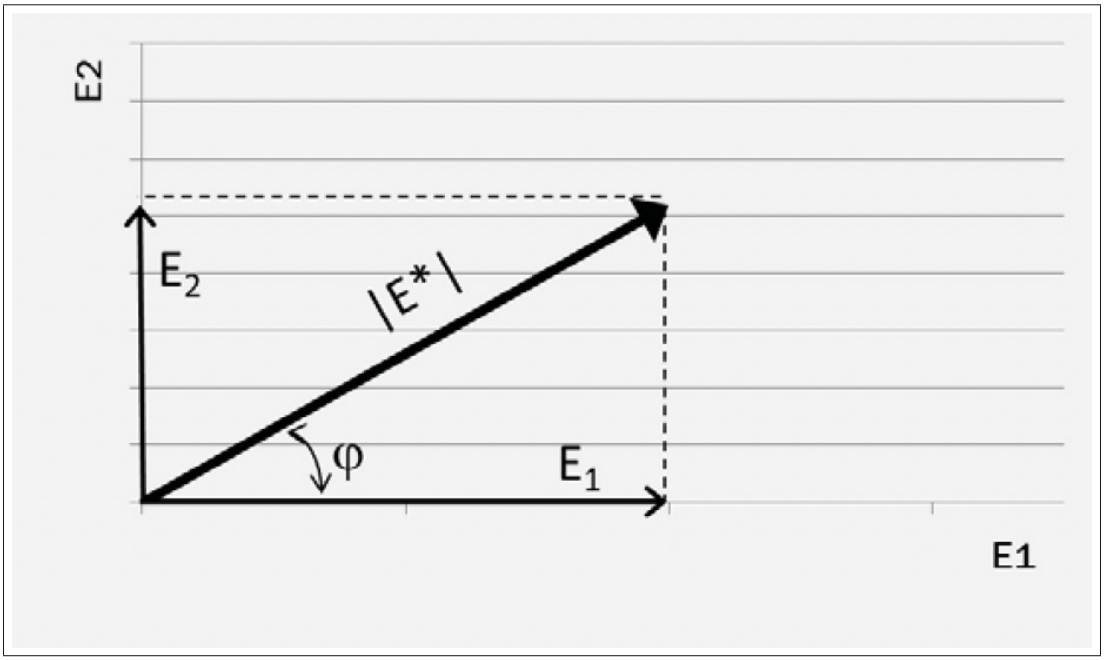

Figure 1.5 The complex modulus vectorial representation
Taken from Carter et al. (2018)

1.2 Bituminous material mechanical models

The complex modulus definition reveals that the bituminous material behavior is comprised of both viscous and elastic regions, which is influenced by a range of temperatures and loading frequencies. Various mechanical models, depicted in Figure 1.6, combine springs and dashpots to examine the asphalt material's elasticity and viscosity. These models range from single to generalized, providing a means for mathematical analysis (Huang, 2004).

1.2.1 Generalized Maxwell Model

Liao (2007) employed the Generalized Maxwell mechanical model in ABAQUS finite element software to simulate the response of HMA materials under traffic loading. One spring and *m* Maxwell elements' pairs included in this model connected in parallel, where each element consists of one spring and one dashpot connected in series, as illustrated in figure 1.7. The model exhibits an additive stress behavior, whereby the relaxation modulus of the entire system

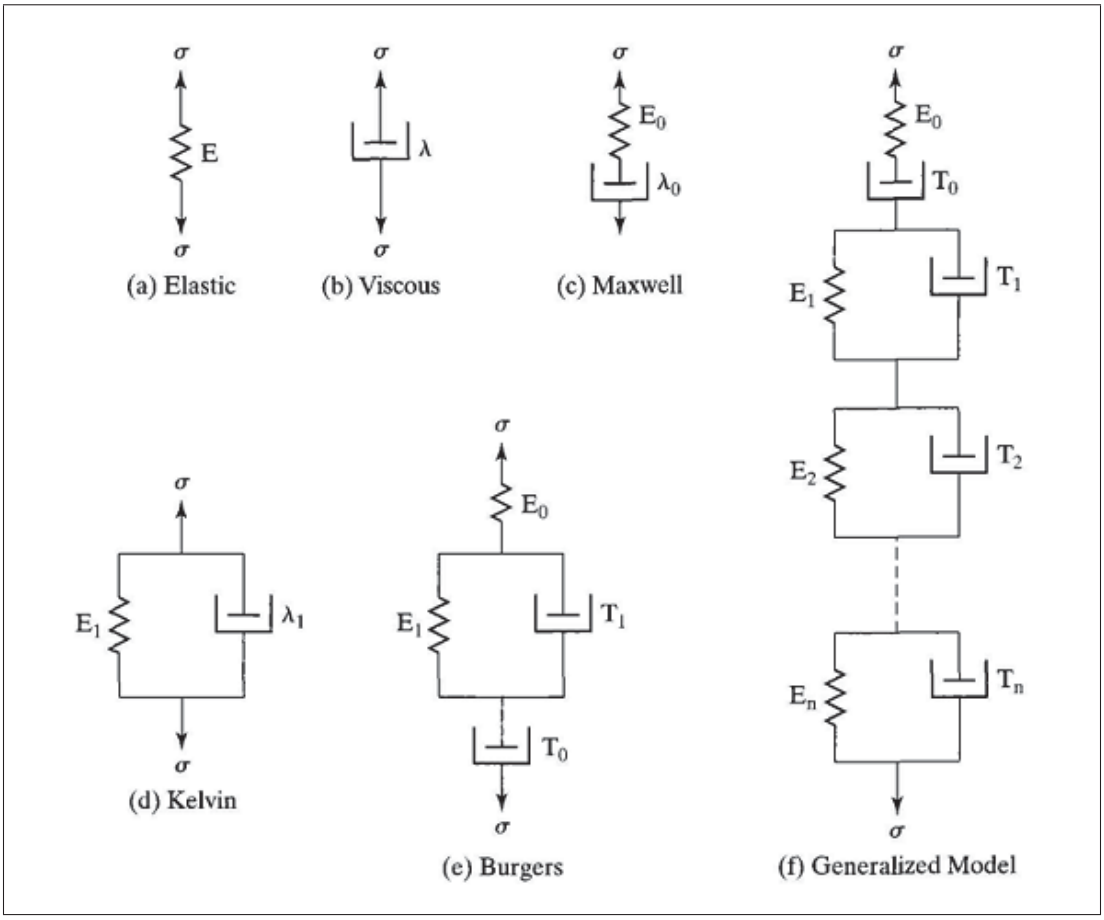

Figure 1.6 Mechanical models for bituminous material behaviour
Taken from Arabani et al. (2014)

serves as the stiffness at equilibrium deformation, as time approaches infinity. When the model experiences a steady strain, the tension on each spring-dashpot pair relaxes exponentially. The relaxation modulus E_i is assigned to the spring and the dashpot is assigned a frictional resistance, η_m, in each Maxwell element. The relaxation modulus for the Generalized Maxwell model can be estimated using equation 1.5, also known as the PRONY series expansion (Liao, 2007).

$$E(t) = E_0 - \sum_{i=1}^{m} E_i(1 - e^{-t/\tau_m}) \tag{1.5}$$

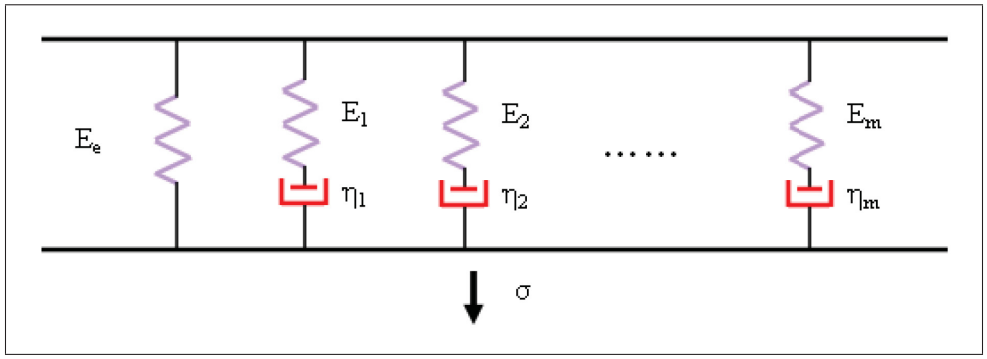

Figure 1.7 Generalized Maxwell Model
Taken from Liao et al. (2007)

In the simulation, the temperature dependency was described using the Williams-Landel-Ferry (WLF) equation, and the time dependency was defined using five PRONY series represented in the form of shear moduli in the ABAQUS software (Liao, 2007).

1.2.2 2S2P1D Model

The 2S2P1D mechanical model, illustrated in Figure 1.8, is a modified version of Huet and Sayegh's model, which was found unsuitable for binders at very low frequencies. This modified model includes a physical spring in parallel with a series connection of one spring, two parabolic elements, and one dashpot. Additionally, a linear dashpot was added to the parabolic elements to improve the simulation of the linear viscoelastic behavior of both aged and unaged bitumen penetration grades. This model was found to be the most effective in accurately simulating the viscoelastic behavior of the bitumen (Tai, Duy-Liem, Vu-Tu & Mai-Lan, 2020).

The 2S2P1D mechanical model presents the stiffness of bituminous material at different temperatures through the complex modulus, which is obtained by adjusting the reference temperature and angular frequency to account for the varying vehicular loading speeds. This process is described by equation 1.8 and is essential for understanding the behavior of the material under different conditions (Carter *et al.*, 2018).

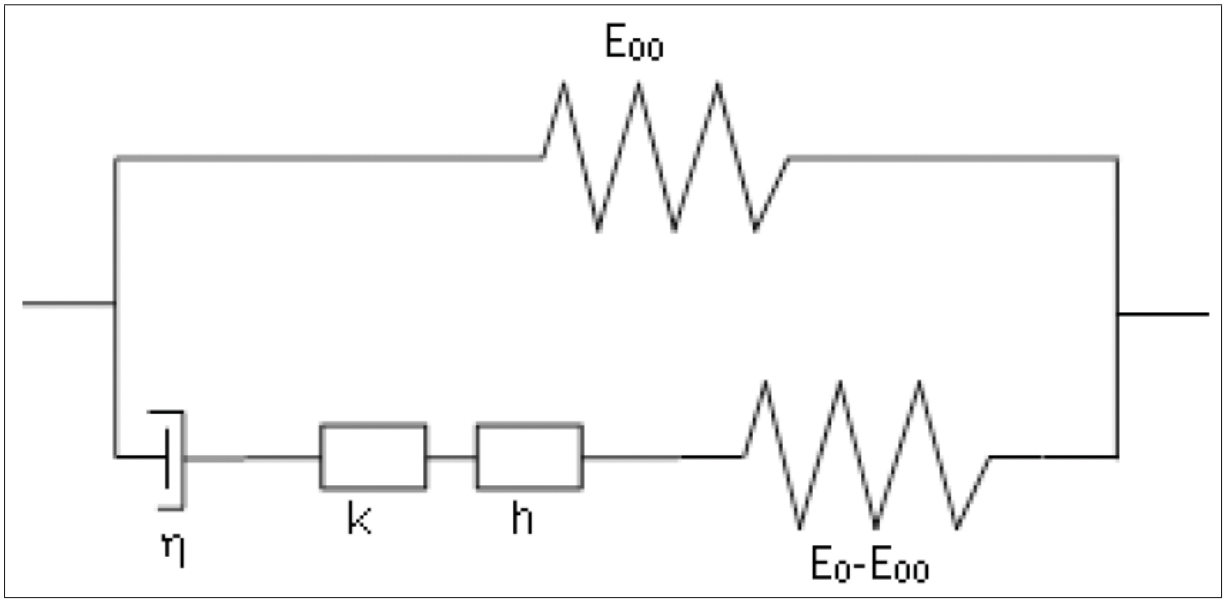

Figure 1.8 Schematic for the 2S2P1D mechanical model
Taken from Olard et al. (2003)

$$E^*(\omega) = E_{00} + \frac{E_0 - E_{00}}{1 + \delta(i\omega\tau(T))^{-k} + (i\omega\tau(T))^{-h} + (i\omega\beta\tau(T))^{-1}} \tag{1.6}$$

The 2S2P1D model calculates the complex modulus of bituminous material based on the temperature and loading cycles through the use of a shift factor applied to the reference temperature and equivalent angular frequencies. The complex modulus equation for this model, shown in equation 1.6, includes exponent parameters h and k with $0 < k < h < 1$, as well as constants δ and β. When the equivalent frequency for time domain vehicular loading and temperature ($\omega\tau(T)$) approaches zero, indicating a very hot surface or a very low level of loading cycles, the asphalt material behaves as a non-linear material in the plastic range, with the stiffness described by the static modulus (E_{00}). Conversely, when $\omega\tau(T)$ approaches infinity, indicating very high loading cycles or a very cold surface, the asphalt material behaves as a glassy linear elastic material, with the stiffness described by the glassy modulus (E_0).

$\omega\tau(T) \approx 0 \rightarrow \frac{E_0 - E_{00}}{1+\delta(i\omega\tau(T))^{-k}+(i\omega\tau(T))^{-h}+(i\omega\beta\tau(T))^{-1}} \approx 0 \rightarrow E^*(\omega) \approx E_{00}$ (Non-linear Plastic behaviour)

$\omega\tau(T) \approx +\infty \rightarrow \frac{E_0 - E_{00}}{1+\delta(i\omega\tau(T))^{-k}+(i\omega\tau(T))^{-h}+(i\omega\beta\tau(T))^{-1}} \approx E_0 - E_{00} \rightarrow E^*(\omega) \approx E_0$ (Glassy Elastic Behaviour)

To accurately model the linear viscoelastic properties of asphalt material, it is necessary to account for both temperature and frequency dependencies. The temperature dependence is described by the temperature shift factor (a_T), which is determined using equation 1.7, and depends on the reference temperature (T_{ref}) and the testing temperature (T). The time constant that varies with temperature ($\tau(T)$) used in the calculation of the complex modulus in the 2S2P1D model can be determined using equation 1.8, which is based on the WLF law ((Carter *et al.*, 2018))

$$\log a_\tau = \frac{-C_1(T - T_{ref})}{T - T_{ref} + C_2} \tag{1.7}$$

$$\tau(T) = a_\tau.\tau(T_{ref}) \tag{1.8}$$

The dynamic modulus ($|E^*|$) of bituminous material, which characterizes its stiffness, is represented by a master curve based on the equivalent frequency $\omega\tau(T)$, which accounts for both loading pulsation and testing temperature. Figure 1.9 illustrates a typical master curve at a reference temperature of 15 $°C$, whose shape is determined by the time shift factor corresponding to different testing temperatures (Carter *et al.*, 2018).

1.3 Application of vehicular loading

In flexible pavements, the wheel path of moving vehicles vehicles induces compression and flexion, leading to small-scale deformations in each layer. The asphalt layers are assumed to sag like a beam under the stress direction. Furthermore, the presence of a tack coat layer as an interface between asphalt layers ensures that there is no slipping between layers, resulting in homogeneous strain at the interlayers. Consequently, the maximum Deformation is happens beneath the lowest bituminous layer (Carter *et al.*, 2018).

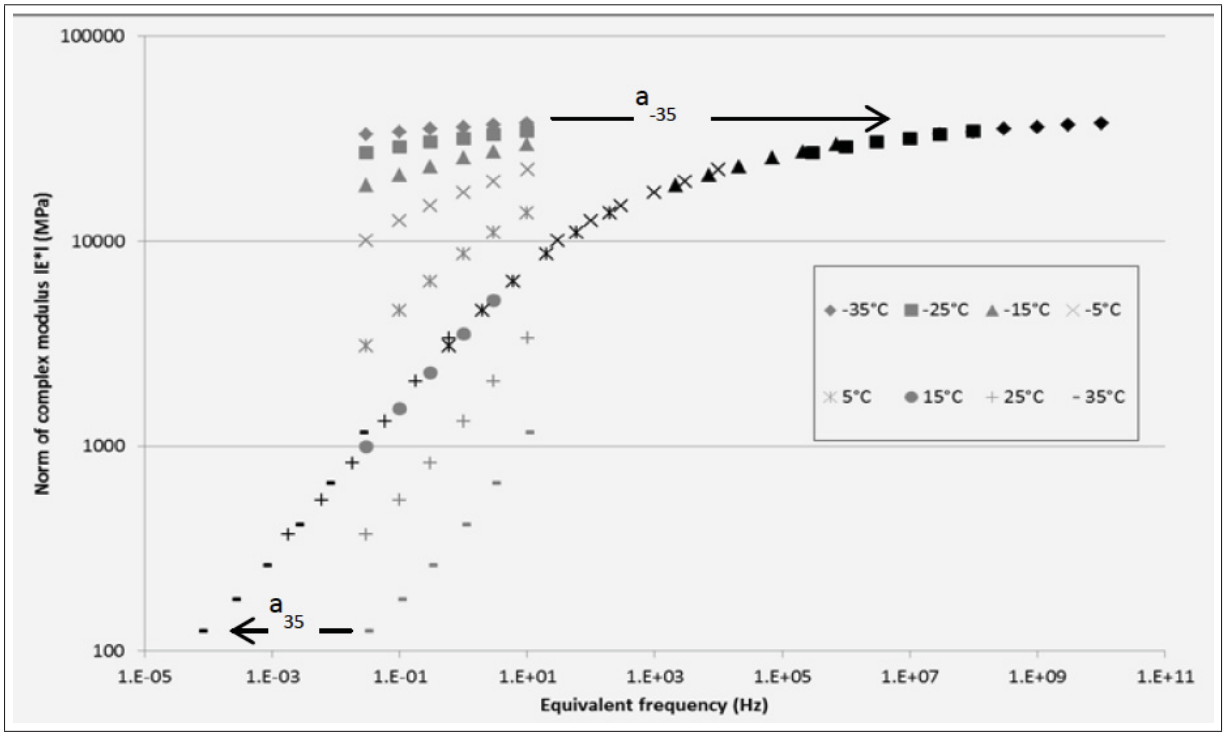

Figure 1.9 Master curve for the complex modulus at the reference temperature of 15 $°C$
Taken from Carter et al. (2018)

The measurement of horizontal deformation at the effective depth is critical aspect of pavement analysis, with longitudinal and transversal directions being commonly considered, as depicted in figure 1.10. The load position, as referenced to the point, is shown on the horizontal axis. The maximum horizontal strain in both directions occurs when the load is positioned directly over the point, with equal magnitudes in both directions. However, in the longitudinal direction, the pavement's flexion under a specific load leads to a lift before and after the loaded point, causing compression strain at the bottom of asphalt layers in that region, and compression at the top. This phenomenon is not observed in the transversal direction.

As previously discussed, flexible asphalt pavements exhibit viscoelastic behavior, which deviates from the isotropic elastic assumptions made in pavement design. Additionally, the response of bituminous material varies with loading frequency. Specifically, higher vehicular speeds

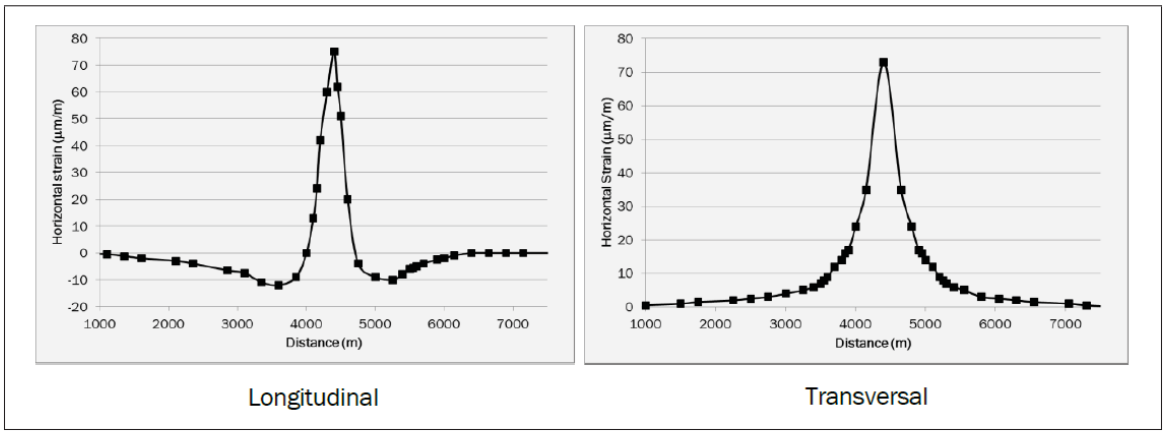

Figure 1.10 An example for the occurred immediate deformation at the bottom of asphalt layers under moving loads
Taken from Carter et al. (2018)

correspond to higher moduli, indicating that asphalt layers behave as a rigid material on highways, but as a compliant material in parking lots and similar settings.

The stiffness of bituminous material is a crucial factor in determining its response to vehicular loading, and its frequency dependence has been shown to vary with different loading speeds. Figure 1.11 depicts the variation in material stiffness, represented by the norm of the complex modulus, over a range of frequencies, from 0.01 Hz (typical of parking lots) to 10 Hz (100 km/h speed) (Carter *et al.*, 2018). Since higher material stiffness leads to greater stresses at a given point, the norm of complex modulus is a valuable tool in simulating and predicting strains in flexible pavements under different speed loading conditions. To this end, the Odemarks' method, described in the following section, is one of the most widely employed and accurate techniques for calculating loading parameters and their distribution in the various layers of a flexible pavement.

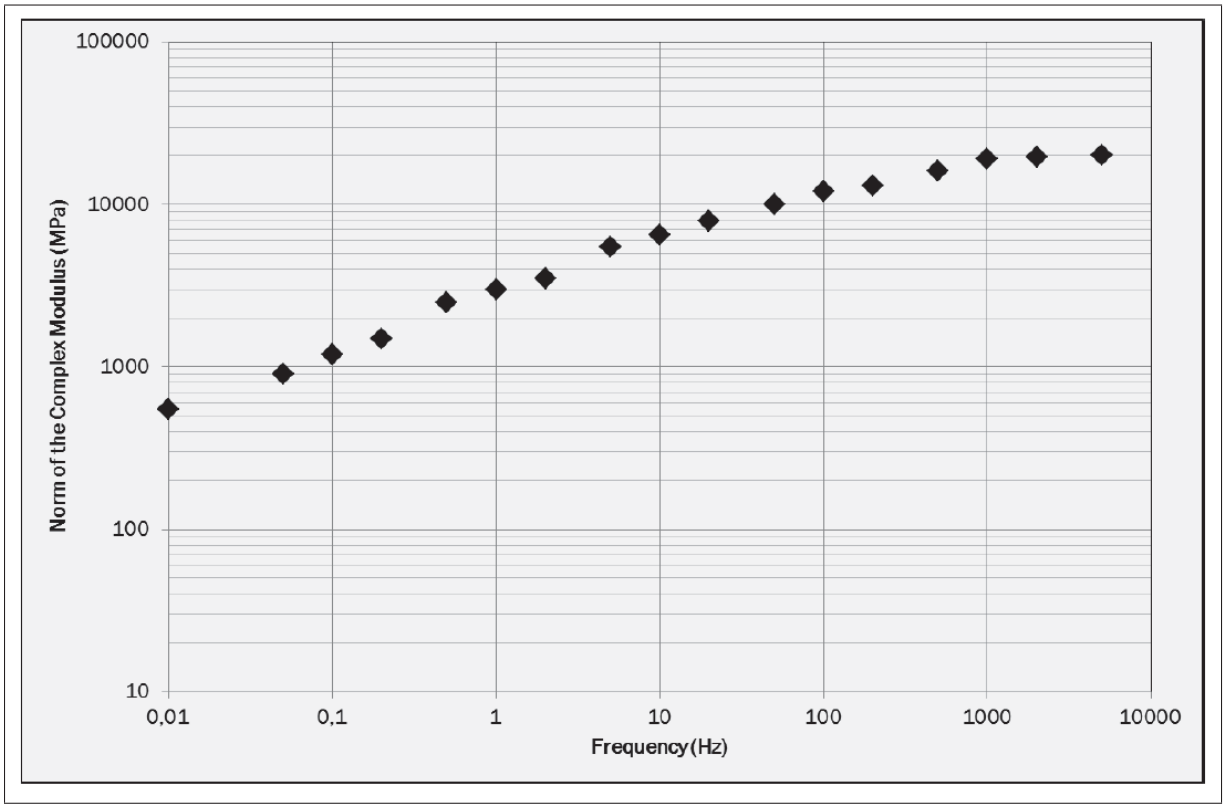

Figure 1.11 Dynamic modulus of GB20 mix under different loading frequencies at -15°*C*
Taken from Carter et al. (2018)

1.3.1 Axle loads

Figure 1.12 depicts a semi-trailer wheel on top of a surface with three configurations: a single axle with a single tyre, a single axle with dual tyres, and a tandem axle with dual tyres. Axle spacing of 23 and 13 feet is not useful in pavement design since there are no load overlaps, rendering them independent. According to the layered theory of flexible pavement design, only the wheels on one side must be considered while applying traffic loads (Huang, 2004).
. The application of traffic loading in asphalt pavements is based on an empirical concept that is time-consuming to calculate. To simplify the procedure of determining the load for each wheel and axle, the AASHTO method converts each load group into an equivalent single axle load, which is commonly accepted as 18 kips (80 KN).

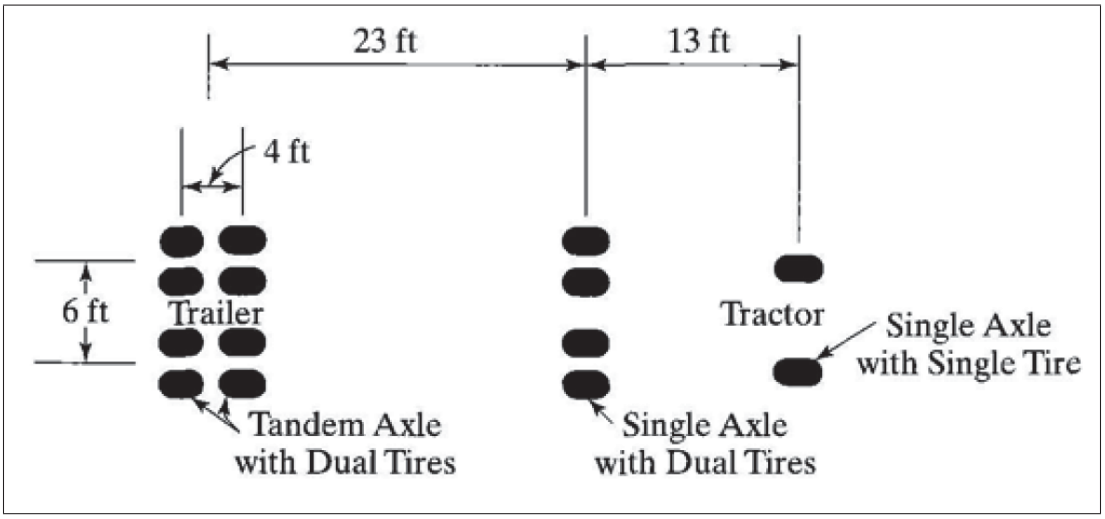

Figure 1.12 Typical semi-trailer wheel spacing
Taken from Huang et al. (2004)

The determination of loading distribution through the various layers of pavement requires an evaluation of the contact area dimensions of the tire, which are contingent upon the contact pressure. In order to calculate the length of the square dimension of the contact area, Equation 1.9 is employed, as detailed by Huang (Huang, 2004). In this equation, A_c is representing surface size of contact area, L represents the circular contact Diameter.

$$L = \sqrt{\frac{A_c}{0.5227}} \tag{1.9}$$

1.3.2 Odemark's Method for Analyzing Traffic Load Distribution

The estimation of the effective loading time for vehicular loading is a critical parameter in determining the equivalent frequency, and it can be calculated using Equation 1.10. This parameter is dependent on the vehicle speed (V_s) and the effective loading length (L_{eff}), and it is fundamental in reaching the equivalent frequency. The Odemark's method is utilized to determine the effective depth of loading, which occurs at the imaginary effective depth based on the trapezoidal model stress distribution. The estimation of the effective depth is accomplished using trigonometric functions based on the Odemark's method, as outlined in NCHRP 1-37A and currently implemented in the MEPDG software version 1.0. The flexibility of asphalt layers and their various characteristics necessitates the calculation of the effective loading length.

$$t_{eff} = \frac{L_{eff}}{V_s} \tag{1.10}$$

$$L_{eff} = 2(a_c + Z_{eff}) \tag{1.11}$$

Due to the viscoelastic properties and adhesion characteristics of bituminous material, the loading time under traffic loads at the bottom of asphalt layers varies from that on top of the surface. Odemark's method employs a $45°C$ isosceles trapezoidal model to determine the effective loading time (t_{eff}), which is directly related to the effective length determined using the radius of tire contact area (a_c) and the effective depth (Z_{eff}). Figure 1.13 illustrates the trapezoidal model and equation 1.10 and 1.11 specify the relationship between the effective loading time and the effective length of loading. The effective depth, represented as the trapezoid's altitude in this model (equation 1.12), is converted from the depth of the layers under consideration (h_i). The short base of the trapezoid represents the contact area's diameter, while the long base represents the effective length of loading (Ghanizadeh & Fakhri, 2018). It is worth noting that the variation

in the stiffness of the surface layer, resulting from different loading speeds and temperatures, only has an impact on the calculation of the effective depth in the 45-degree trapezoidal model. This model is used for determining the effective loading length by transferring the length of the tire contact area based on the layers' thickness and their stiffness (E_i - E_n) and the subgrade layer's stiffness (E_{SG}).

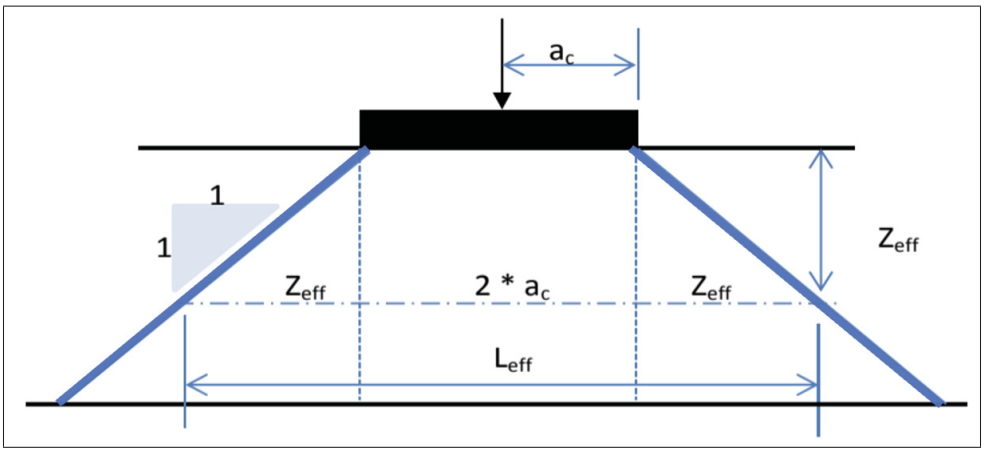

Figure 1.13 Effective length by equivalent thickness of layers
Taken from Ghanizadeh et al. (2018)

$$Z_{eff} = \sum_{i=1}^{n} (h_i \sqrt[3]{\frac{E_i}{E_{SG}}}) + h_n \sqrt[3]{\frac{E_n}{E_{SG}}} \tag{1.12}$$

1.3.3 Immediate Deformation Data Collection

The strain gauge technique is a widely used method for measuring the dynamic deformation of flexible pavement structures due to traffic loads. Linear displacement sensors (LDS) are typically installed either horizontally or longitudinally within or beneath the asphalt layers to detect the instantaneous tension and compression deformation. The placement of sensors depends on the data analysis approaches utilized. Figure 1.14 provides an example of strain gauges placed within an asphalt layer for measuring the deformation induced by traffic stress applied on the surface. This method enables the collection of accurate and reliable data on

the dynamic behaviour of flexible pavements under traffic loads, which is crucial for effective pavement design and maintenance.

Figure 1.14 H-type asphalt strain gauges installed within the asphalt layers
Taken from Correia et al. (2018)

N.S. Correia and J.G. Zornberg conducted an experimental investigation to evaluate the immediate and permanent deformation caused in geogrids inside asphalt structures exposed to repetitive loading from moving loads. Mechanical extensometers linked to the geogrids were used to measure both types of deformations. Their study revealed that the permanent geogrid strains were gradually mobilized and eventually reached a final profile beyond which additional straining was unlikely to occur. The installation plan for two horizontal and longitudinal strain gauges is shown in Figure 1.15, while Figure 1.16 illustrates the permanent deformation beneath the wheel path between two asphalt layers based on the distance from the loading wheel

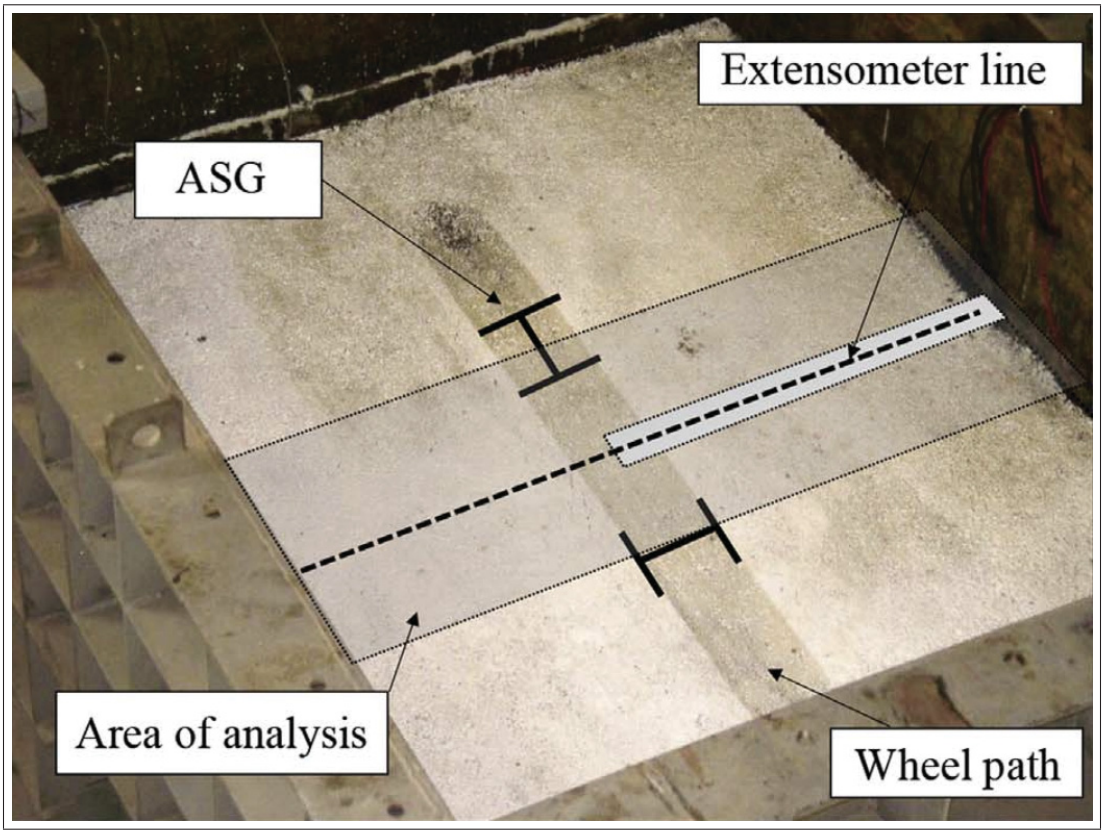

Figure 1.15 Installation plan of the strain gauges beneath the wheel path
Taken from Correia et al. (2018)

In 2021, Youness Berrada and his team conducted an empirical study to investigate the influence of low-temperature surface cracking on the performance of hot-mix asphalt layers subjected to vehicular loads (Berraha *et al.*, 2020). The study involved measuring the deformation data using five TML strain gauges that were installed longitudinally beneath the wheel path before and after inducing an idealized crack beneath the asphalt layer. The experimental setup plan view is depicted in Figure 1.17. The objective of the study was to evaluate the impact of cracking on the mechanical response of asphalt layers to vehicular loads, with the findings expected to provide insight into the potential for premature cracking of asphalt pavement and inform efforts to improve pavement performance.

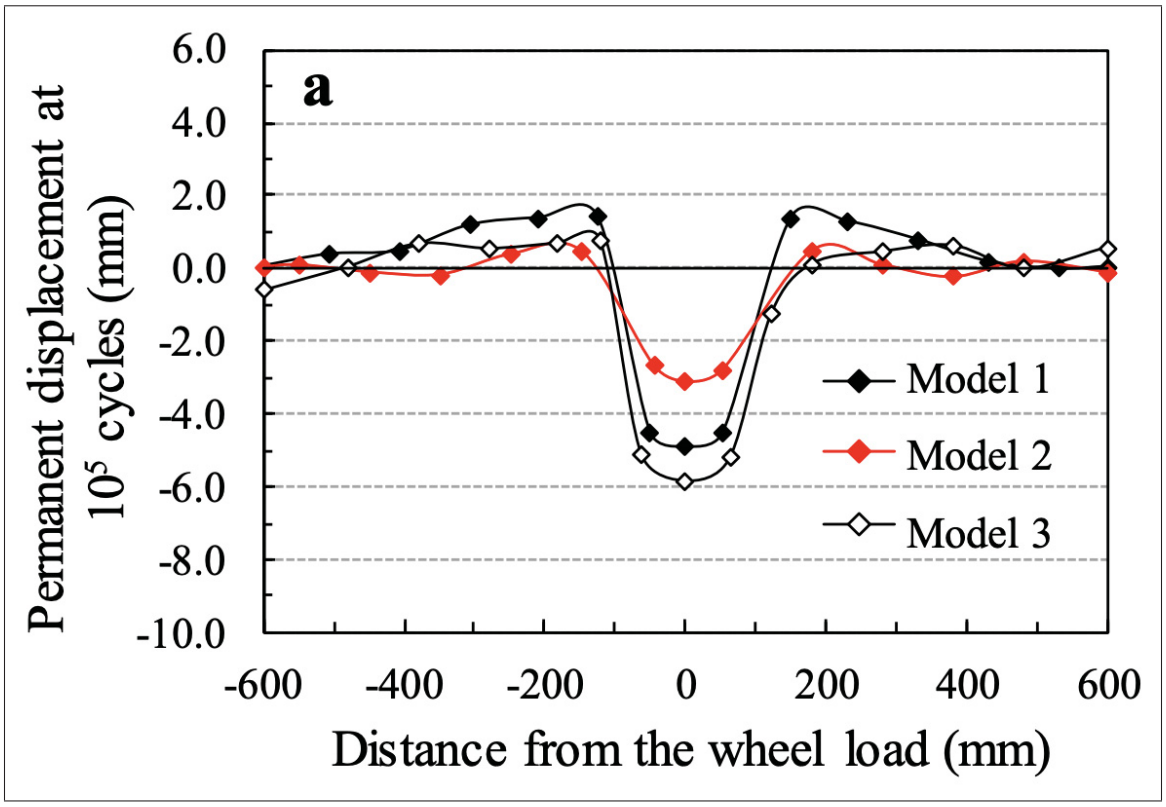

Figure 1.16 Longitudinal permanent deformation
Taken from Correia et al. (2018)

Strain gauges have been used to measure the immediate deformation at the bottom of the surface at different temperatures. The investigation conducted by Youness Berrada and his team in 2021 aimed to study the impact of low-temperature surface cracking on the behaviour of hot-mix asphalt layers under vehicular loads. Five TML strain gauges were implanted in a longitudinal direction underneath the wheel path to collect deformation data before and after the idealized crack at the bottom of the asphalt layer, as illustrated in the plan view shown in Figure 1.18. The results obtained from the TML1, TML2, TML3, TML4 and TML-REF strain gauges at the tested temperature of $16°C$ have been presented in Figure 1.18 (Berraha *et al.*, 2020).

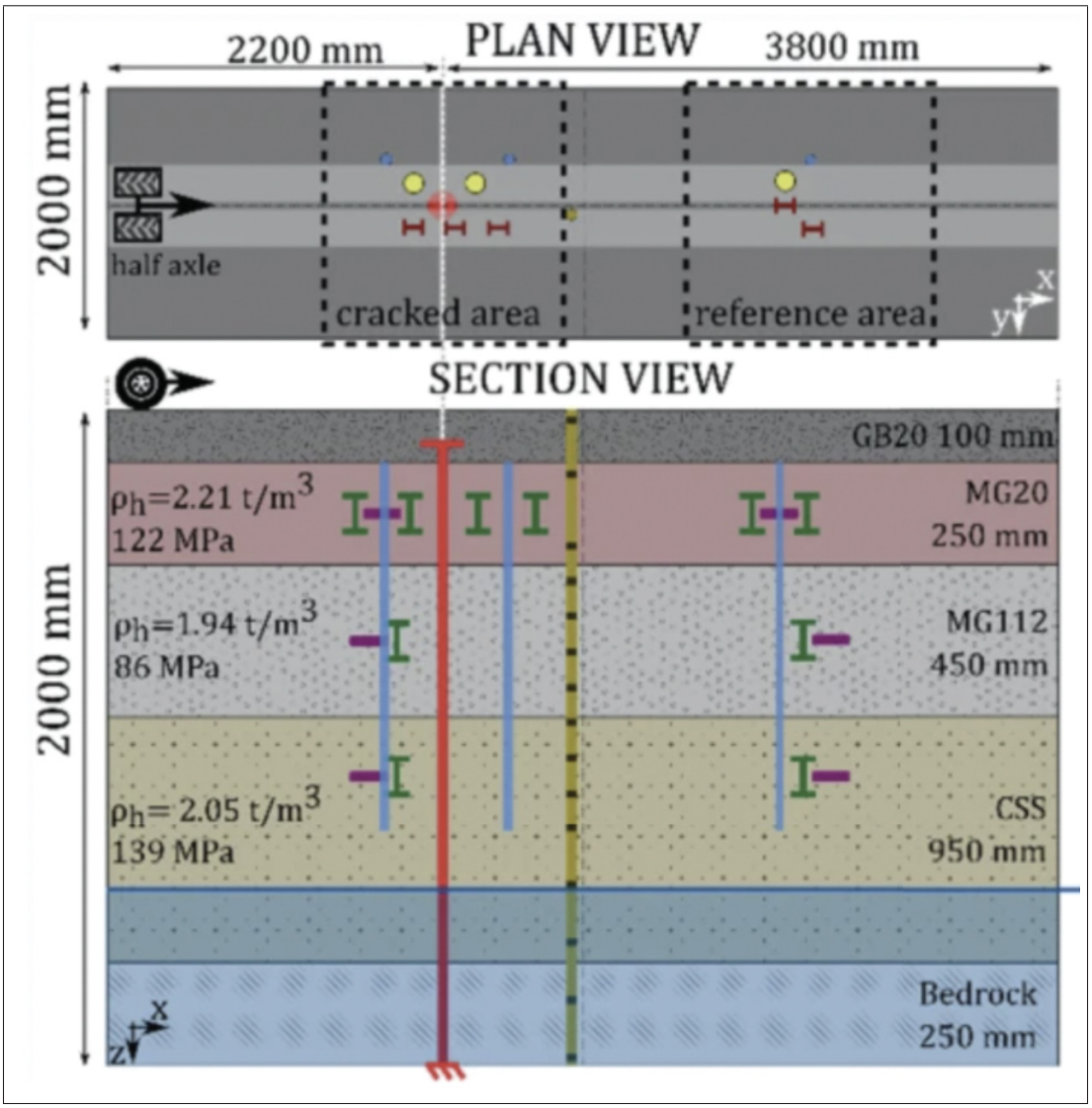

Figure 1.17 Positions of the strain gauges at the bottom of the surface
Taken from Berraha et al. (2020)

1.3.4 Conversion Techniques between Time-Domain and Frequency-Domain Data

Bituminous materials exhibit viscous behavior, which is related to the loss component of the complex modulus in the frequency domain. However, all data measurements related to vehicular loading are time-based. Therefore, to correlate laboratory tests based on mechanical models with field measurements, it is necessary to convert the data between the time domain and

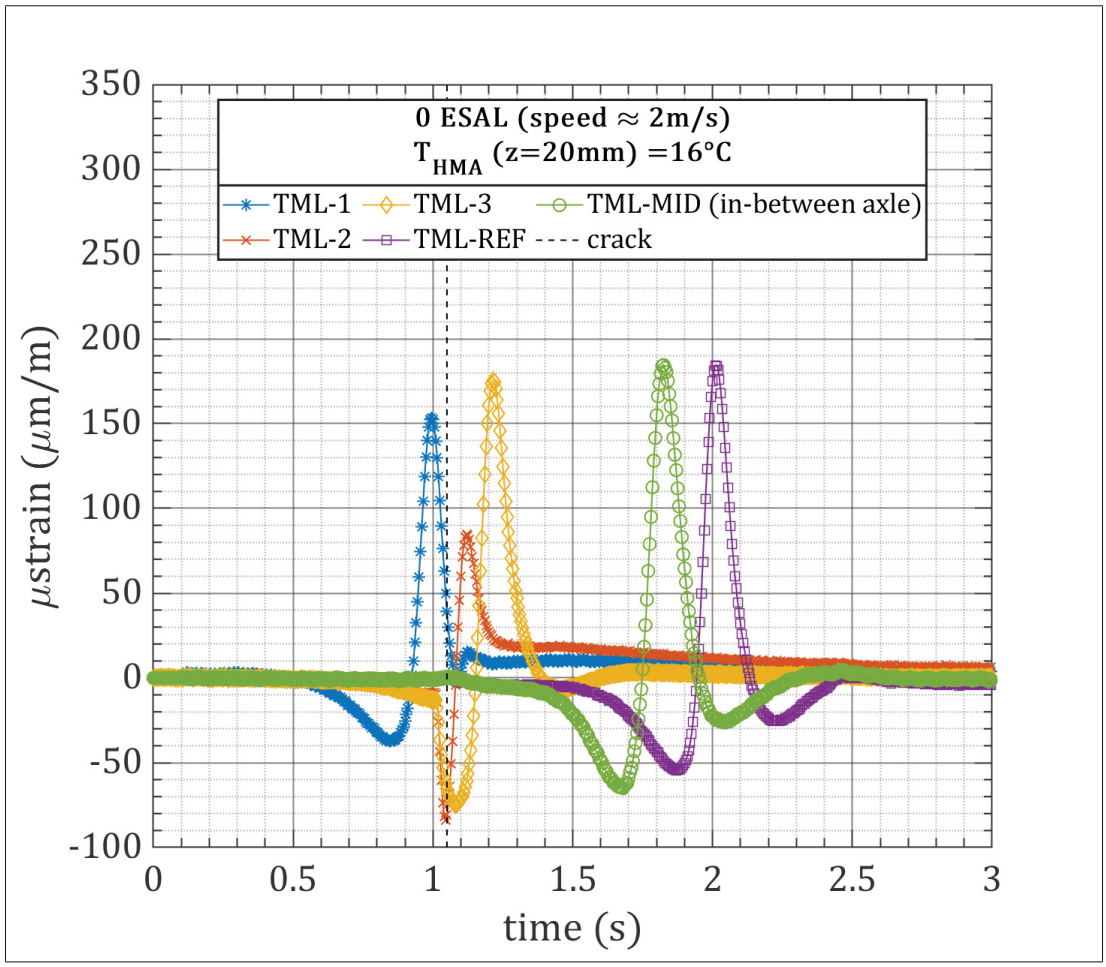

Figure 1.18 TML strain gauges records at 16°*C*
Taken from Berraha et al. (2020)

frequency domain. One approach for this conversion is the Fourier transform, which transforms time-domain data into frequency-domain data. Conversely, the inverse Fourier transform converts frequency-domain data back into time-domain data. Other techniques used for the conversion include the Laplace transform, Z-transform, and wavelet transform. The choice of technique depends on the nature of the data and the desired accuracy of the conversion. It is essential to have a clear understanding of the limitations of each method to ensure that the conversion does not lead to significant errors in the analysis of bituminous material behavior under traffic loading.

The determination of stiffness in asphalt mixes relies on the dynamic modulus instead of the complex modulus, as prescribed by the MEPDG method. Several methods based on rheology have been developed to convert time-domain data to frequency-domain data, with Dongre and colleagues proposing the concept of angular frequency "ω" as the most prevalent approach due to its reduced error rates during the analysis of HMA responses. In accordance with Equation 1.13, the total recording time by the strain gauges (T_t) established by Equation 1.10 as effective loading time at the bottom of asphalt layer can be converted to frequency in (Hz), and frequency can be further converted to angular frequency in (Hz or Radian per second) using Equation 1.14 (D"Angelo, Dongre & Myers, 2006).

$$f = \frac{1}{T_t} \tag{1.13}$$

$$\omega = 2\pi f \tag{1.14}$$

Al-Qadi and his colleagues identified two primary sources of error in the MEPDG method for approximating the frequency to determine the dynamic modulus in their research. The first source of error is the Odemark's method's inability to accurately estimate the loading pulse time, while the second is the inaccurate conversion method used to estimate the angular frequency from the loading pulse time. To overcome these issues, the compressive stress pulse can be used to obtain the equivalent frequency by applying Fast-Fourier Transform (FFT) (Al-Qadi *et al.*, 2008).

1.3.4.1 Fourier Analysis on the Time domain Loading Signals

Fourier analysis provides a pair of transforms between the time and frequency domains. A function of data sets in the time domain, denoted by "$x(t)$" can be transformed to the frequency domain using integral equation 1.15 as a function of frequency intervals ($X(f)$), and the inverse of this operation is represented by equation 1.16. During the 1960s, Cooley and Tukey introduced an algorithm named the Fast-Fourier transform (FFT), designed for efficiently

computing complex Fourier series using machines (Cooley & Tukey, 1965). The FFT analysis is applicable to finite sets of data sampled at discrete time points. Prior to the FFT algorithm, data must be digitized.

$$X(f) = \int_{-\infty}^{+\infty} x(t) e^{-j2\pi ft} dt \tag{1.15}$$

$$x(t) = \int_{-\infty}^{+\infty} X(f) e^{j2\pi ft} df \tag{1.16}$$

The Fast-Fourier Transform (FFT) technique offers a streamlined approach for calculating the Discrete Fourier Transform (DFT), which is a discrete form of the Continuous Fourier Transform. Continuous Fourier Transform is a mathematical tool used to represent a continuous-time signal as a superposition of complex exponential functions with varying magnitudes and phases. It provides a representation of the signal in the frequency domain, showing how much of the signal is made up of different frequencies. Unlike the Continuous Fourier Transform that requires integrating from negative to positive infinity, the DFT is computed by summing a finite set of data points indexed by "n" from "0" to "N-1", as presented in equation 1.17 (Ramirez, 1985). The FFT is particularly useful for computing the DFT of a large number of data points, thereby reducing the computational complexity of the Fourier analysis.

The discrete Fourier transform (DFT) is a computational method that is applied to a finite set of sampled data points. In this context, the frequency domain is also a discrete set of frequencies, with each frequency value being represented by a specific index. Specifically, the k^{th} frequency, denoted as "X_k", corresponds to k/N, where k is the index of the frequency component and N is the total number of samples. The time domain is represented by the sample index n, which corresponds to time t. Therefore, the DFT algorithm enables the conversion of a time-domain signal into a discrete set of frequency components (i.e., spectral analysis) by calculating the summation of the product of each sampled point and a complex exponential function at each frequency value, as shown in equation 1.17 (Ramirez, 1985).

$$X_k = \sum_{n=0}^{N-1} x_n . e^{-j2\pi kn/N} \tag{1.17}$$

The Discrete Fourier Transform (DFT) representing in the equation 1.17 can be expressed in the matrix 1.18, where matrix "X" represents the frequency data points and matrix "x" represents the time-based data. The "ω_n" matrix includes the multiplier factors on the time-based data matrix, which is valued as $\omega_n = e^{-j2\pi k/N}$. By applying the DFT matrix, the data vector "x" with "n" pieces of information is multiplied in the NxN matrix "ω_n". Thus, "n^2" multiplications are required to conduct the DFT matrix multiplication. However, the Fast Fourier Transform (FFT) technique is used to expedite and streamline the calculation process of the DFT by performing the same analysis and producing identical results. The FFT algorithm requires only "$n.\log 2(n)$" operations to perform the necessary calculations, whereas the DFT requires "n^2" operations. It is important to note that for optimal utilization of the FFT algorithm, the quantity of data points utilized in the FFT analysis should be a power of two (2^n).

$$\begin{bmatrix} X_0 \\ X_1 \\ X_2 \\ \vdots \\ X_n \end{bmatrix} = \begin{bmatrix} 1 & 1 & 1 & \dots & 1 \\ 1 & \omega_n & {\omega_n}^2 & \dots & {\omega_n}^{n-1} \\ 1 & {\omega_n}^2 & {\omega_n}^4 & \dots & {\omega_n}^{2(n-1)} \\ \vdots & \vdots & \vdots & \ddots & \vdots \\ 1 & {\omega_n}^{(n-1)} & {\omega_n}^{2(n-1)} & \dots & {\omega_n}^{(n-1)^2} \end{bmatrix} \begin{bmatrix} x_0 \\ x_1 \\ x_2 \\ \vdots \\ x_n \end{bmatrix} \tag{1.18}$$

In 2004, Al-Qadi and colleagues conducted a study to investigate the accuracy of the theory of elasticity in determining the shape and timing of compressive stress pulses in a multi-layered system. To achieve this, they utilized the NonPAS program to determine the compressive stress pulse shapes at different depths and in various road sections. The compressive stresses were calculated for different radial distances at intervals of 1 cm, such that the stress value equaled one percent of the maximum amount. Next, by taking into account the assumed vehicle speed, the compressive stress pulse in the distance domain was transformed into the time domain (Al-Qadi *et al.*, 2008).

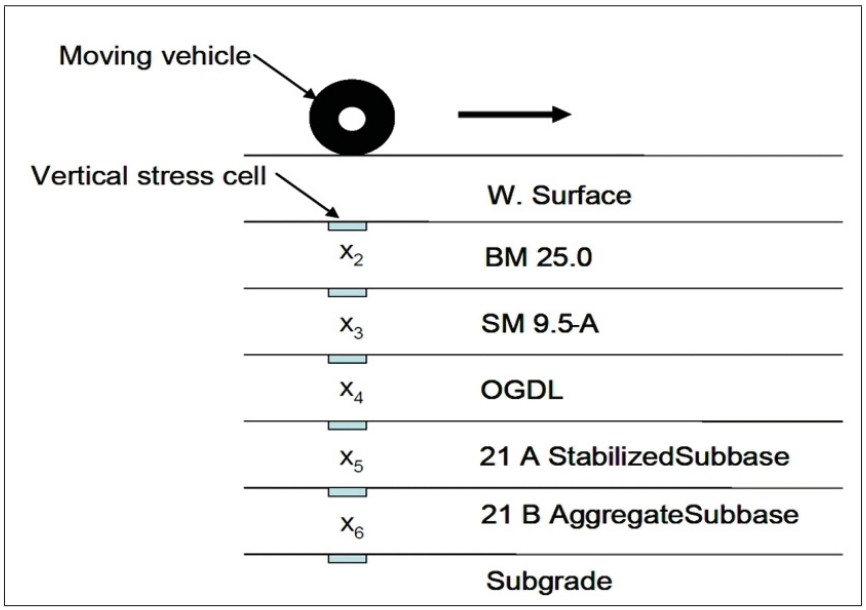

Figure 1.19 Normalized signals providing vertical stress cells in the pavement cross-section of the Virginia roadway Taken from Al-Qadi et al. (2008)

Based on the research conducted by Al-Qadi and colleagues, an amplitude-frequency chart can be generated using the FFT algorithm and equations for each section at various depths and vehicular speeds. The frequency of different speeds can be approximated by applying equation (equation 1.19), which assumes a reference vehicle speed of 100 km/h. Ultimately, the equivalent frequency for the loading pulse can be determined by evaluating the area underneath the amplitude-frequency chart, as depicted in figure 1.20.

$$f_V = 0.01 f_{100} \tag{1.19}$$

The frequency for a vehicular speed of "V" is represented as f_v, while the estimated equivalent frequency for the speed of 100 km/h is represented as f_{100}. This estimation can be achieved by using the equation (1.19), which provides an approximation for the frequency at any given speed. The amplitude-frequency chart, drawn using the FFT algorithm and equations for each section in different depths for all vehicular speeds, provides valuable insight into the frequency

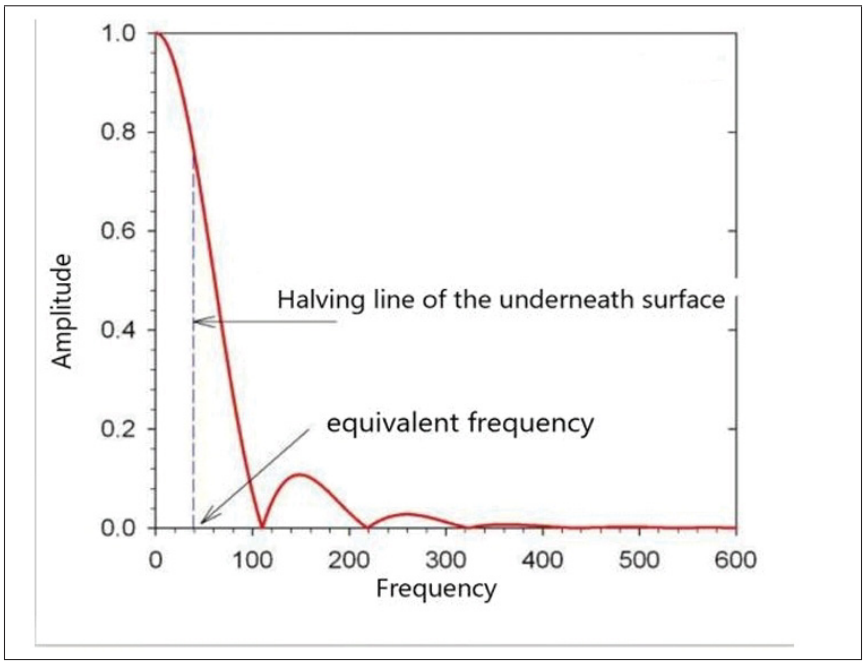

Figure 1.20 The amplitude-frequency chart
Taken from Al-Qadi et al. (2008)

distribution. By measuring the surface underneath this chart, the equivalent frequency for the loading pulse can be accurately determined, as demonstrated in figure 1.20.

In 2019 a study on Frequency-Domain Analysis of Pavement Response was conducted by scholars from Texas A&M University and published in the Journal of Transportation Engineering. The researchers used a high-speed profilometer to collect deformation signals from the bottom of the asphalt layer in time-domain under vehicular loading. Subsequently, the collected data was processed and examined using Fourier analysis in Microsoft Excel to convert the discrete data to their corresponding frequency domain. The researchers used a 2D FE model to replicate the pavement behaviour and confirm their results. The findings indicated that the Fourier analysis technique is an effective and dependable method for transforming pavement deformation signals from the time to frequency domain. Additionally, the study recommended that frequency-domain analysis of pavement response could provide valuable insights into pavement performance and be beneficial in developing more precise pavement design and maintenance strategies (Wang, Chen, Nie, Wang & Shu, 2019).

The study conducted by Yang et al. (Yang, Zhang, Hu & Wei, 2020) aimed to investigate the effects of temperature on asphalt pavement performance by analyzing the deformation signals in different temperature conditions. The authors collected the deformation signals beneath the asphalt layer using strain gauges and then used Fourier analysis to transform the data into the frequency domain. The measured strain amplitudes showed that the pavement's stiffness increased with temperature, and the dominant frequencies of the deformation signals shifted to higher frequencies as the temperature increased. The findings indicated that the Fourier analysis technique is an effective and reliable method for analyzing the effects of temperature on asphalt pavement performance. The study provides valuable insights into the pavement's response to temperature changes, which can be used for developing more accurate pavement design and maintenance strategies.

Rizvi et al. (2019) conducted a study to evaluate the in-situ viscoelastic properties of asphalt concrete using frequency domain analysis. The authors collected pavement deformation signals under vehicular loading using a Falling Weight Deflectometer (FWD) and then transformed the data into the frequency domain using Fourier analysis. The resulting complex modulus of the asphalt concrete increased with frequency, indicating higher stiffness at higher frequencies. In addition, the phase angle of the complex modulus decreased with frequency. The study concluded that frequency domain analysis is a valuable tool for evaluating the in-situ viscoelastic parameters of bituminous material, providing important insights for pavement design and maintenance strategies.

1.4 Methods of Flexible Pavement Design

Professor E.J. initiated the construction of the first asphalt road, paving the way for the evolution of asphalt pavement design through three distinct phases. The first phase, prior to the early 1920s, was characterized by empirical pavement design that lacked an understanding of material mechanics. In the second phase, elastic mechanistic-empirical pavement design, which was widely accepted until the early 1990s, assumed the homogeneity and isotropic linear elasticity of asphalt mixes, despite the viscoelastic behavior of bituminous materials in reality. The third

and current phase of pavement design methods is viscoelastic mechanistic-empirical pavement design, which recognizes the viscoelastic behavior of bituminous materials under dynamic traffic loads and applies viscoelastic theory to account for this behavior (Liao, 2007). The KENPAVE software currently utilized to design flexible and rigid pavements is based on the viscoelastic characteristics of bituminous materials. Furthermore, the OPECC web-based pavement design platform developed by École de Technologie Superieure (ÉTS) is also described in the subsequent sections.

1.4.1 KENPAVE software

Yang H. Huang, at the University of Kentucky, developed KENPAVE, a software with two primary modules: KENLAYER for flexible pavement analysis and KENSLAB for rigid pavement analysis. The software divides each year into a maximum of 12 damage analysis periods, with 12 load groups in each period. KENPAVE is capable of analyzing linear, nonlinear, and viscoelastic material characteristics for each pavement layer. The design life for each load group is determined by summing the damages produced by fatigue, rutting, and overall deformation. KENLAYER's key advantage over other programmes is its ability to solve for linear-elastic, nonlinear-elastic, and viscoelastic material characteristics, as well as perform damage analysis, fatigue damage, and rutting distresses to evaluate pavement design life. The efficacy of KENPAVE has been demonstrated through the incorporation of the software in the pavement management system of various state departments of transportation (Rind, Memon & Qureshi, 2017).

1.4.1.1 KENLAYER computer program

The primary goal of this software is to achieve pavement design life. To accomplish this, KENPAVE calculates the damage caused by fatigue cracking and permanent deformation for each of the 12 months of the year and then aggregates this damage over all 12 load groups. Figure 1.21 depicts an n-layer system in cylindrical coordinates, which is modelled in the KENLAYER software, with the infinite n_{th} layer thickness. The elasticity and Poisson ratio of the i_{th} layer are E_i and ν_i, respectively.

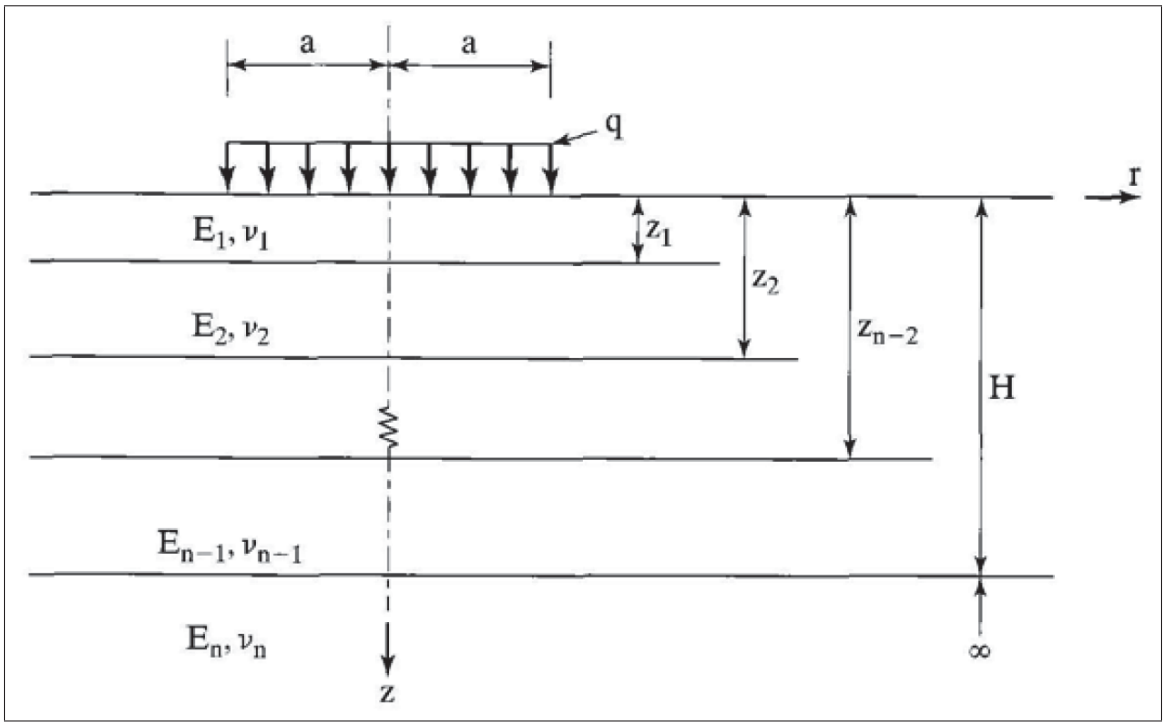

Figure 1.21 Schematic of a modelled n-layer flexible pavement system in KENPAVE
Taken from Huang et al. (2004)

This software employs the Hankel transform method to solve the governing differential equation for axisymmetric elasticity problems, which involves a constant load (q) distributed across a circular contact area of radius (a_c). The stress function for each layer contains four integration constants, except for the bottom layer, which has only two constants. The total number of unknowns in an n-layer system is $4n - 2$, which is determined by two boundary conditions and $4(n - 1)$ continuity requirements. These continuity requirements include vertical stress, vertical displacement, shear stress, and radial displacement continuity at each of the $n - 1$ interfaces, with the continuity of shear stress and radial displacement being replaced by the loss of shear stress both above and below the interface for a frictionless interface (Huang, 2004).

1.4.2 Impact of loading frequency

The calculation of loading frequency can vary depending on the methodology employed, and this can have a substantial effect on the stiffness value used in pavement design. The stiffness of pavement is a crucial input parameter in empirical and mechanical-empirical pavement design. In the case of viscoelastic materials such as bituminous mixes, the frequency of loading is significant, while in the case of granular materials, it does not have any impact. Figure 1.9 illustrates that the modulus values of pavement vary significantly with loading frequency. For instance, the modulus values rise from approximately 3000 MPa at 1 Hz to around 6500 MPa at 10 Hz. Consequently, it is essential to utilize the right loading frequency for pavement design to attain accurate results. These varying values of modulus can be utilized in KENPAVE software to determine stress and strain. If a single layer of asphalt mix is positioned over the subgrade and an Equivalent Single Axle Load (ESAL) is utilized as load, the vertical deformation under the bituminous layer varies from 954 when 3000 MPa is utilized to 654 when 6500 MPa is employed. The difference is nearly 50%, which significantly affects pavement design life. Therefore, it is crucial to accurately estimate the loading frequency while calculating the stiffness value in pavement design.

1.5 Summary

Flexible pavement is the most commonly used road construction, which is designed to distribute traffic loads uniformly throughout all layers from top to bottom. It is composed of asphalt and granular material layers, each having specific characteristics that contribute to the pavement's overall performance. Asphalt layers are stiffer and have higher moduli than granular layers, resulting in them absorbing a greater volume of stresses. As a result, the most significant deformation for design purposes occurs under the lower asphalt layer. This is a crucial design consideration since the ability to predict deformations in the lower asphalt layer accurately will enable pavement designers to evaluate and improve pavement performance.

The complex modulus is a crucial parameter used in the laboratory testing and simulation of bituminous materials to assess their stiffness. Due to its complex nature, the modulus exhibits different behaviour under varying external conditions and does not have a constant value for a given material. Furthermore, the complex modulus is time-dependent since loading speed and weather conditions are time-based. Laboratory tests and mechanical models employed in simulation software rely on evaluating the complex modulus and the behaviour of bituminous materials in the frequency domain. However, converting from the time-domain to the frequency-domain can significantly affect the accuracy and reliability of the results obtained. Therefore, ensuring a proper conversion is imperative for the validity of the findings.

CHAPTER 2

RESEARCH METHODOLOGY

Since the decline of the empirical method before the early 1920s, the design of flexible pavements has progressed to a stage where mechanical models define the viscoelastic behaviour of asphalt in design and simulation techniques by employing mathematical transforms. To enhance the precision of the design methods, researchers have focused on examining changes in the behaviour of asphalt layers under traffic loads in field studies and simulating the behaviour of bituminous materials. In this project, two mathematical approaches have been combined to transform time-domain vehicular loading signals to the frequency-domain, resulting in the development of a tool to estimate the equivalent frequency for traffic loading on the surface of flexible pavements with a high degree of accuracy, using mechanical models and simulation methods.

2.1 Problem statement

In the design process, the material stiffness is a critical characteristic described by the complex modulus in bituminous materials. This modulus is estimated using the 2S2P1D model in laboratory tests, based on the equivalent loading frequency that represents traffic loading parameters and surface temperatures. Vehicular loads distribute in the time domain on top of the surface layer through the wheel path. However, there are few reliable conversion techniques available to accurately measure the acceptable equivalent frequency for actual time-domain loading parameters. In the absence of an alternative method to compute this parameter, the equivalent frequency serves as a reference for the entire repeating loading duration and is considered to be 0.01Hz for parking lots and 10Hz for highways. Inaccuracies in this parameter can result in significant calculation errors in structural response simulations. Therefore, it is essential to follow an initial structure that provides accurate frequency parameters in various situations when designing pavement structures subjected to moving loads.

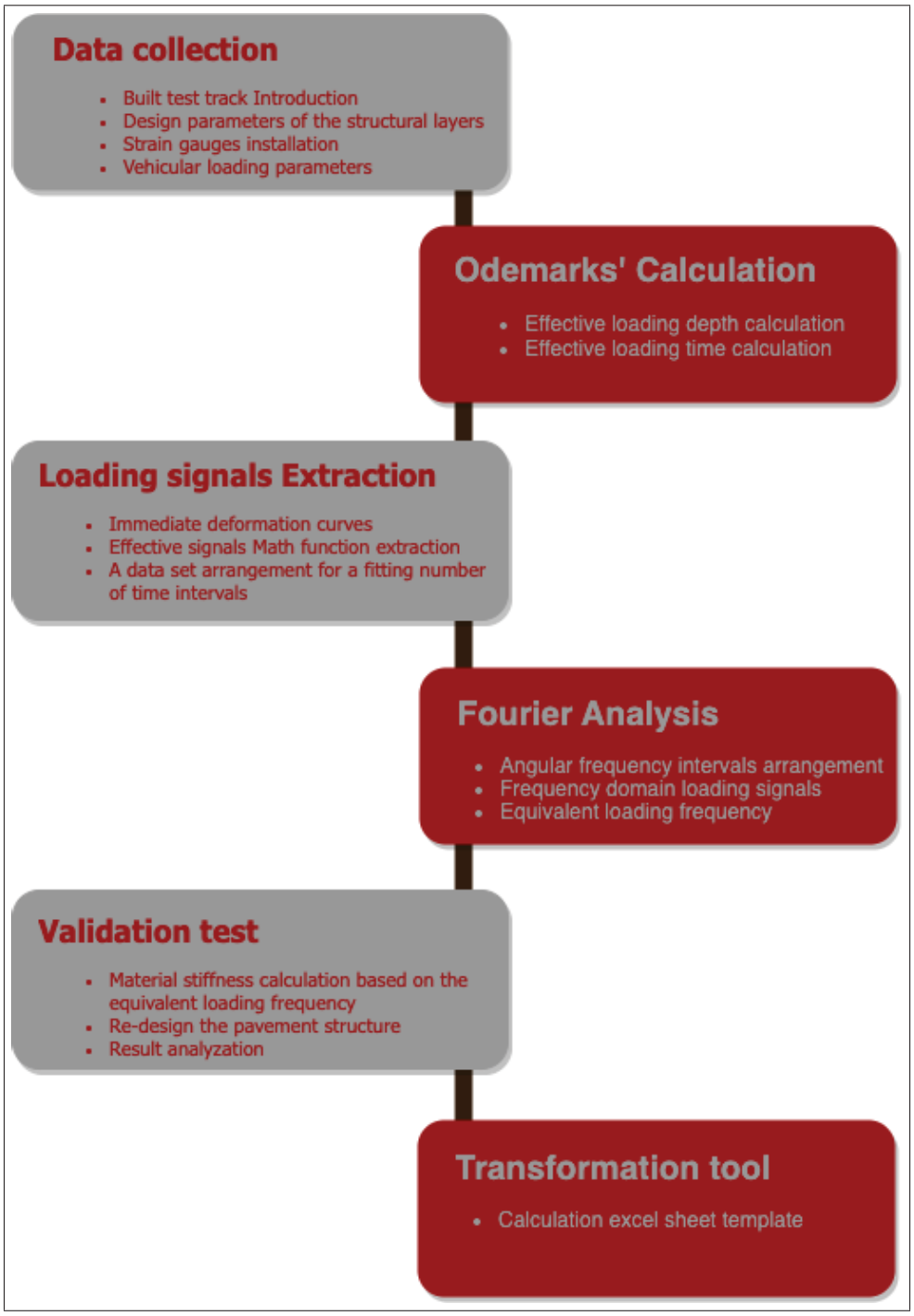

Figure 2.1 Project method's diagram

2.2 Objective

The principal aim of this study is to formulate a conversion tool that enables the computation of the equivalent traffic loading frequency across diverse scenarios. To this end, an additional objective involves an in-depth inquiry into a mathematical procedure for the determination of the equivalent frequency of loading signals. These signals are sourced from strain gauges meticulously positioned at the substrate of an asphalt layer within a specially constructed experimental track. The process is illustrated in Figure 2.1 diagram.

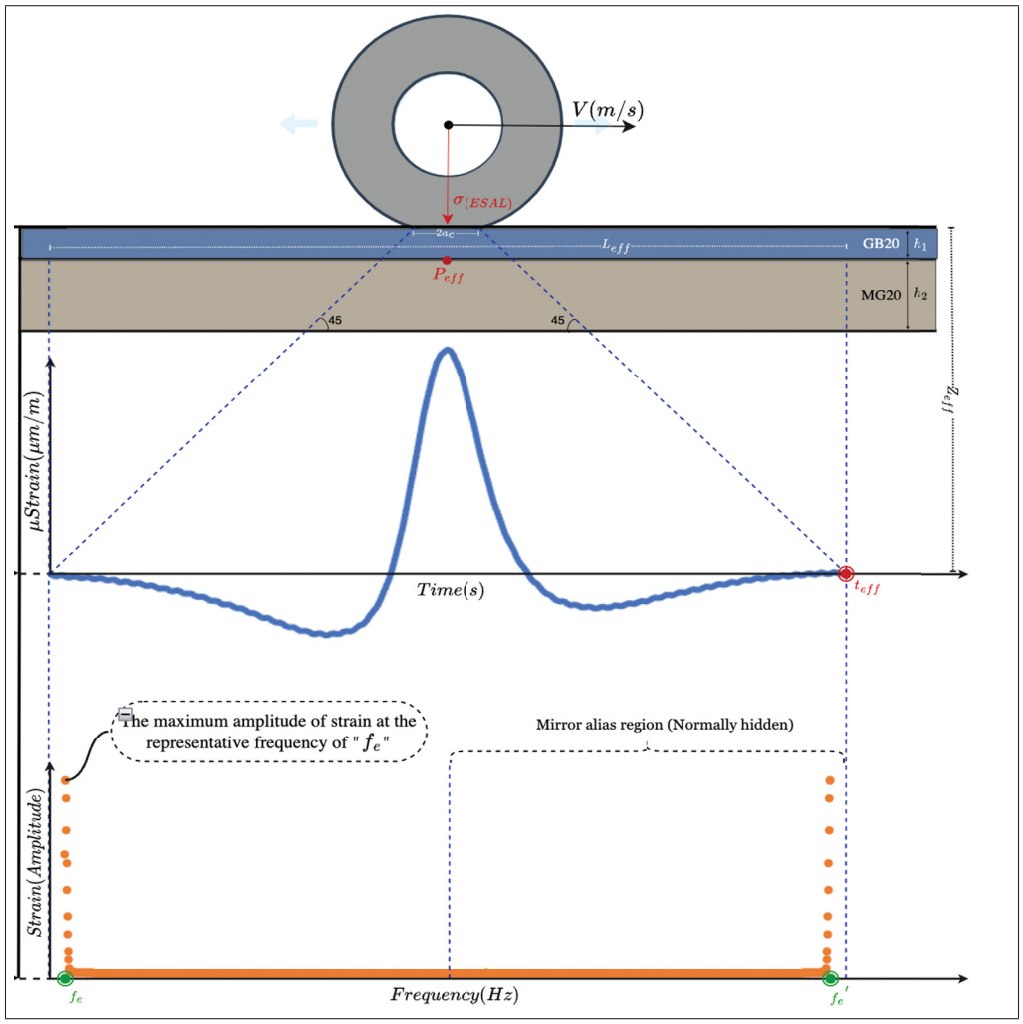

Figure 2.2 Schematic of signals' transformation from the vehicular loading in time domain to the equivalent frequency domain

These gauges record the instantaneous deformation data under vehicle loading and collect them as longitudinal loading signals. The effective loading signals are then extracted from the entire signal range (three seconds) using the Odemark method. To convert the loading signals from time-domain to frequency-domain, Microsoft Excel Fourier analysis is used, but all data points need to be a power of two, which is not always the case. In this study, a modified time interval of 0.0005s is used to reach a proper power of two (2048) and applied to the mathematical function of each signal retrieved through CurveExpert software. The Microsoft Excel Fourier Analysis is then used to transfer the signals from the time domain to the frequency domain for four different temperatures, and the equivalent loading frequency is determined for each temperature. The asphalt layer's stiffness is recalculated based on the equivalent loading frequency to validate the method. The process is repeated to compare the equivalent frequency with the primary loading frequency. A Microsoft Excel calculation tool is developed based on various temperature, vehicular loading, and pavement structural parameters for method validation, which is detailed in Appendix I.

2.3 Data collection

In 2021, Youness Berraha conducted research on the effect of low-temperature surface cracking on hot mixed asphalt layer behavior under vehicular loads. He gathered deformation data using implanted strain gauges, which are also used as a database for this study. The loading system involves equivalent load cycles of 2.43 ESAL and is applied in a one-way wheel path at a speed of 2.0 m/s on the asphalt surface at an expected radius of the circular contact area of 120 mm. The internal test track has a total dimension of 6 m length, 2 m depth, and 2 m breadth.

Table 2.1 2S2P1D parameters for the GB20 mix layer produced in Quebec
Taken from Berraha et al. (2020)

$E_\infty(Mpa)$	$E_0(Mpa)$	K	H	δ	τ_E	β
25	41000	0.17	0.56	2.25	1.5	400

In the plan view depicted in Figure 2.3, the 6-meter-long track is divided into two main areas of interest: the reference area, which represents the original pavement structure, and the cracked area, which includes an idealized transverse crack. The GB20 asphalt mix, manufactured in Québec, was the single asphalt layer utilized in the study, and the 2S2P1D parameters were applied to simulate the complex modulus of a typical HMA GB20. These parameters are detailed in Table 2.1 (Berraha *et al.*, 2020).

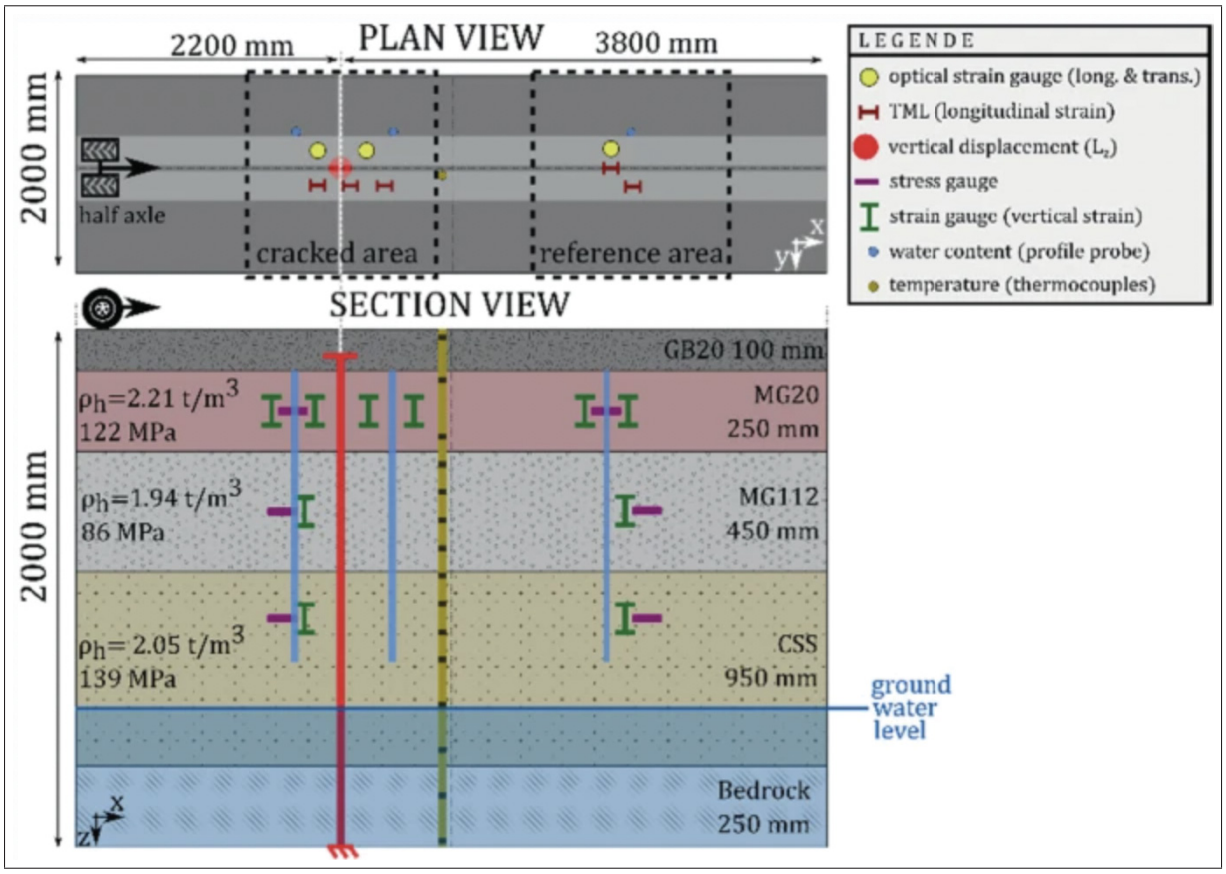

Figure 2.3 Plan and side view of the indoor test structure track
Taken from Berraha et al. (2020)

Figure 2.4 depicts the placement of five H-beam longitudinal strain gauges on the top of the MG20 layer and beneath the GB20 asphalt layer at 100 mm depth, in different positions. Among them, TML-1, 2, 3, and TML-REF are situated under the wheel path, while TML-MID is positioned between the wheel tracks. The purpose of TML-MID is to measure the longitudinal deformation under wheel path while ignoring the influence of the interface.

This study utilized deformation data collected by three H-beam longitudinal strain gauges: TML-1, TML-2, and TML-REF, which were strategically installed to measure longitudinal deformation at different positions along the asphalt layer. The TML-1 and TML-2 were placed before and immediately after the idealized crack, respectively, while TML-REF was placed far after the crack. The collected deformation data was then utilized for the computations in this

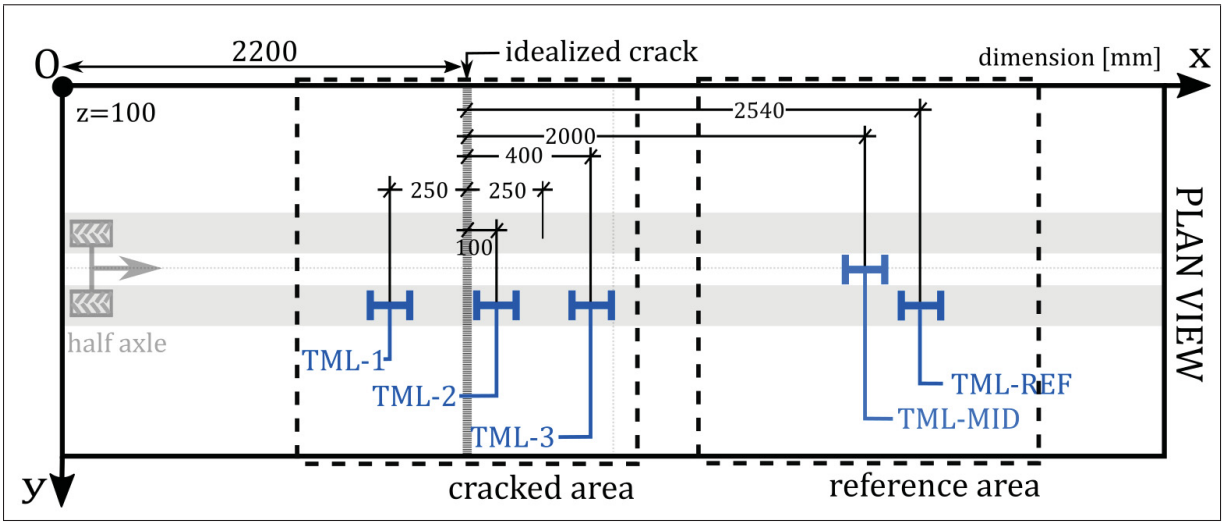

Figure 2.4 Plan view of the position of the strain gauges on top of sub-grade
Taken from Berraha et al. (2020)

study. The data was gathered at four distinct internal asphalt layer temperatures, which were -8, 6, 16, and 20 $^{\circ}C$.

Figure 2.5 displays the longitudinal deformation data obtained by TML-REF at a temperature of 6 $^{\circ}C$. The strain diagram, plotted using strain gauges, illustrates the maximum longitudinal tension (ε_t) at the effective point, which is when the wheel is precisely positioned on top of the effective point (p_{eff}), and the maximum longitudinal pressure before the effective point occurs in the loading area (ε_{cd}) and the unloading area (ε_{ca}). The tension peak of the strain diagram is located in the centre of the total loading period, which is divided into loading period ($T_{loading} = t_{eff}/2$) and unloading period ($T_{unloading} = t_{eff}/2$), when the delay response time of the asphalt layer is disregarded. Consequently, only the time (not the deformation types) between the beginning of the loading area (t_1) and the end of the unloading area (t_2) are considered effective loading time ($t_{eff} = t_1 - t_2$).

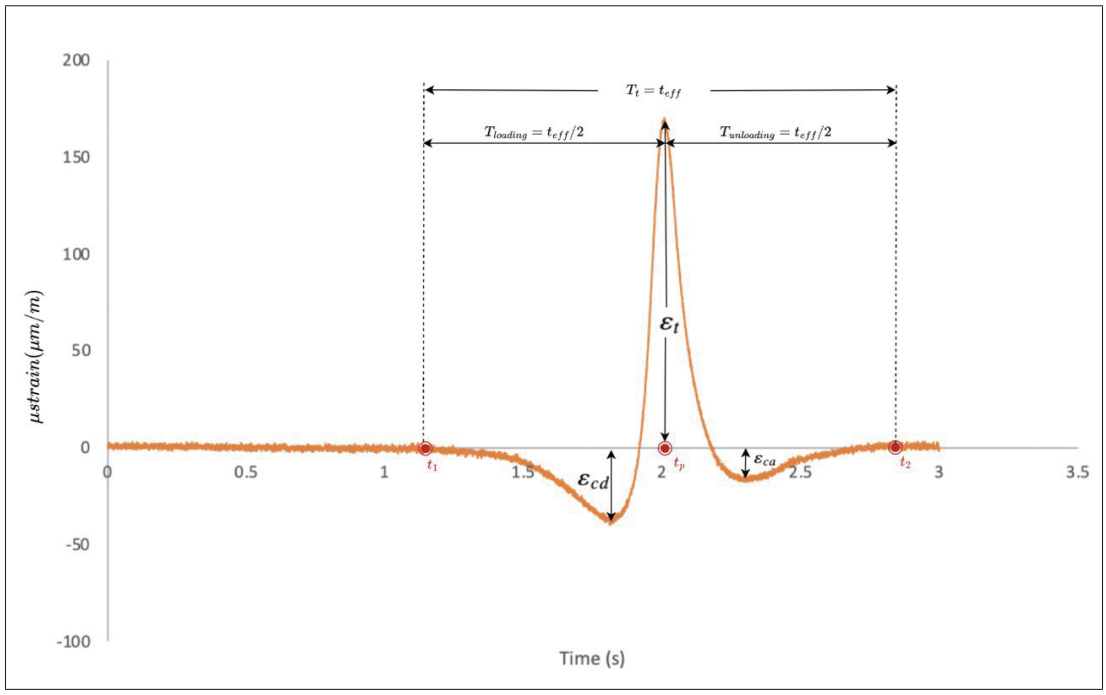

Figure 2.5 Longitudinal deformation fluctuation at the bottom of the HMA layer under the vehicle passage

2.4 Estimation of the effective loading time

In estimating the effective loading time, it is important to note that this period varies across the depth of the asphalt layer due to its stiffness. Hence, the effective loading time beneath the asphalt layer is not equivalent to the time taken for the vehicle tire to press any point on the surface. To account for this, the Odemark technique is utilized to transform the thickness of the asphalt layer (h_1) into the effective depth (Z_{eff}) using equation 1.12. The effective loading length ($L_{eff}(m)$) can be calculated using the $45°C$ trapezoidal model (Figure 1.13), which considers the effective depth and the length of the tire's contact area. Subsequently, the effective loading time (t_{eff}) is estimated using equation 1.10.

Based on the Odemark method, the analysis of the test track in this study requires consideration of the stiffness and depth of the first two layers in order to calculate the effective depth (Z_{eff}) accurately. As per (Diffiné, 2012) study, for the ALIZÉ simulation, the dynamic modulus of

the GB20 mixture layer is evaluated at 22000 (Mpa) with a loading frequency of 30 (Hz) and a temperature of 5°C. In this project, the loading frequency is assumed as an initial value of 1 Hz for the vehicular speed of 2 (m/s) at the bottom of the asphalt layer to start the conversion process. This will estimate the GB20 layer's stiffness based on 2S2P1D model, at the recording temperatures of -8, 6, 16, and 20 °C, as presented in Table 2.2. The stiffness for each temperature is extracted from the 2S2P1D calculation as presented in figure 2.6 and 2.7 by the red circles.

.

Table 2.2 The Odemarks' parameters of the first two layers.

GB20 (Asphalt layer)					MG20 (Subgrade layer)	
$\|E^*\|(Mpa)$, $-8°C$	$\|E^*\|(Mpa)$, $6°C$	$\|E^*\|(Mpa)$, $16°C$	$\|E^*\|(Mpa)$, $20°C$	$h_1(mm)$	$E(Mpa)$	$h_2(mm)$
23578	13660	7055	4924	100	122	250

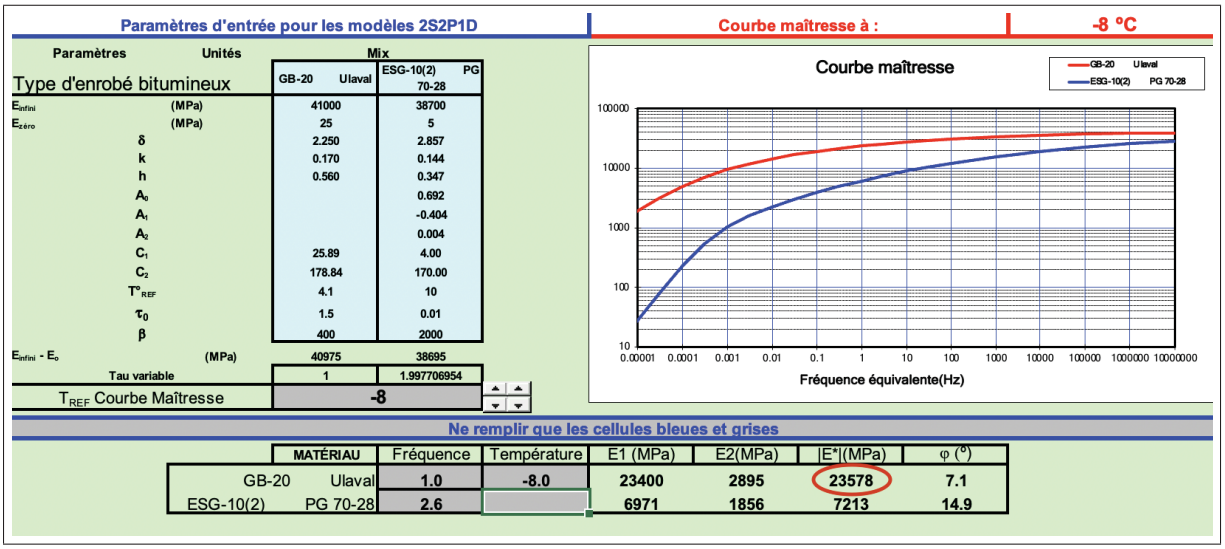

Figure 2.6 Dynamic modulus of GB20 layer for the loading frequency of 1 Hz at -8°C

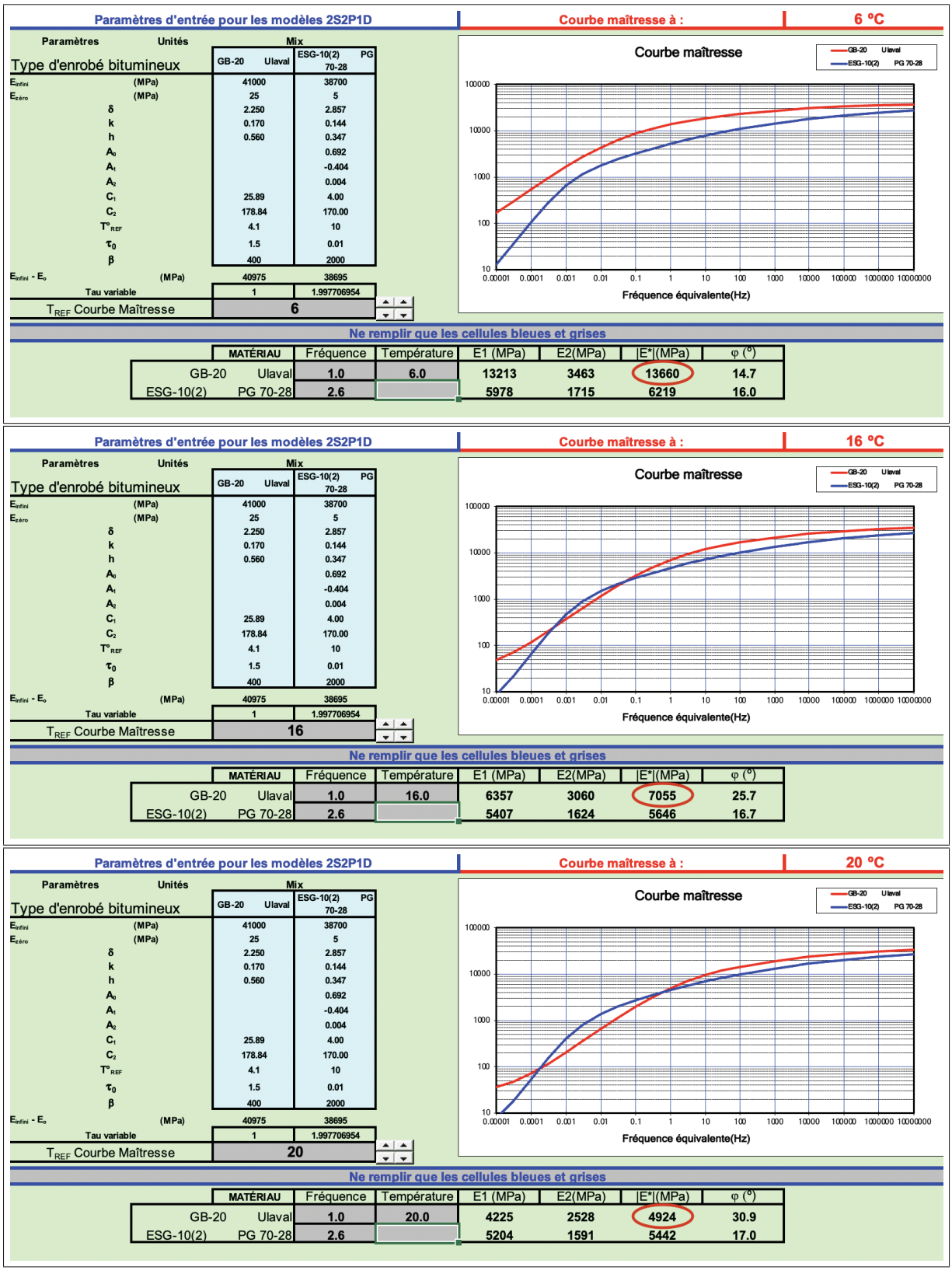

Figure 2.7 Dynamic modulus of GB20 layer for the loading frequency of 1 Hz at 6,16 and 20°C

2.5 Analysis of Longitudinal Loading Signals Under the Wheel Path Using Recorded Data

The longitudinal deformation of asphalt pavement under the wheel path is a crucial factor in pavement performance assessment. In this study, digital discrete data points were recorded by strain gauges every 0.0005 seconds to capture the immediate deformation response. A primary database table was created to store the recorded data over the full wheel passage period of 3 seconds at four different temperatures (-8, 6, 16 and 20$°C$) corresponding to different weather conditions. The deformation data points were represented by a set of numbers from 0 to 5999, reflecting the time interval at which the data was recorded. The total loading signals were obtained by plotting the deformation data for each strain gauge at each temperature, resulting in a total of 12 signals. The recorded data and total loading signals were analyzed to gain insight into the pavement's response to vehicular loading. The figure 2.8 shows all 12 recorded strain gauge signals under the whole vehicle passage.

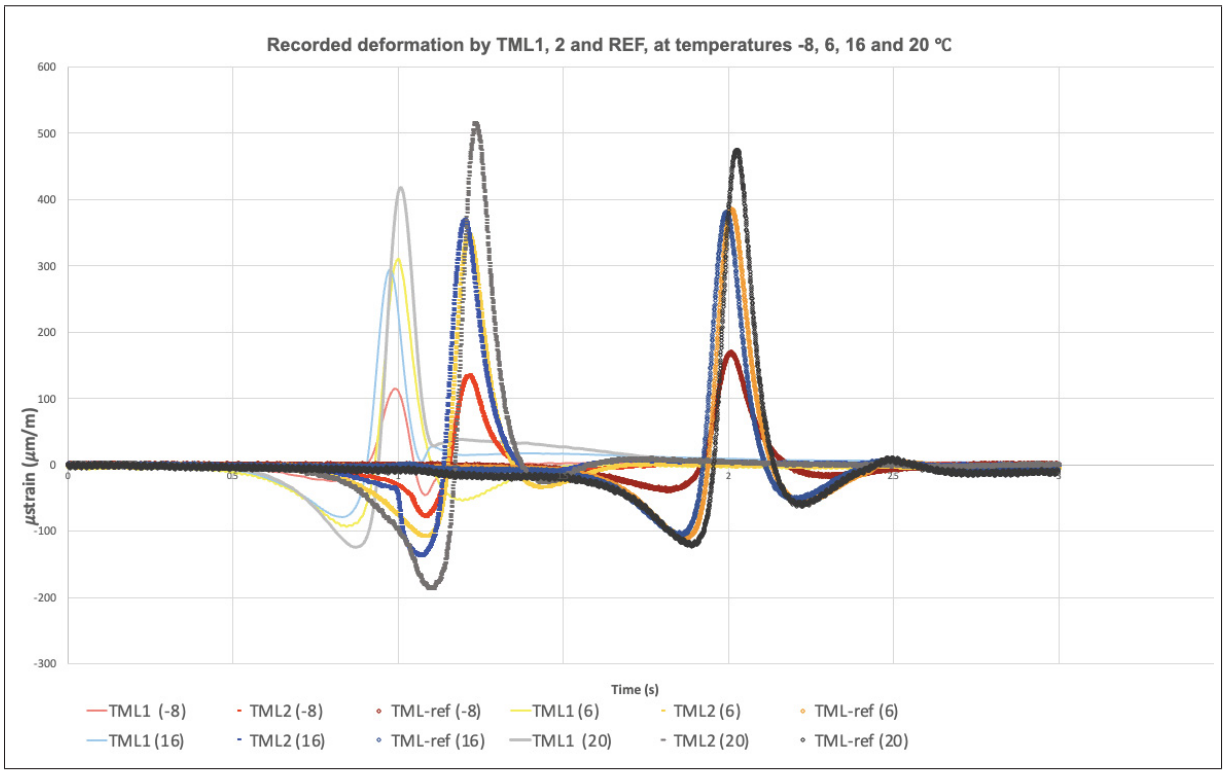

Figure 2.8 All 12 recorded strain gauges signals under the whole vehicle passage

2.5.1 Extracting Effective Loading Signals from Longitudinal Deformation Data Recorded by Strain Gauges

To accurately determine the equivalent loading frequency for each collected data, it is essential to extract the effective loading signals from the total signals, which refers to the maximum deformation values recorded by the strain gauges from the beginning of loading to the end of unloading point. This can be achieved by using the "ADDRESS(MATCH(MAX()))" function in Microsoft Excel on each column in the primary database table, which technically isolates the effective loading signals for each temperature. The effective loading time (t_{eff}) is determined by the time factor representing the peak (t_p) when the centre of the wheel contact area is located precisely on top of the strain gauges, as shown in Figure 2.5. The number of effective loading signals' cells can be calculated using equation 2.1, and subsequently, $\frac{N_{eff}}{2}$ cells before and after the signals' peak are chosen to be extracted. The extracted cells are arranged in the effective

deformation table, where each signal represents the recorded deformation in a time range of 0 to t_{eff} for each temperature and TML strain gauge, by intervals of $\Delta t = 0.0005$.

$$N_{eff} = \frac{t_{eff}}{\Delta t} + 1 \tag{2.1}$$

2.5.2 Optimizing cell numbers of loading signals to powers of two

As highlighted in section 1.4.4, the Fourier transform is only applicable to signals' data points generated with a number of samples that are a power of two. However, the effective loading signals obtained from the strain gauge readings in this study are generated at intervals of 0.0005s, which results in different numbers of data points for the effective loading signals at different temperatures, without necessarily being a power of two. To address this, the number of data points of the effective loading signals is fixed to the nearest power of two. This is achieved by finding the nearest power of two to the original cell numbers of the signals, and then adjusting the time interval accordingly. The modified time interval ($\Delta t'$) for each signal is computed using equation 2.2, which takes into account the effective loading time (t_{eff}) of each signal.

$$\Delta t' = \frac{t_{eff}}{N' - 1} \tag{2.2}$$

To apply the Fourier transform to the effective loading signals, it is necessary to find the mathematical function that accurately represents each signal. This mathematical representation is used to calculate the modified time factors (t_n), which are determined based on the effective loading time (t_{eff}) for each signal. This enables the modified time factors to be calculated as $t_n = n.\Delta t'$, where n ranges from 0 to $N' - 1$, where N' is the closest power of two to the number of data points in each signal. By resetting the effective loading signals to a fixed power of two number of time factors, it is possible to apply the Fourier transform to each signal with the appropriate resolution and accuracy.

2.5.2.1 Mathematical Function Estimation of the Effective Loading Signals

For the purpose of this project, the software called CurveExpert Professional 2.7.3 has been utilized to obtain the mathematical functions that accurately represent the effective loading signals for each temperature. CurveExpert is a widely-used cross-platform software that specializes in curve fitting and data analysis. It offers a range of powerful tools including smoothing techniques, spline types, and both nonlinear and linear regression models to facilitate the process of modeling data (Hyams, 2011). By utilizing this software, we can efficiently and effectively find the most suitable mathematical functions that represent the effective loading signals for each temperature.

Figure 2.9 demonstrates that there are various regression models that can be used to fit the curve and generate different constant coefficients. In this research, the Rational Model is selected as the most suitable curve function to approximate the effective loading signals accurately. The mathematical functions of the selected Rational Model for each signal are employed on their modified time factors (x parameters) to calculate the modified deformation values (y parameters). Therefore, the four reference effective signals are adjusted and graphed in power of two points. This approach allows for a more precise analysis of the signals, which is necessary for accurate results. It should be noted that the Rational Model is one of the commonly used regression models in curve fitting due to its simplicity and ability to capture both the linear and nonlinear behavior of the data.

2.5.3 Converting the effective loading signals to the frequency domain by using Fourier analysis

To analyze the effective loading signals in the frequency domain, a Fourier transform is used. However, as mentioned in the previous section, the effective loading signals are modified to have a fixed number of time factors that is a power of two. Therefore, in order to create the transformed table to present the equivalent frequency signals, the angular frequency interval $\Delta\omega$ must first be calculated for each signal. This is done by using equation 2.3, which determines the angular frequency factors for each effective loading time. The resulting angular frequency factors (ω_k)

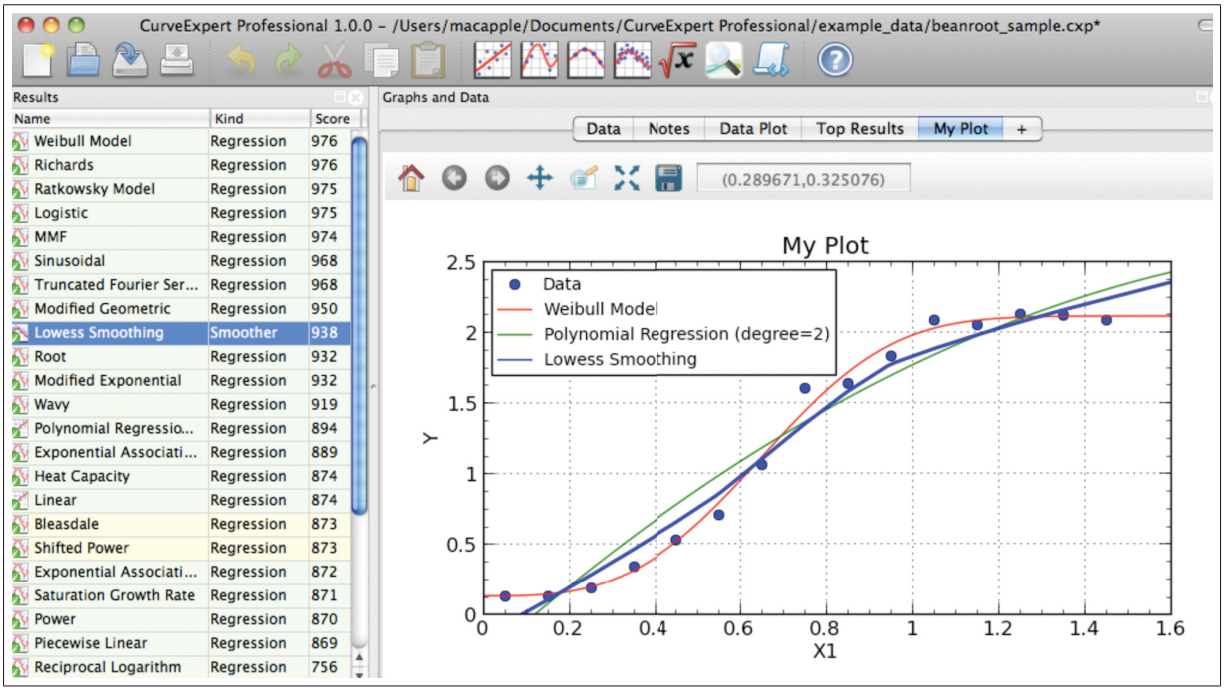

Figure 2.9 An example of curve fitting function of the CurveExpert tool
Taken from Hyams et al. (2011)

are calculated as $(k.\Delta\omega)$, where (ω_k) ranges from 0 to ω_{max}, which is the maximum angular frequency that can be represented based on the Nyquist criterion. These angular frequency factors are then set in the angular frequency columns for each signal in the transformed table, which is used to analyze the signals in the frequency domain.

$$\Delta\omega = 2\pi\Delta f = \frac{2\pi}{N'\Delta t'} \tag{2.3}$$

The sampling rate of a signal imposes a limit on the highest frequency that can be represented in the signal, which is known as the Nyquist frequency. Robert W. Ramirez has stated that the Nyquist frequency is equal to $1/2\Delta t$ for a fixed signal's time interval. Thus, equation 2.4 is used to calculate the maximum allowable angular frequency for each signal, where the coefficient "k" ranges from 0 to $(N'/2) - 1$. This equation ensures that the frequencies beyond the Nyquist frequency are excluded to avoid aliasing in the frequency domain.

$$\omega_{max} = \frac{\pi}{\Delta t'} \tag{2.4}$$

The deformation data obtained by applying the math functions of each signal are prepared to be transformed to the frequency domain using Fourier analysis. The conversion involves selecting the column of adjusted deformation cells, which are then transformed to the strain amplitude column of the frequency domain table. This transformation is achieved by applying the Fourier analysis, which is a Microsoft Excel add-in function. The process of the Fourier data analysis is illustrated in Figure 2.10 ($Data > DataAnalysis > FourierAnalysis > inputrange - outputrange$). The resulting output is a column of N' sets of complex numbers, each comprising a real part and an imaginary part. To refine the complex values of the strain amplitude columns to real numbers, the "IMABS" function is applied. The "IMABS" function is a built-in function in Microsoft Excel that returns the absolute value (modulus) of a complex number. The frequency loading signals are then presented for the determined temperatures, based on the angular frequency factors ranging from 0 to ω_{max} and their corresponding representing strain amplitude.

2.5.3.1 Determining the Equivalent frequency for the Loading Signals

In this project, the angular frequency factor of the strain curves' peak is considered as the equivalent loading frequency for each effective loading signal. The frequency domain signals are obtained by using 1024 points with different angular frequency intervals due to the viscoelastic behaviour of bituminous material at different temperatures. In order to improve the accuracy in determining the X and Y factors for the signal peaks, a mathematical proportionality is applied to adjust the two biggest amplitude values. This results in the provision of equivalent frequency values in Rad/s and Hz in the equivalent loading frequency table for each effective loading signal. In order to determine the equivalent frequency of the loading signals at various effective loading times, a mathematical function is derived by performing a three-degree polynomial regression on the equivalent angular frequency values by using the CurveExpert software.

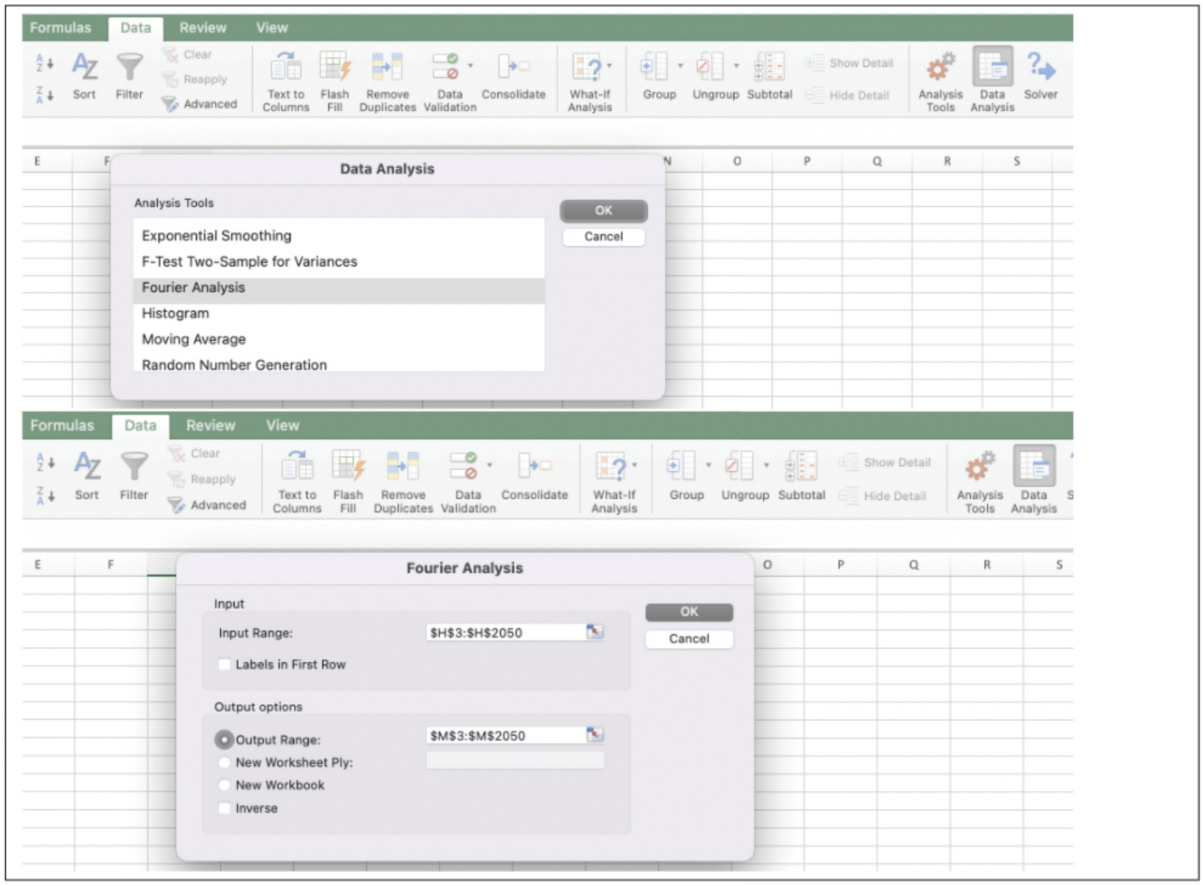

Figure 2.10 Application of the Fourier Analysis in Microsoft Excel

2.6 The equivalent loading frequency validation

In order to validate the conversion tool developed in this study, the equivalent frequency values obtained for each signal's effective loading time need to be tested. To do this, the estimated equivalent frequencies are used as initial loading frequencies in the 2S2P1D mechanical model for each testing temperature, resulting in a new dynamic modulus. This new modulus is then used to recalculate the effective loading time in the Odemark method, leading to rectified equivalent loading frequencies. This process is repeated until an acceptable level of matching is achieved between the equivalent loading frequencies and the initial loading frequencies. It should be noted that the GB20 ULAVAL stiffness calculation method considers a reference temperature of

15°C. Figure **??** illustrates the approximate stiffness provided in MPa for each initial frequency input in Hz and surface temperature in °C, based on the 2S2P1D mechanical model.

2.7 Development of a Conversion Method to transform Loading Signals to the Frequency Domain

Validation tests are utilized to obtain accurate equivalent loading frequency by replacing the initial loading frequency with the calculated equivalent loading frequencies. In this study, the equivalent loading frequency values are computed and validated for moving loads with a speed of 2 (m/s) on top of a single asphalt layer of GB20 mixture at -8, 6, 16 and 20 °C. The resulted equivalent loading frequencies are unique to different loading parameters, such as vehicular loading speed, temperature and material stiffness, which consequently affect the effective loading time (t_{eff}) at the bottom of the asphalt layer. It can be inferred that each equivalent loading frequency is specific to each effective loading time calculated based on the loading and material parameters. The CurveExpert software is used to apply a three-degree polynomial regression to the resulted equivalent frequencies for each effective loading time to find the conversion curve for extracting the equivalent frequency.

To calculate the equivalent loading frequency for every effective loading time, a three-phased mathematical conversion tool is developed in Microsoft Excel. This conversion tool includes the use of the 2S2P1D mechanical model to calculate the material stiffness, Odemarks' calculation to determine the effective loading time for loading and pavement parameters, and the conversion curve function to find the equivalent loading frequency. The developed conversion tool is explained in detail in the APPENDIX chapter.

CHAPTER 3

RESULTS AND DISCUSSION

This research aims to improve the accuracy of vehicular loading calculations on flexible pavements by developing a method to convert loading signals from the time domain to the equivalent angular frequency parameter in the frequency domain. The conversion of loading signals is crucial in achieving accurate loading calculations with higher precision. In this chapter, a detailed description of the methodology used in the research is presented, including an illustration and explanation of the results for each phase. The final equivalent angular frequency charts are created using data collected from strain gauges in the field study. The outcome of this project is the development of a calculation tool that computes the equivalent loading frequency, which is made available in the appendix.

3.1 Strain gauges records

The present study utilizes the immediate deformation data obtained from three strain gauges, namely TML1, TML2, and TML-REF, which were placed at the bottom of the asphalt layer of the ULAVAL test track at various locations, as the primary data source for calculations. These records encompass the strain values for each time factor, every 0.0005 second of the entire wheel path on the surface, from 0 to 3 seconds, which constitutes the complete duration of the vehicle's motion. Notably, the strain values differ for each time factor, depending on the location of the strain gauges and the ambient temperature during testing. All data were compiled in a Microsoft Excel sheet and organized into a primary database table in the time domain. Subsequently, the data were plotted, yielding the 12 loading signals for each strain gauge under varying test temperatures, as depicted in Figure 3.1.

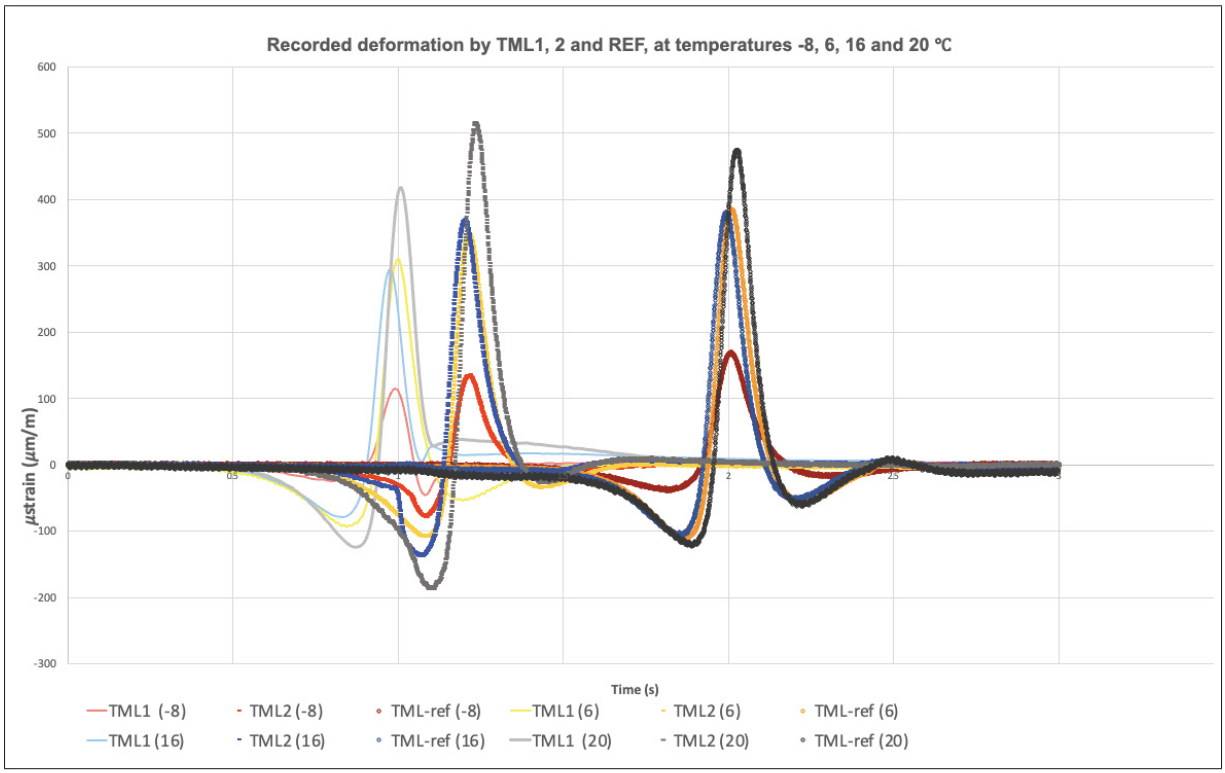

Figure 3.1 All 12 recorded strain gauges signals under the whole vehicle passage

The initiation of loading for each signal is contingent on their longitudinal distance from the initial position of the vehicle, resulting in temporal variations among them. The maximum deformation value of these signals is highly dependent on the temperature of the GB20 layer, with the highest deformation recorded at $20°C$, as evidenced by the grey-colored curves. Conversely, the red curves indicate deformation signals at -8$°C$, with the lowest deformation amplitude peak under the moving load. To determine the effective loading signals, it is necessary to calculate the effective loading time for each test temperature and subsequently extract the deformation variation range of each signal. At reduced temperatures, the asphalt layer demonstrates increased stiffness when contrasted with elevated temperatures. Consequently, the visual assessment indicates an extended period of effective loading experienced during the testing at -8 degrees Celsius compared to the wavelength observed at 20 degrees Celsius. Furthermore, the strain gauges register more substantial peak deformation values at higher temperature levels.

3.2 The results of Odemarks' method

To initiate the conversion of loading signals to their corresponding frequency domain, it is essential to determine the effective loading time from the complete loading signals that are measured using the strain gauges. Although an estimate of the effective loading time can be obtained visually from the overall signals, a more precise effective loading time is required for each temperature condition. Therefore, the Odemark method is employed in conjunction with the design specifications of the asphalt (GB20) and subgrade (MG20) layers of the test track to obtain an accurate determination of the effective loading time. The Odemarks' method was employed to determine the effective loading depth (Z_{eff}) for the effective loading signals based on the the Tyre contact area radius ($a_c = 120mm$), vehicle speed ($V_c = 2(m/s)$) and the structural parameters provided in table 3.1. Subsequently, the effective loading length (L_{eff}) was calculated based on the obtained depth, as illustrated in Figure 1.13 and presented in the second and third rows of Table 3.2. Finally, dividing the effective length by the velocity of the vehicle enabled the derivation of the effective loading times (t_{eff}) for each temperature, which are provided in the last row of Table 3.2.

.

Table 3.1 The Odemarks' parameters of the first two layers.

GB20 (Asphalt layer)					MG20 (Subgrade layer)	
$\|E^*\|(Mpa)$, $-8°C$	$\|E^*\|(Mpa)$, $6°C$	$\|E^*\|(Mpa)$, $16°C$	$\|E^*\|(Mpa)$, $20°C$	$h_1(mm)$	$E(Mpa)$	$h_2(mm)$
23578	13660	7055	4924	100	122	250

Table 3.2 The Odemarks' results of the effective loading time calculation.

Test Temperatures T_{eff}	$-8°C$	$6°C$	$16°C$	$20°C$
Effective Depth Z_{eff} (mm)	1078.16	981.98	886.70	843.1
Effective Length L_{eff} (mm)	2396.32	2203.96	2013.40	1926.03
Effective Time t_{eff} (s)	1.2	1.1	1	0.96

3.3 Effective loading signals

The effective loading signals underneath the wheel path were extracted from the entirety of the strain gauge data and are illustrated in four charts as presented in Figure 3.2 and 3.3. These charts depict the effective loading signals throughout the effective loading time (t_{eff}), spanning from the initiation of the loading period until the completion of the unloading time, as recorded by the TML1, TML2, and TML-REF.

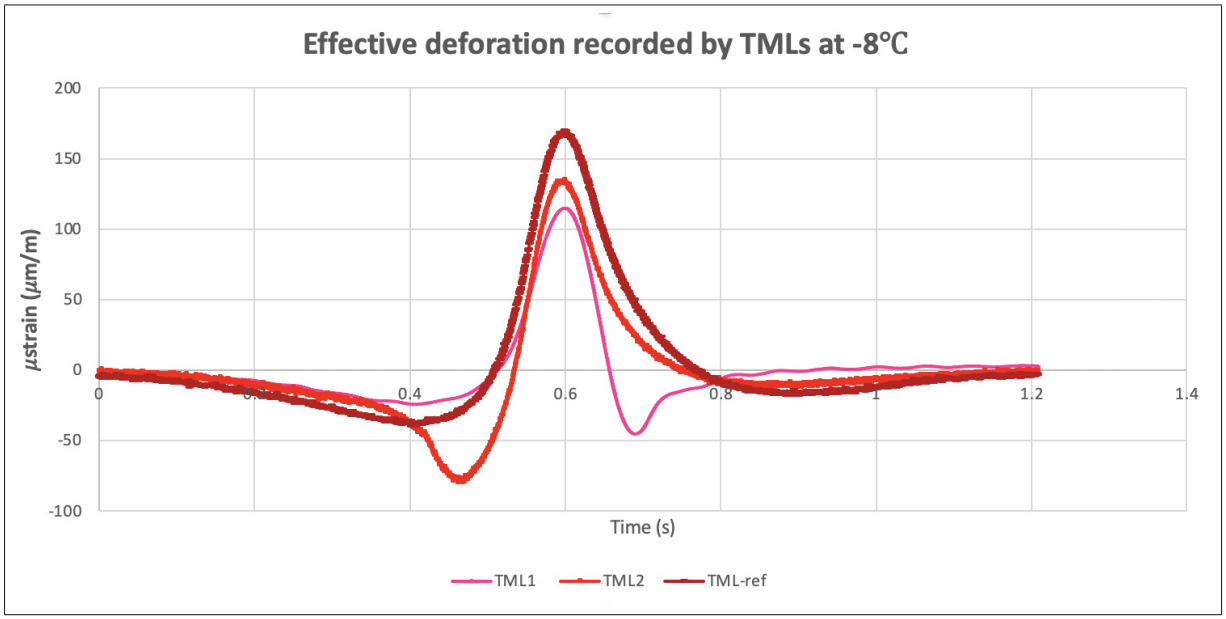

Figure 3.2 Extracted effective strain records at -8°C

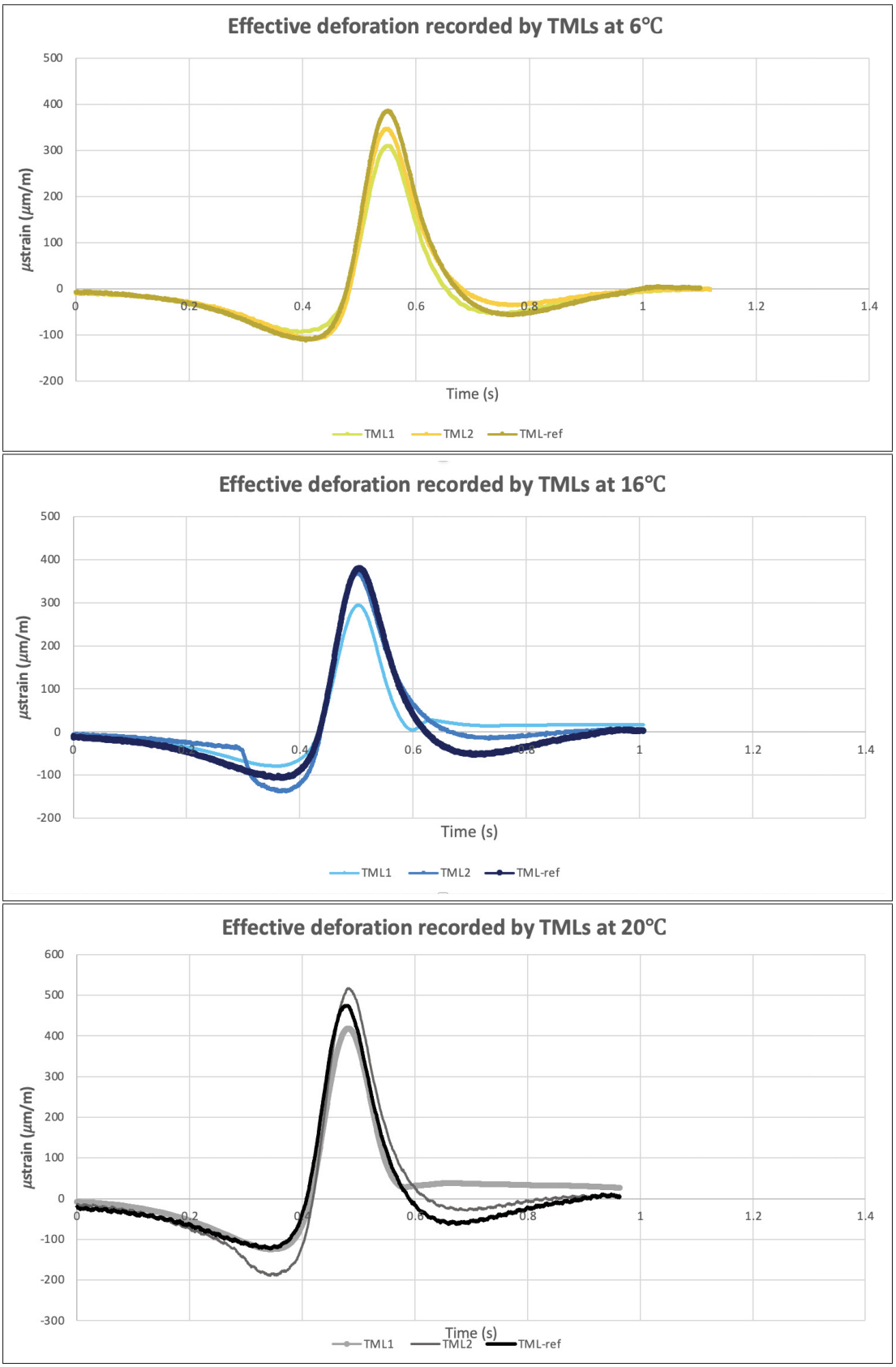

Figure 3.3 Extracted effective strain records at 6, 16, 20°*C*

All the effective loading signals are generated based on a single loading pulse, without considering the location of the strain gauges. These signals depict the immediate longitudinal deformation from time zero to t_{eff}, distinct for each temperature tested as presented in Table 3.2. The idealized crack within the cracked area between TML-1 and TML-2 does influence the deformation signals recorded by these gauges at the bottom of the GB20 layer, as evidenced by a shift in the signal flow before and after reaching its peak. Furthermore, due to TML-REF's installation location, which is sufficiently far from the idealized crack in the referenced area, the recorded signal at this position is not impacted by the crack. Consequently, the TML-REF signals are utilized as reference loading signals for extracting the mathematical function of the signals.

3.3.1 Extraction of Mathematical Functions from Signals

In the previous chapter, the methodology of extracting the mathematical functions from deformation signals for specified time factors was presented out using CurveExpert Professional 2.7.3 software. The deformation data, recorded during effective loading time, was imported into the input table of the CurveExpert software. Regressions were performed on the time factors and deformation columns, and the most accurate regression function for each signal was selected. To obtain the highest accuracy, the signals were divided into two halves, before and after the peak point. Consequently, two functions were calculated for each signal; one for the first half of the time factors' column and the other for the second half. The results of all divided signals are presented in figures 3.4 to 3.11. In the derived equations, the parameter "x" represents the time interval values, and the "y" parameter represents the deformation outcome. The Rational Model's regression, based on the CurveExpert results, was found to be the most accurate match to the real data signals. These regression functions were subsequently set in a Microsoft Excel table and applied to the power of two number of modified time factors.

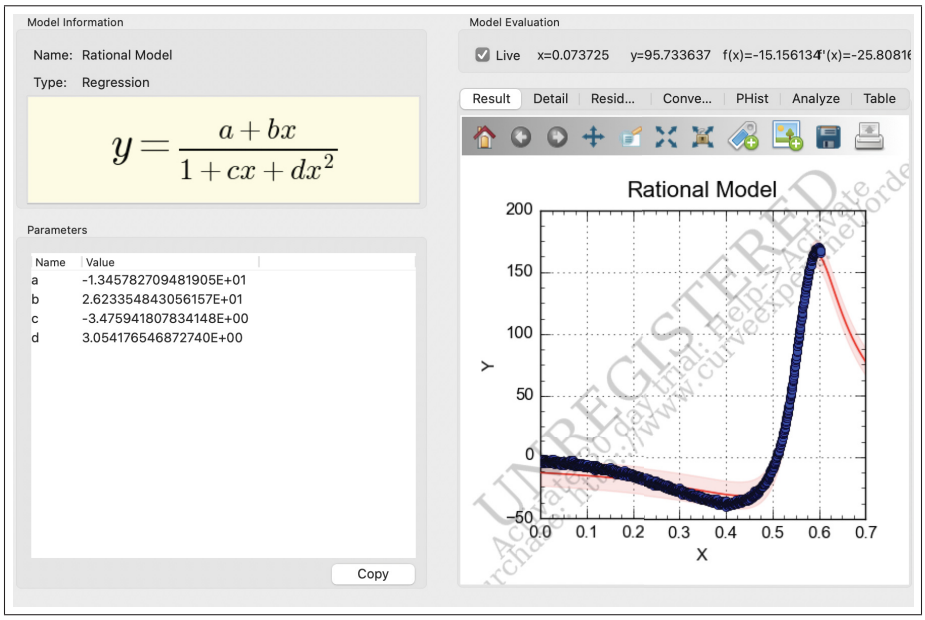

Figure 3.4 Math function for the first half of TML-REF signal at $-8°C$

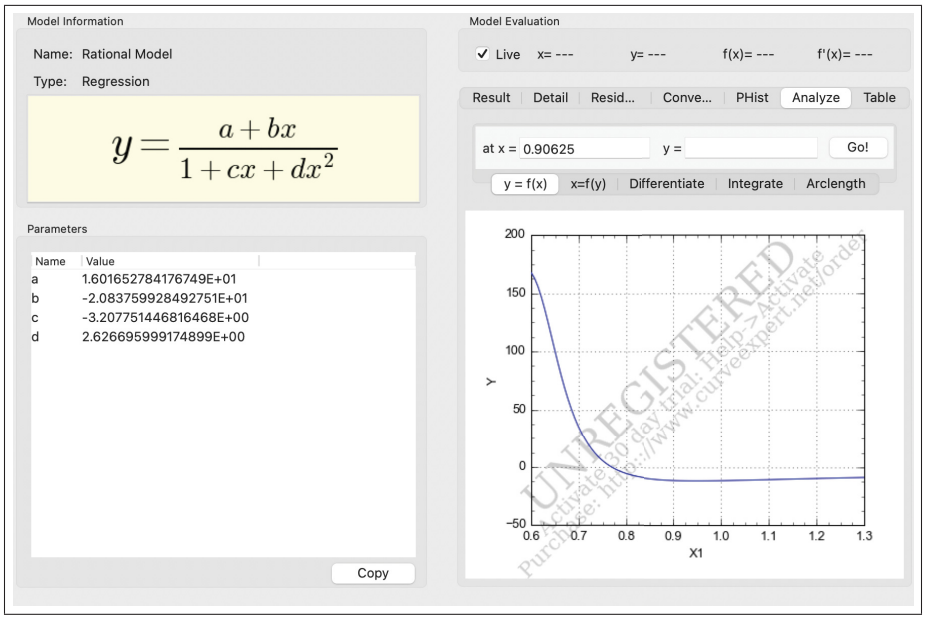

Figure 3.5 Math function for the second half TML-REF signal at $-8°C$

The strain gauges' measurements along the under wheel path reveal that longitudinal strains remain close to zero when unaffected by moving loads, across all testing temperatures. Consequently,

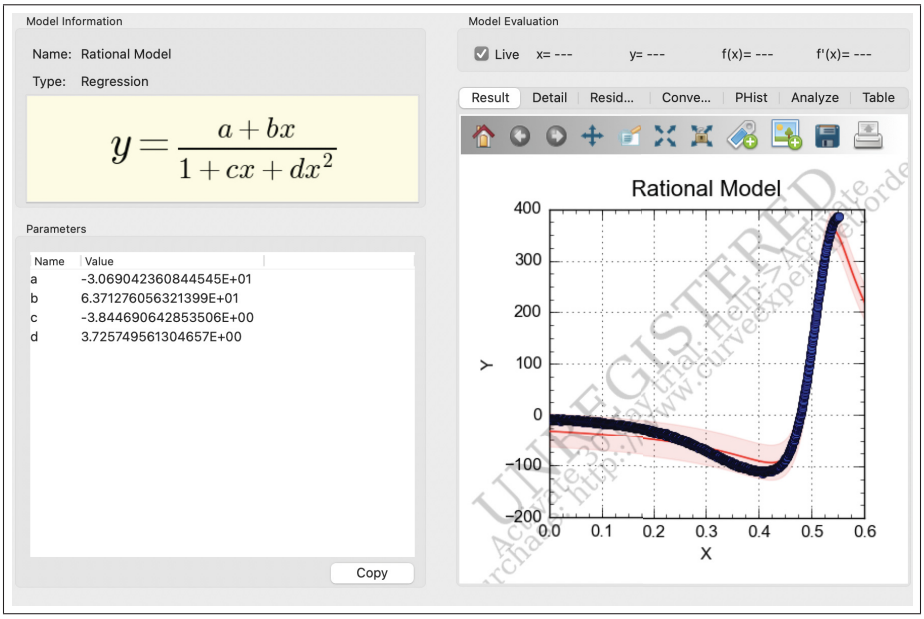

Figure 3.6 Math function for the first half of TML-REF signal at 6°*C*

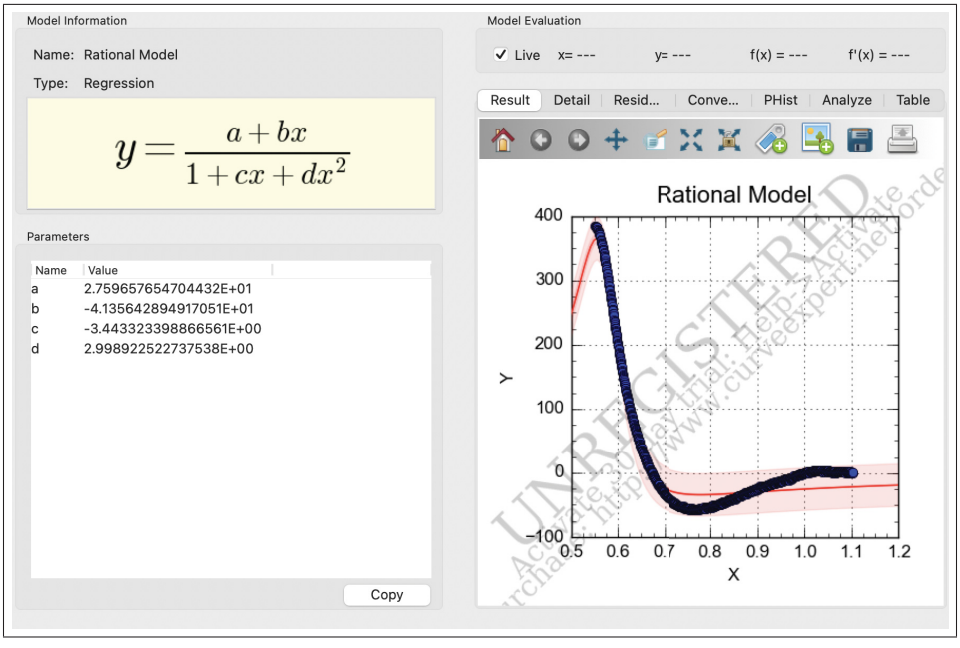

Figure 3.7 Math function for the second half TML-REF signal at 6°*C*

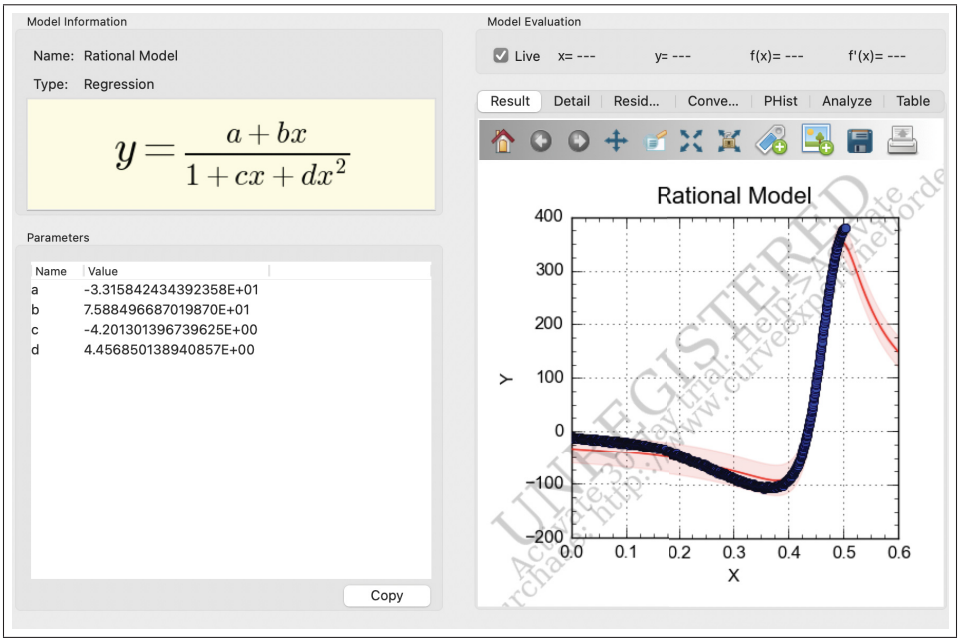

Figure 3.8 Math function for the first half of TML-REF signal at 16°C

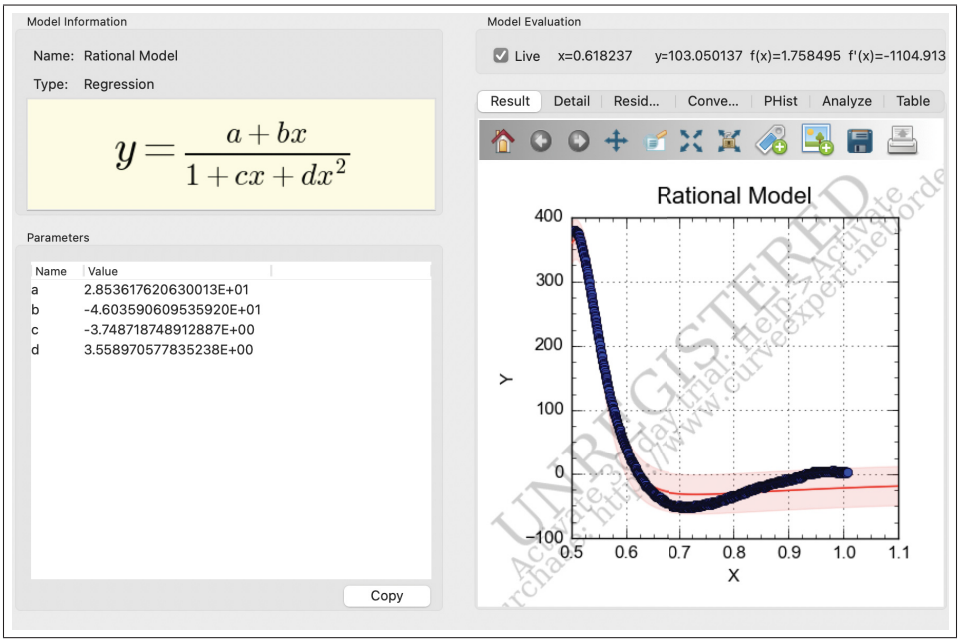

Figure 3.9 Math function for the second half TML-REF signal at 16°C

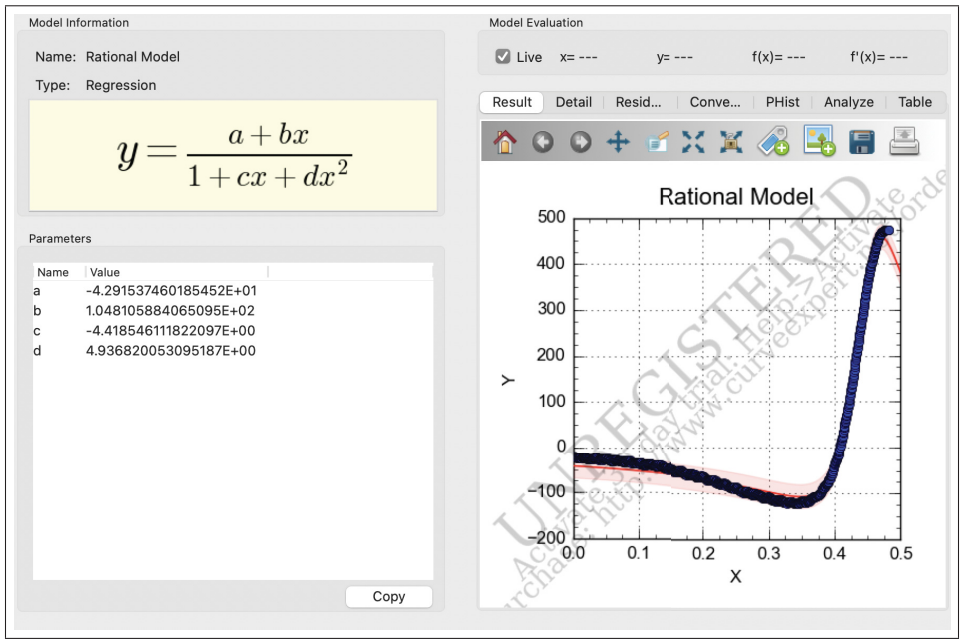

Figure 3.10 Math function for the first half of TML-REF signal at 20°*C*

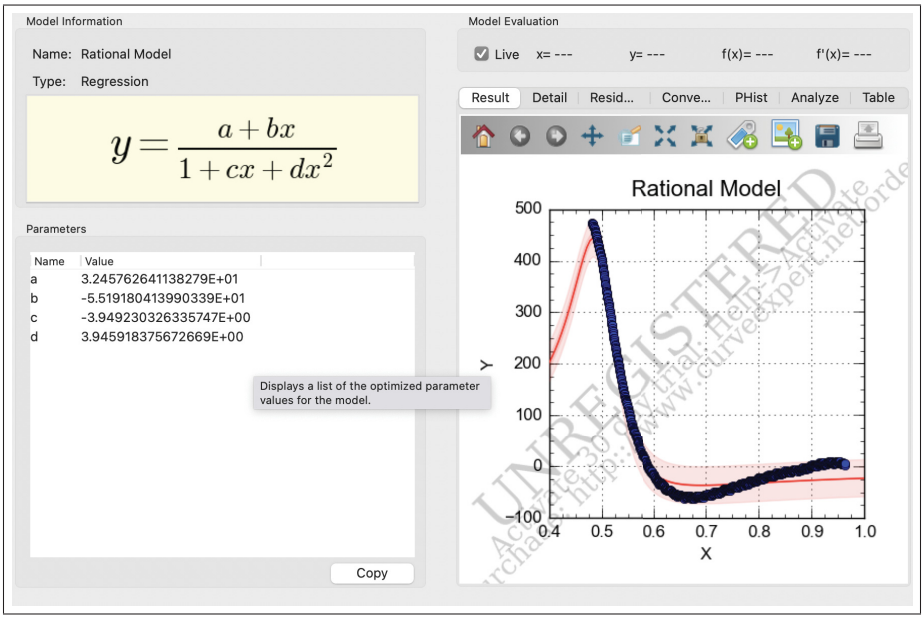

Figure 3.11 Math function for the second half TML-REF signal at 20°*C*

the effective loading signals neither commence nor conclude at zero. Furthermore, during the signal's transition to the frequency domain, only the wavelength and the peak or form of the time domain signals play a significant role in determining the equivalent loading frequency.

3.3.2 Signals modification to power of two number of time intervals

In accordance with the measurements of the effective loading time for each temperature tested (1.2, 1.11, 1.02, and 0.96 seconds), the nearest power of two to the number of time factors is determined to be N'=2048. As a result of this number of time factors the smallest difference from the interval of 0.0005 seconds is obtained. The modification of the curves necessitates the computation of modified time intervals ($\Delta t'$) for each curve based on its corresponding effective loading time, utilizing Equation 2.2. The calculated modified time intervals, represented as "x" values, are then imported into the signals' mathematical functions. The obtained values for modified time intervals at temperatures of -8, 6, 16, and 20 $^{\circ}C$, are presented in Table 3.3 for the recorded referenced loading signals.

Table 3.3 The modified time intervals calculated for each reference signal (Sec).

$\Delta t'(-8^{\circ}C)$	$\Delta t'(6^{\circ}C)$	$\Delta t'(16^{\circ}C)$	$\Delta t'(20^{\circ}C)$
0.000585	0.000538	0.000491	0.00047

The adjusted signals consist of 2048 cells in row for time intervals and for the strain amplitude values obtained from the mathematical functions in time domain for all reference signals. This way, they will be appropriate for Fourier transform from time domain to frequency domain. The effective reference signals are plotted in Figure 3.12 and 3.13.

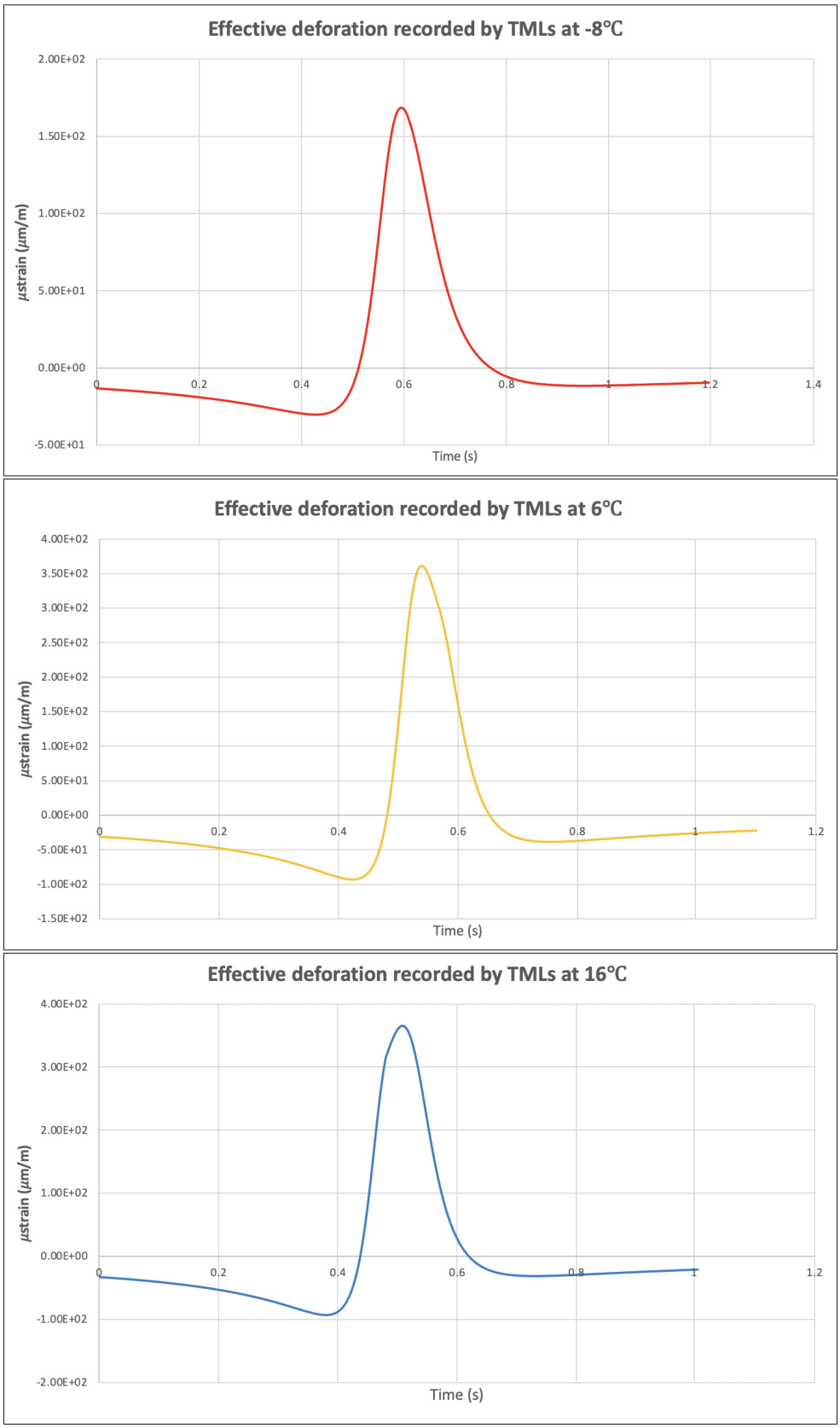

Figure 3.12 Modified TML-REF graphs at -8, 6 and 16°*C* in 2047 time intervals

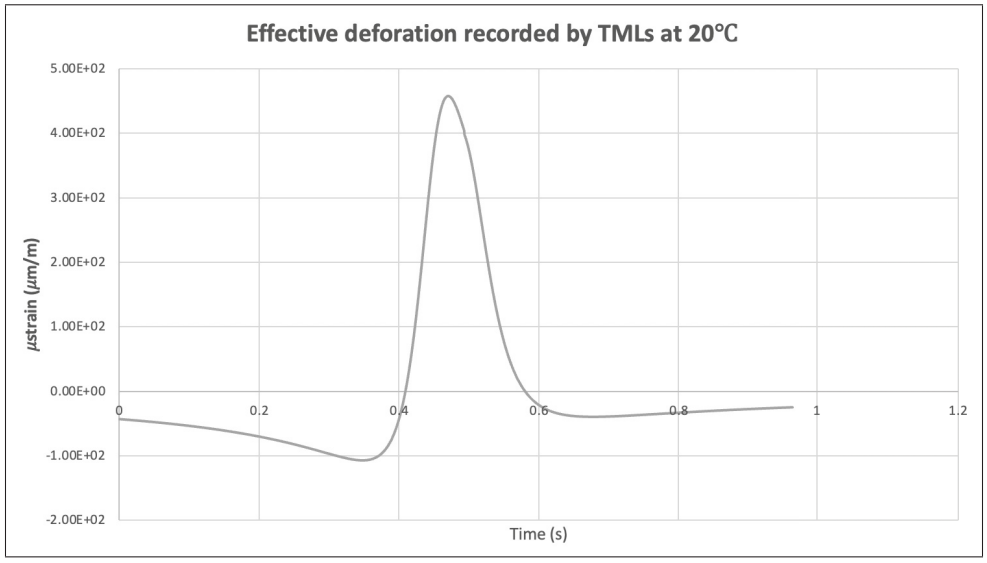

Figure 3.13 Modified TML-REF graphs at 20°C in 2047 time intervals

3.4 Converting the loading signals to the frequency domain

During the transformation process from the time to frequency domain in the present study, it is necessary to determine the angular frequency intervals ($\Delta\omega$) for each reference loading signal to reach the angular frequency factors (ω_k). These values are computed in radians per second (Rad/s), using the equation 2.3 (provided in table 3.4).

Table 3.4 The angular frequency intervals calculated for each reference signal (Rad).

$\Delta\omega(-8°C)$	$\Delta\omega(6°C)$	$\Delta\omega(16°C)$	$\Delta\omega(20°C)$
5.2415	5.699	6.2383	6.5213

In accordance with the definition of the Nyquist frequency (ω_{max}), the angular frequency factors must be specified in the table from 0 to the 1024th factor (i.e., the first half of each signal). Consequently, the corresponding strain amplitude values, derived via Fourier analysis in Microsoft Excel, ranging from the first to the 1024th amplitude.

3.4.1 Calculation of the Angular Frequency Equivalent to the Loading Signals

The present study involves the visualization of the transformed signals in the frequency domain, which have been graphed in the range from zero to the Nyquist frequency (1024th angular frequency factor), as depicted in figures 3.14 to 3.17. To generate the charts, the angular frequency representative (ω) for each temperature was assigned to the "X" axis, while the transformed TML-REF strain amplitude ($\Delta\omega$) was designated to the "Y" axis.

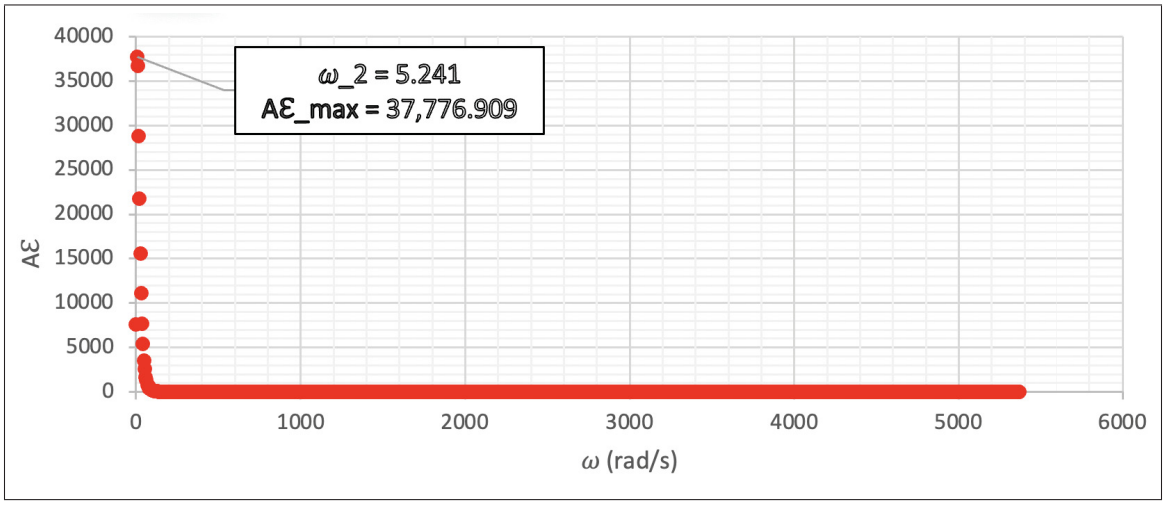

Figure 3.14 Equivalent loading signal in the frequency domain at $-8°C$

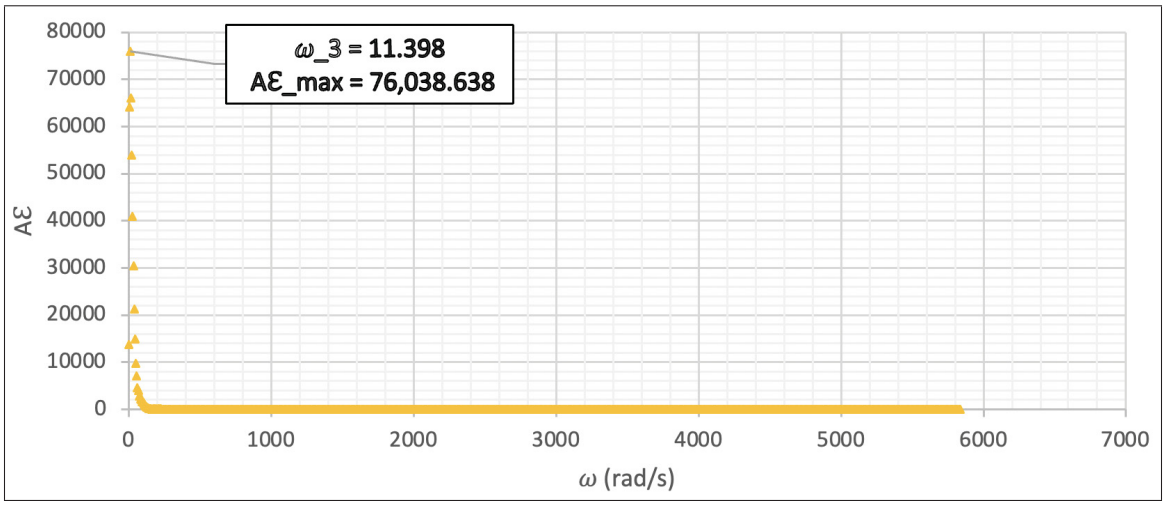

Figure 3.15 Equivalent loading signal in the frequency domain at 6°C

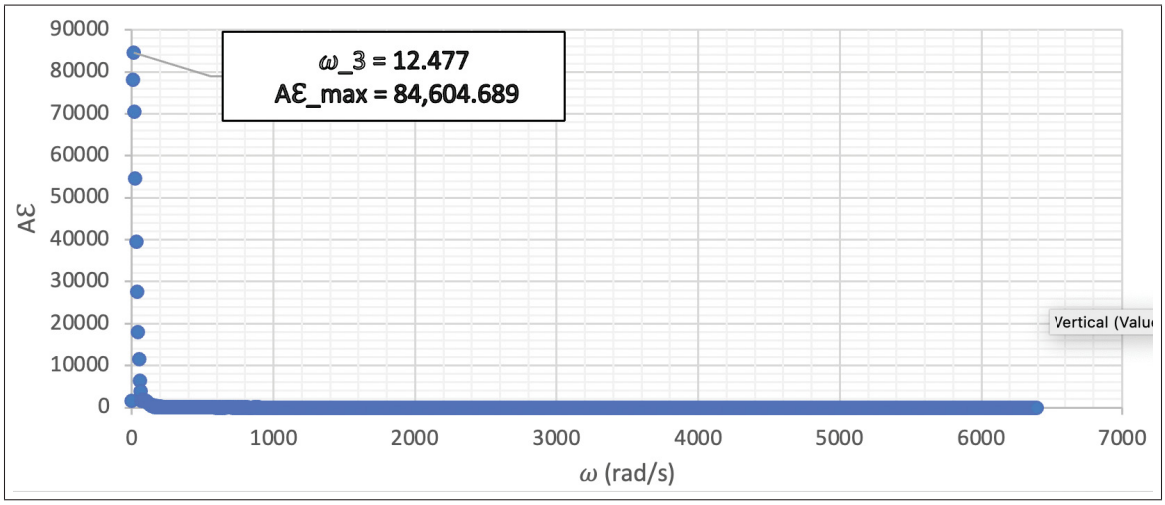

Figure 3.16 Equivalent loading signal in the frequency domain at 16°C

In order to determine the equivalent angular frequency for each loading signal, it is necessary to identify the peak amplitude for each frequency domain signal. Accordingly, the equivalent angular frequency was estimated for a vehicle speed of 2(m/s) traveling on a single asphalt layer of the ULAVAL test track at four different test temperatures (-8, 6, 16, and 20 °C), which are labeled in the signal charts. However, the strain amplitude for the second and third frequency factors exhibited a narrow difference with uneven gaps between the values for each signal. To

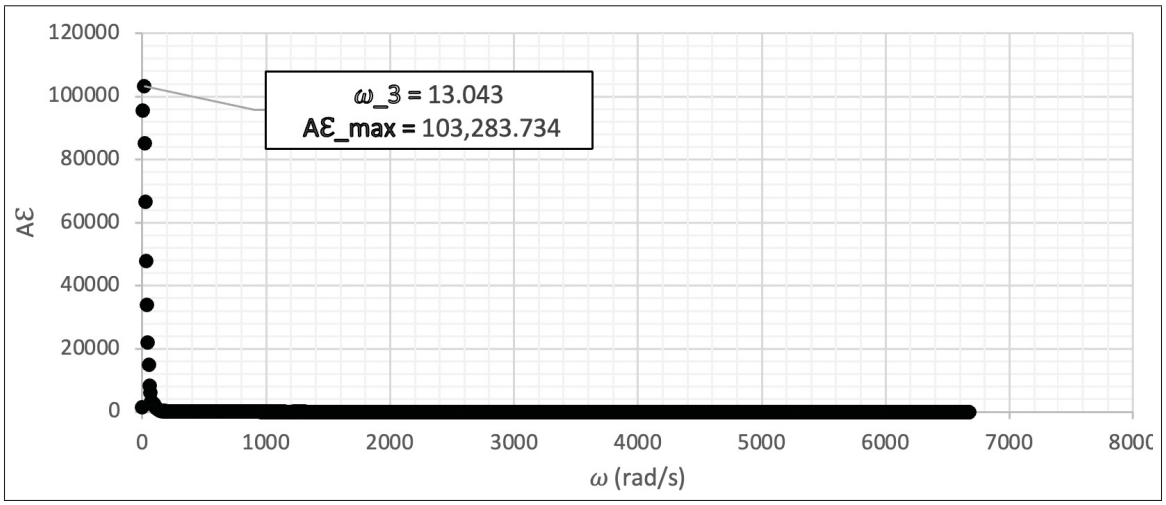

Figure 3.17 Equivalent loading signal in the frequency domain at 20°C

obtain the most accurate angular frequency factor of the peak, mathematical interpolation was applied, and the results are presented in Table 3.5 as the equivalent angular frequency for each loading signal. In the last row of the table, the equivalent frequencies in Hz were calculated using equation 1.14. It is worth noting that the equivalent angular frequencies were calculated based on the four different effective loading times, which were determined using the fixed vehicular speed for each temperature and the asphalt stiffness that varies with speed and temperature. Therefore, it is more appropriate to state that the four equivalent angular frequencies were calculated for four different effective loading times that can vary depending on the temperature and vehicle speed.

Table 3.5 The equivalent frequency for each effective loading time calculated based on different testing temperatures.

T (°C)	-8	6	16	20
$t_{eff}(s)$	1.2	1.1	1	0.96
$\omega_{eq}(Rad/s)$	7.826	8.79	9.48	9.91
$F_{eq}(Hz)$	1.244	1.399	1.508	1.577

The present study utilizes CurveExpert software to generate a mathematical function by depicting a The three-degree Polynomial regression curve for the equivalent angular frequency values

obtained from the loading signals. Figure 3.18 displays the obtained function, which is applied to the effective loading time column ranging from 0 to the maximum value of effective loading time. Parameter X represents the effective loading time and the parameter Y represents the equivalent loading frequency. The corresponding graphical representation is depicted in figure 3.19.

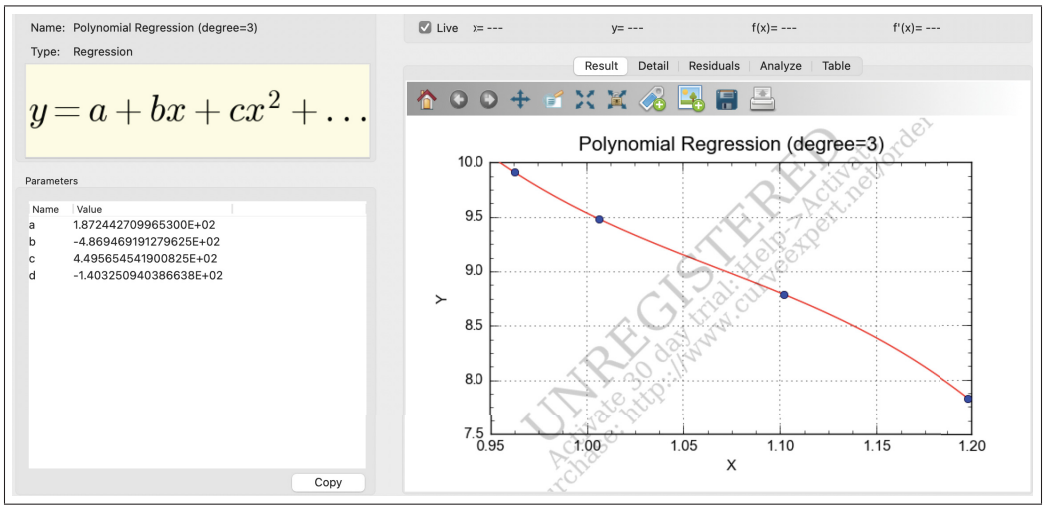

Figure 3.18 CurveExpert function result for the equivalent frequency for the effective loading time

3.5 Validation Outcomes of the Methodology

As stated earlier, the initial loading frequency of 1 Hz was adopted in this investigation to achieve an approximate asphalt material stiffness. However, the equivalent frequency values calculated for each signal at temperatures of -8, 6, 16, and 20$^{\circ}C$ are dissimilar and do not align with the initial assumption. Therefore, The result values of the equivalent frequency for each temperature are replaced to the initial loading frequency in the 2S2P1D mechanical model to calculate the dynamic modulus again. As a result, the material stiffness for each temperature under the revised loading frequencies changes, which in turn modifies the effective loading times (t_{eff}) calculated by the Odemarks method, as shown in Table 3.5.

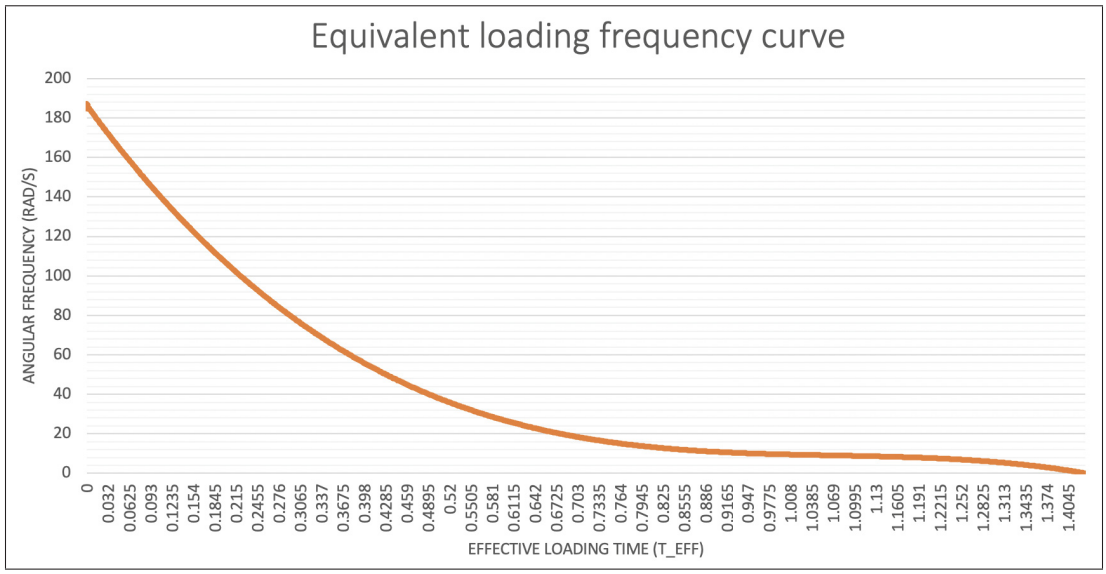

Figure 3.19 The three-degree Polynomial regression curve for the equivalent angular frequency based on the effective loading time.

Table 3.6 Modified pavement and loading parameters based on 2S2P1D model and Odemark method

$T(°C)$	-8	6	16	20
$\|E\|_{GB20}(MPa)$	23974	14382	7879	5754
$t_{eff}(s)$	1.201	1.11	1.021	0.981

The reprocessing method for calculating the effective loading times based on the new frequency inputs resulted in a marginal increase in the recalculated effective loading times compared to the first results. The effective loading times obtained through this method were imported into the CurveExpert math function result to obtain the approximate equivalent angular frequency curve, and the corresponding equivalent frequencies were tabulated in Table 3.7. Since the normal equivalent frequencies remain largely unchanged, this table provides an acceptable representation of the equivalent loading frequencies for a speed of 2 (m/s) on a single layer of asphalt at temperatures of -8, 6, 16, and 20 $°C$.

Table 3.7 Reprocessed equivalent loading frequencies for each effective loading times

T ($°C$)	-8	6	16	20
$t_{eff}(s)$	1.201	1.11	1.021	0.981
$\omega_{eq}(Rad/s)$	7.786	8.72	9.36	9.71
$F_{eq}(Hz)$	1.240	1.390	1.49	1.55

3.6 Conclusion and Future Research Work

The primary objective of this study is to develop a calculation method that utilizes the Odemarks' method and Fourier analysis to estimate the equivalent loading frequency for vehicular loading conditions on a single asphalt layer pavement at different temperatures. The methodology employed in this study involves obtaining the effective loading time at the bottom of the GB20 layer of the ULAVAL test track and extracting the structural parameters based on the 2S2P1D mechanical model. Strain gauges installed at the bottom of the test track surface layer are used to record the immediate deformation at -8, 6, 16 and 20 $°C$, which serve as the loading signals for this study. The effective loading signals are then transferred to the frequency domain using Microsoft Excel Fourier analysis to obtain the equivalent frequencies for each recorded loading signal. After validation of the results, the final equivalent frequency values for each effective loading time are imported into CurveExpert software to generate a base chart that is acceptable for obtaining the equivalent frequency for every effective loading time. Consequently, a conversion tool is developed to calculate the equivalent frequency for loading signals using an initial loading frequency input. If no gaps exist between the outcome equivalent frequency and the initial input frequency, the initial frequency is renewed by the outcome and this process will continue in a loop and explained more in the APPENDIX chapter. The limitations of this study are listed in the following items.

- Given that the strain gauges were installed between the GB20 and MG20 layers without any interlayers in place, the effective loading time results obtained using Odemarks' method in this study only account for the behavior of a single surface layer. To improve the generalizability and accuracy of Odemarks' results in all scenarios, it is necessary to perform similar calculations using strain gauge recordings from different types of flexible pavements.

- In this research, the CurveExpert software is utilized to extract the mathematical functions of loading signals, which are subsequently modified in length to fit a power of two number of data cells, a necessary step to transfer to the frequency domain through Fourier analysis. While the accuracy of CurveExpert results for the entire signal length is insufficient, it is acceptable for preserving the shape of the signals if they are divided into two halves. Nevertheless, it is imperative to develop a more accurate method for adjusting the length of signals while retaining their shape to achieve greater precision in the frequency domain results.

- In this study, a mathematical interpolation method is employed to determine the maximum strain amplitude value between the second and third intervals in the frequency domain. Obtaining an accurate equivalent loading frequency is crucial, and to achieve this, it is more imperative to use a larger power of two number as the number of frequency factors (N'). This approach results in a higher accuracy in determining the equivalent frequency.

APPENDIX I

EQUIVALENT FREQUENCY CONVERSION TOOL

1. Introduction

The accurate transformation of loading signals from the time domain to the frequency domain is essential for ascertaining the equivalent loading frequency, which, in turn, is a critical parameter for bituminous material pavement design. To facilitate this, the present study proposes a conversion tool built on the Microsoft Excel platform that employs the 2S2P1D mechanical model, Odemark method, and Fourier analysis. This conversion tool adopts a loop calculation method, which iteratively refines the initial loading frequency input until the final output (i.e., the equivalent frequency) equals the imported input value.

2. A Methodology for Estimating Stiffness using the 2S2P1D Model

The first step of this study involves calculating the stiffness of the asphalt layer (GB20) using the 2S2P1D mechanical model. This is achieved by inputting the assumed design temperature and a loading frequency (typically 1 Hz) into the 2S2P1D Excel sheet to start the process, which estimates the dynamic modulus ($|E|$) of the material. This modulus serves as a key input for the subsequent Odemark method, which determines the effective loading time (t_{eff}).

3. Estimation of the effective loading time through the Odemarks Method

The Odemark method is employed to determine the effective loading time (t_{eff}) by first calculating the effective loading depth (Z_{eff}), which further defines the effective loading length (L_{eff}) through the $45°C$ trapezoidal Odemark model. The computation is carried out using Microsoft Excel, requiring input of the pavement and loading parameters such as vehicle tire contact area with the surface ($a_c(mm^2)$), thickness of the asphalt layer ($h_{GB20}(mm)$), thickness of the sub-grade layer ($h_{SG}(mm)$), dynamic modulus of the asphalt material ($|E|_{GB20}(MPa)$), and dynamic modulus of the sub-grade material ($E_{SG}(MPa)$). Addition of the vehicle speed

($V_c(mm/s)$) as input parameter leads to estimation of the effective loading time using equation 1.10, whereby L_{eff} is divided by V_c.

4. Determination of Equivalent Frequency using Computed Effective Loading Time

In this stage, the methodology of this project involves utilizing a conversion calibration chart to determine the equivalent frequency of the effective loading time. The conversion calibration curve, which estimates the equivalent frequencies for each effective loading time (for each temperature), was developed using CurveExpert software by employing a three-degree polynomial regression. The resultant effective loading time is subsequently entered into the math function of the conversion chart, illustrated in Figure I-1. The equivalent loading frequency can be expressed in both Hz and Rad/s, however, calibration is required for it to be considered valid.

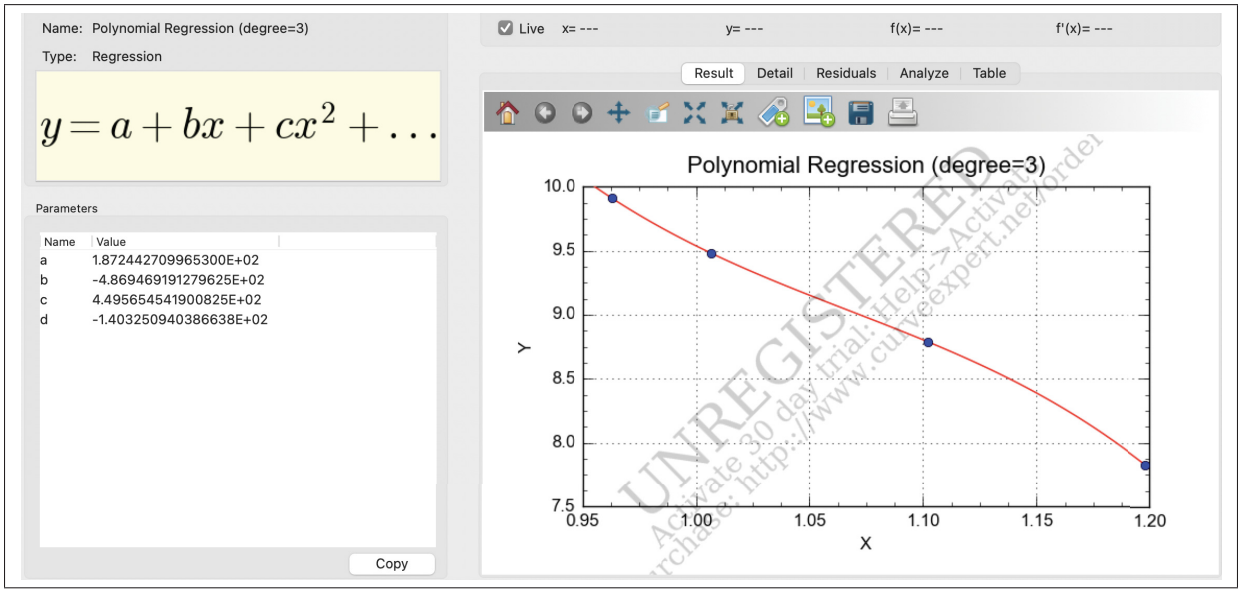

Figure-A I-1 Conversion curve and it's math function for equivalent frequency based on the effective loading time

5. The equivalent frequency calibration

As previously mentioned, the 2S2P1D model relies on the initial loading frequency input to determine the stiffness of the asphalt layer, which in turn allows for the calculation of the effective loading time under a specific moving load. In this study, the initial loading frequency was taken as 1 Hz to start the calculation. However, in order to refine the effective loading time, the frequency must be calibrated by adjusting the designed equation with the calculated equivalent loading frequency. This iterative process involves replacing the initial loading frequency with the calculated equivalent frequency until the difference between the two values is insignificant. By iteratively refining the estimated effective loading time and corresponding equivalent frequency, a more accurate representation of the pavement response to vehicular loading can be obtained. This approach accounts for the variability in pavement material properties and loading conditions, which can affect the effective loading time and ultimately the equivalent frequency parameter.

BIBLIOGRAPHY

Al-Qadi, I. L. & Wang, H. (2009). *Evaluation of pavement damage due to new tire designs*.

Al-Qadi, I. L., Loulizi, A., Elseifi, M. & Lahouar, S. (2004). The Virginia Smart Road: The impact of pavement instrumentation on understanding pavement performance. *Journal of the Association of Asphalt Paving Technologists*, 73(3), 427–465.

Al-Qadi, I. L., Xie, W. & Elseifi, M. A. (2008). Frequency determination from vehicular loading time pulse to predict appropriate complex modulus in MEPDG. *Asphalt Paving Technology-Proceedings*, 77, 739.

Alfaqawi, R. (2012). *Using recycled aggregate in hot asphalt mixtures in Gaza Strip*. (Ph.D. thesis, M. Sc Thesis, University of Nottingham, UK).

Ara, I., Vicente-Rodriguez, G., Jimenez-Ramirez, J., Dorado, C., Serrano-Sanchez, J. & Calbet, J. (2004). Regular participation in sports is associated with enhanced physical fitness and lower fat mass in prepubertal boys. *International journal of obesity*, 28(12), 1585–1593.

Arabani, M. & Kamboozia, N. (2014). New achievements in visco-elastoplastic constitutive model and temperature sensitivity of glasphalt. *International Journal of Pavement Engineering*, 15(9), 810–830.

ASTM, D. (2009). Standard practice for roads and parking lots pavement condition index surveys.

Badeli, S. (2018). *Evaluation of the damage of an asphalt mix under repeated freeze-thaw cycles*. (Ph.D. thesis, École de technologie supérieure).

Barber, E. (1947). Application of triaxial compression test results to the calculation of flexible pavement thickness. *Highway Research Board Proceedings*, 26.

Barksdale, R. D. (1971). Compressive stress pulse times in flexible pavements for use in dynamic testing. *Highway research record*, 345(4), 32–44.

Berraha, Y., Perraton, D., Doré, G. & Vaillancourt, M. (2020). Cracked asphalt pavement behaviour under thermal and load cycles–laboratory investigation using accelerated loading system. *RILEM International Symposium on Bituminous Materials*, pp. 497–504.

Brown, S. (1973). Determination of Young's modulus for bituminous materials in pavement design. *Highway Research Record*, (431).

Burmister, D. M., Palmer, L., Barber, E. & Middlebrooks, T. (1944). The theory of stress and displacements in layered systems and applications to the design of airport runways. *Highway Research Board Proceedings*, 23.

Carter, A., Donovan, H., MacInnis,Keith, S. & Todd. (2018). *Hot Mix Asphalt: Canadian technical Asphalt Association; Alan Carter, Hugh Donovan, Keith MacInnis and Todd Strynadka*. CTAA.

Chabot, A., Tamagny, P., Duhamel, D. & Poché, D. (2006). Visco-elastic modeling for asphalt pavements–software ViscoRoute. *Proceedings of the 10th International Conference on Asphalt Pavements, Québec*, 2, 5–14.

Chabot, A., Chupin, O., Deloffre, L. & Duhamel, D. (2010). Viscoroute 2.0 A: tool for the simulation of moving load effects on asphalt pavement. *Road Materials and Pavement Design*, 11(2), 227–250.

Chadbourn, B., Dai, S., Davich, P., Siekmeier, J. & Van Deusen, D. (2002). Pavement Designer's Guide for MnDOT Flexible Pavement Design. *MnPAVE Beta Version*, 5(1).

Cooley, J. W. & Tukey, J. W. (1965). An algorithm for the machine calculation of complex Fourier series. *Mathematics of computation*, 19(90), 297–301.

Correia, N. & Zornberg, J. (2018). Strain distribution along geogrid-reinforced asphalt overlays under traffic loading. *Geotextiles and Geomembranes*, 46(1), 111–120.

Cross, S. A. & Shrestha, P. P. (2005). *Guidelines for Using Prime and Tack Coats*.

D"Angelo, J. A., Dongre, R. N. & Myers, L. A. (2006). *Conversion of testing frequency to loading time: Impact on performance predictions obtained from mechanistic-empirical pavement design guide*.

David W. Janisch, F. S. G. (1998). sponsored by Minnesota Local Road Research Board. *Minnesota Department of Transportation*.

De Jong, D. (1979). Computer Program BISAR, Layered systems under normal and tangential loads. *External Report, Koninkljke/Shell-Laboratorium*.

Dejong, D., Peutz, M. & Korswagen, A. (1973). Computer Program, BISAR, Layered Systems under Normal and Tangential Surface Loads, Koninklijke Shell Laboratorium, External Rept. *AMSR-000673, Amsterdam, Netherlands*.

Di Benedetto, H. & Corté, J.-F. (2004). *Matériaux routiers bitumineux: Constitution et propriétés thermomécaniques des mélanges*. Hermès science publications.

Di Benedetto, H. & Corté, J.-F. (2005). Matériaux routiers bitumineux 2: constitution et propriétés thermomécaniques des mélanges, 1ère éd. Coll.«Mécanique et Ingénierie des Matériaux». Paris: Hermes Science.

Diffiné, T. (2012). *Analyse des déformations d'une chaussée contenant des matériaux bitumineux recyclés à froid*. (Ph.D. thesis, École de technologie supérieure).

Dinata, D. I., Rahmawati, A. & Setiawan, D. (2017). Evaluasi Tebal Perkerasan Lentur dengan Metode Analisa Komponen dari Bina Marga 1987 dan Metode AASHTO 1993 Menggunakan Program KENPAVE (Studi Kasus: Jalan Karangmojo-Semin Sta 0+ 000 sampai Sta 4+ 050). *Semesta Teknika*, 20(1), 8–19.

Duncan, J. M., Monismith, C. L. & Wilson, E. L. (1968). Finite element analysis of pavements. *Highway Research Record*, 228, 18–33.

Ekwulo, E. & Eme, D. (2010). Fatigue and rutting strain analysis of flexible pavements designed using CBR methods. *Afr J Environ Sci Technol*, 3.

Elseifi,Mostafa A, A.-Q. I. Y. & Jun, P. (2006a). Viscoelastic modeling and field validation of flexible pavements. *Journal of engineering mechanics*, 132(2), 172–178.

Elseifi,Mostafa A, D.-S. H. A.-Q. I. L. Y. & Shih-Hsien. (2006b). Viscoelastic model to describe mechanical response of bituminous sealants at low temperature. *Transportation research record*, 1958(1), 82–89.

Elseifi, M. A., Al-Qadi, I., Yoo, P. J. & Janajreh, I. (2005). Quantification of pavement damage caused by dual and wide-base tires. *Transportation research record*, 1940(1), 125–135.

Erlingsson, S. & Ahmed, A. (2013). Fast layered elastic response program for the analysis of flexible pavement structures. *Road Materials and Pavement Design*, 14(1), 196–210.

Ghanizadeh, A. R. & Fakhri, M. (2018). Quasi-static analysis of flexible pavements based on predicted frequencies using Fast Fourier Transform and Artificial Neural Network. *International Journal of Pavement Research and Technology*, 11(1), 47–57.

Harichandran, R., Baladi, G. & Yeh, M. (1989). Development of a computer program for design of pavement systems consisting of bound and unbound materials. *Department of Civil and Environmental Engineering, Michigan State University*.

Hayhoe, G. F. (2002). *LEAF: A new layered elastic computational program for FAA pavement design and evaluation procedures*. Citeseer.

Heck, J., Piau, J., Gramsammer, J., Kerzreho, J. & Odeon, H. (1998). Thermo-visco-elastic modelling of pavements behaviour and comparison with experimental data from LCPC test track. *Proc. of the 5th BCRA*, 6–8.

Huang, Y. H. (1967). Stresses and displacements in viscoelastic layered systems under circular loaded areas. *Intl Conf Struct Design Asphalt Pvmts*.

Huang, Y. (1985). A computer package for structural analysis of concrete pavements. *Third International Conference on Concrete Pavement Design and RehabilitationPurdue University, School of Civil Engineering; Federal Highway Administration; Portland Cement Association; Transportation Research Board; Federal Aviation Administration; and Indiana Department of Highways.*, (1 Volume).

Huang, Y. (2004). Pavement Analysis and Design Pearson Education. *Upper Saddle River, NJ, USA*.

Huet, C. (1963). *Étude par une méthode d'impédance du comportement viscoélastique des matériaux hydrocarbonés [Study of the viscoelastic behavior of bituminous mixes by method of impedance]*. (Ph.D. thesis, Ph. D. thesis, Faculte des Sciences de Paris, Paris (in French)).

Hwang, D. & Witczak, M. (1979). Program DAMA (Chevron), User's Manual. *Department of Civil Engineering, University of Maryland*.

Hyams, D. G. (2011). CurveExpert professional documentation. Release.

Islam, M. R., Mannan, U. A., Rahman, A. & Tarefder, R. A. (2014). Simplified thermal stress model to predict low temperature cracks in flexible pavement. In *Pavement Materials, Structures, and Performance* (pp. 251–261).

Janisch, D. W. & Gaillard, F. S. (1998). *Minnesota seal coat handbook*.

Jones, A. (1962). Tables of stresses in three-layer elastic systems. *Highway Research Board Bulletin*, (342).

Khazanovich, L. & Wang, Q. (2007). MnLayer: high-performance layered elastic analysis program. *Transportation Research Record*, 2037(1), 63–75.

Kopperman, S., Tiller, G. & Tseng, M. (1986). ELSYM5, Interactive microcomputer version, User's manual. *Rep. No. FHWA-TS-87*, 206.

Kruntcheva, M. R., Collop, A. C. & Thom, N. H. (2005). Effect of bond condition on flexible pavement performance. *Journal of transportation engineering*, 131(11), 880–888.

Liao, J. & Sargand, S. (2010). Viscoelastic FE modeling and verification of a US 30 perpetual pavement test section. *Road materials and pavement design*, 11(4), 993–1008.

Liao, Y. (2007). *Viscoelastic FE modeling of asphalt pavements and its application to US 30 perpetual pavement*. (Ph.D. thesis, Ohio University).

Liu, Y. (2016). *Novel Parylene Filters for Biomedical Applications*. (Ph.D. thesis).

MEPDG, A. (2004). Inc, ERES Consultants Division. *Guide for the mechanistic-empirical design of new and rehabilitated pavement structures*.

Meunier, M. (2012). *Prédiction de l'orniérage lié aux déformations permanentes des enrobés bitumineux*. (Ph.D. thesis, École de technolgie supérieure).

Mohammadi, M., Pishdad-Bozorgi, P., Huang, Y. & Lovell, C. (2021). Frequency domain analysis of dynamic strains in asphalt pavements using a Fourier series approach. *International Journal of Pavement Engineering*, 22(5), 599–610.

Olard, F. & Di Benedetto, H. (2003). General "2S2P1D" model and relation between the linear viscoelastic behaviours of bituminous binders and mixes. *Road materials and pavement design*, 4(2), 185–224.

Pagen, C. A. (1965). Rheological response of bituminous concrete. *Highway Research Record*, (67).

Park,SW, S. & RA0942. (1999). Methods of interconversion between linear viscoelastic material functions. Part I—A numerical method based on Prony series. *International journal of solids and structures*, 36(11), 1653–1675.

PDG, M. (2004). NCHRP-Guide for mechanistic-empirical design of new and rehabilitated pavement structures. National Cooperative Highway Research Program. *Transportation Research Board, National Research Council, Washington, DC, USA*.

Pereira, T. D. d. C. P. (2014). *Rigid pavements distresses-pavement condition index evaluation*. (Ph.D. thesis).

Pirabarooban, S., Zaman, M. & Tarefder, R. A. (2003). Evaluation of rutting potential in asphalt mixes using finite element modeling. *The Transportation Factor 2003. Annual Conference and Exhibition of the Transportation Association of Canada.(Congres et Exposition Annuels de l'Association des transport du Canada) Transportation Association of Canada (TAC)*.

Raad, L. & Figueroa, J. L. (1980). Load response of transportation support systems. *Journal of Transportation Engineering*, 106(1).

Ramirez, C., Diego, A., Pouget, S., Di Benedetto, H. & Olard, F. (2015). Viscoelastic behaviour characterization of a gap-graded asphalt mixture with SBS polymer modified bitumen. *Materials Research*, 18(2), 373–381.

Ramirez, R. W. (1985). The FFT Fundamentals and Concepts, Tektronix. *Inc., Englewood Cliffs 1985*.

Rind, T. A., Memon, N. A. & Qureshi, A. S. (2017). Analysis and Design of Flexible Pavement Using Empirical-Mechanistic Based Software (KENPAVE). *International Conference on Sustainable Development in Civil Engineering*.

Roberts, F. L., Kandhal, P. S., Brown, E. R., Lee, D.-Y. & Kennedy, T. W. (1991). Hot mix asphalt materials, mixture design and construction.

Secor, K. E. & Monismith, C. L. (1961). Analysis of triaxial test data on asphalt concrete using viscoelastic principles. *Highway Research Board Proceedings*, 40.

Siddharthan, R. V., Krishnamenon, N., Sebaaly & E, P. (2000). Finite-layer approach to pavement response evaluation. *Transportation research record*, 1709(1), 43–49.

Siddharthan, R. V., Krishnamenon, N., El-Mously, M. & Sebaaly, P. E. (2002). Investigation of tire contact stress distributions on pavement response. *Journal of Transportation Engineering*, 128(2), 136–144.

Siddharthan,Raj V, Y. J. S. & E, P. (1998). Pavement strain from moving dynamic 3D load distribution. *Journal of Transportation Engineering*, 124(6), 557–566.

Tai, N., Duy-Liem, T., Vu-Tu, N. & Mai-Lan. (2020). Finite element implementation of Huet-Sayegh and 2S2P1D models for analysis of asphalt pavement structures in time domain. *Road Materials and Pavement Design*, 1–25.

Tanquist, B., Dai, S., Davich, P., Siekmeier, J. & VanDeusen, D. (2002). Pavement Designer's Guide Mn/DOT Flexible Pavement Design MnPAVE Beta Version 5.1. *MnDOT Office of Materials and Road Research, Maplewood, Minnesota*.

Uddin, W., Hackett, R. M., Joseph, A., Pan, Z. & Crawley, A. B. (1995). Three-dimensional finite-element analysis of jointed concrete pavement with discontinuities. *Transportation Research Record*, 1482, 26–32.

Uzan, J. (1994). Advanced backcalculation techniques. In *Nondestructive Testing of Pavements and Backcalculation of Moduli: Second Volume*. ASTM International.

Van Cauwelaert, F. & Lequeux, D. (1986). Computer programs for the determination of stresses and displacements in four layered structures. Water Experiment Station, US Army Corps of Engineers, Vicksburg, Miss.

Van Cauwelaert, F. J., Alexander, D. R., White, T. D. & Barker, W. R. (1989). Multilayer elastic program for backcalculating layer moduli in pavement evaluation. In *Nondestructive testing of pavements and backcalculation of moduli*. ASTM International.

Wang, G., Chen, W., Nie, Q., Wang, Y. & Shu, X. (2019). Behavior of Composite Foundations Reinforced with Rigid Columns. *Journal of Transportation Engineering, Part B: Pavements*, 145(4), 04019032.

Warren, H. & Dieckmann, W. (1963). Numerical computation of stresses and strains in a multiple-layer asphalt pavement system. *International Report, Chevron Research Corporation, Richmond, CA*.

Williams, M. L., Landel, R. F. & Ferry, J. D. (1955). The temperature dependence of relaxation mechanisms in amorphous polymers and other glass-forming liquids. *Journal of the American Chemical society*, 77(14), 3701–3707.

Williams, T. (2000). The Glass Menagerie. Tennessee Williams: Plays 1937-1955. *The Library of America*, 393–466.

Yang, X., Zhang, Y., Hu, X. & Wei, J. (2020). Investigating the effects of temperature on asphalt pavement performance using frequency domain analysis. *Construction and Building Materials*, 241, 117992.

Yusoff, M., Airey, G. et al. (2010). The 2S2P1D: An excellent linear viscoelastic model. *Journal of Civil Engineering, Science and Technology*, 1(2), 1–7.